



Corso di dottorato di ricerca in:

“Scienze Biomediche e Biotecnologiche”

*in convenzione con Centro di Riferimento Oncologico di Aviano, IRCCS*

Ciclo 34°

Titolo della tesi

“MOLECULAR INSIGHTS INTO EPITHELIOID SARCOMA”

Dottorando

Del Savio Elisa

Supervisore

Dott.ssa Maestro Roberta

Co-supervisore

Dott. Sigalotti Luca

**Anno 2022**

## **ABSTRACT**

Epithelioid Sarcoma (ES) is a very rare and aggressive mesenchymal tumor characterized by the loss of expression of the SWI/SNF component SMARCB1, which accounts for the designation of ES as an “epigenetic-driven tumor”. From a pathological standpoint, ES is distinguished into classic or conventional type (a.k.a “distal type”) ES and proximal ES. This pathological distinction seems to identify two clinically different entities, with C-ES featuring a relatively indolent clinical course, and P-ES showing a more aggressive phenotype. What are the molecular bases of this pathological and clinical dichotomy is still undefined. A better understanding of the molecular features of the two histopathological variants would provide better tools for differential diagnosis (currently based on not well-defined morphological features) and, given the apparent differential clinical behavior of the two variants, would result also into better prognostic criteria.

Bearing this in mind, my thesis work was focused on the molecular characterization of ES and in particular on the identification of the molecular properties that differentiate P-ES and C-ES. By exploiting RNA and microRNA profiling, we were able to corroborate the notion that P-ES and C-ES actually represent two distinct entities also from a transcriptional standpoint, with the more aggressive P-ES variant featuring an enrichment in biological processes related to cell proliferation and chromatin remodeling. We then focused on miRNAs and addressed their role in shaping the transcriptome of P-ES and C-ES. To this end, RNA and miRNA data were integrated through the use of different bioinformatic approaches and several candidate gene/miRNA pairs possibly involved in ES pathogenesis were identified. Specifically, we were able to validate the implication of miR-137 and miR-24-3p in the up-regulation of EZH2 and MYC observed in P-ES. Furthermore, we identified an unprecedented gene pair, HELLS/miR-24-3p, possibly implicated in the epigenetic regulation of P-ES.

Overall, this work provides molecular evidence for the pathological differentiation of ES into two variants, indicates that the more aggressive P-ES variant likely exhibits further drift toward epigenetic deregulation, and supports the implication of miRNAs in the distinctive features of P-ES and C-ES.

# INDEX

<b>1. INTRODUCTION.....</b>	<b>5</b>
1.1 SOFT TISSUE SARCOMAS.....	6
1.2 EPITHELIOID SARCOMA (ES).....	8
1.2.1 Pathological and molecular features.....	9
1.2.2 Deregulated pathways in ES.....	12
1.2.3 Therapy.....	13
1.3 EPIGENETICS AND SARCOMAS.....	14
1.3.1 Chromatin remodeling complexes.....	17
1.3.2 Histone modifiers.....	20
1.3.3 MicroRNAs.....	22
<b>2. AIM.....</b>	<b>25</b>
<b>3. RESULTS.....</b>	<b>27</b>
3.1 Transcriptome analysis: whole cohort.....	28
3.2 Transcriptome profiling: selected cohort.....	30
3.3 miRNA profiling: selected cohort.....	36
3.4 miRNA targeting validation.....	42
<b>4. DISCUSSION.....</b>	<b>44</b>
<b>5. MATERIAL AND METHODS.....</b>	<b>48</b>
5.1 Epithelioid sarcoma samples.....	49
5.2 RNA extraction.....	49
5.3 RNA-Sequencing and data processing.....	49
5.4 miRNA-Sequencing and data processing.....	50
5.5 Graphical representation of data.....	51
5.6 Functional annotation analyses.....	51
5.7 Cell cultures and miRNA mimics transfection.....	52
5.8 Quantitative Real-Time PCR.....	53
5.9 Western blotting.....	53



<b>6. REFERENCES.....</b>	<b>54</b>
<b>7. ACKNOWLEDGMENTS.....</b>	<b>70</b>
<b>8. PUBLISHED ARTICLES.....</b>	<b>72</b>

# **1. INTRODUCTION**

## 1.1 SOFT TISSUE SARCOMAS

Sarcomas are mesenchymal tumors conventionally distinguished into soft tissue sarcomas (STSs) and bone sarcomas. STSs represent a heterogeneous group of malignancies that are classified into nearly 70 histopathological subtypes (Fig. 1.1.) that often differ also for clinical behaviour and therapeutic treatment (Sbaraglia et al., 2020; WHO, 2020).

The annual incidence of STSs is about 50 cases per 1 million population, that corresponds to less than 1% of all malignant tumors in the adult and 12-15% of pediatric tumors (Stiller et al., 2013). Thus, STSs are formally considered as rare tumors (WHO, 2020).

Clinically, STSs range from low-grade neoplasms to high-grade, very aggressive malignancies with an elevated propensity to recurrence and metastatization. The 5-year overall survival for STSs is 57%-62% considering STSs as a whole, but the clinical course is highly influenced by the disease stage, the anatomical site and the histological subtype (Grünewald et al., 2020).

From a genetic point of view, sarcomas are distinguished into tumors with a near-diploid karyotype and simple driver alterations (e.g. fusion genes or activating mutations) and tumors with complex and unbalanced karyotypes, characterized by genomic instability and multiple aberrations. Unfortunately, the cell of origin of sarcomas is unknown in the vast majority of cases, which prevents reconstruction of the pathogenic pathways sustaining sarcoma development (Taylor et al., 2011; Schaefer et al., 2018).

Both genetic and epigenetic phenomena may concur to promote STS development and progression (Taylor et al., 2011; Nacev et al., 2020). For instance, dedifferentiated liposarcomas are typified by the amplification of chromosome 12q that results in the overexpression of MDM2 and CDK4; myxoid liposarcomas are characterized by the expression of a fusion protein involving DDIT3/CHOP; gastrointestinal stromal tumors are hallmarked by the oncogenic activation of KIT or PDGFRA. The driver alteration may impinge upon a specific pathway or have broader effects as in the case of STSs driven by genes implicated in epigenetic gene regulation. Among these, the epithelioid sarcoma.

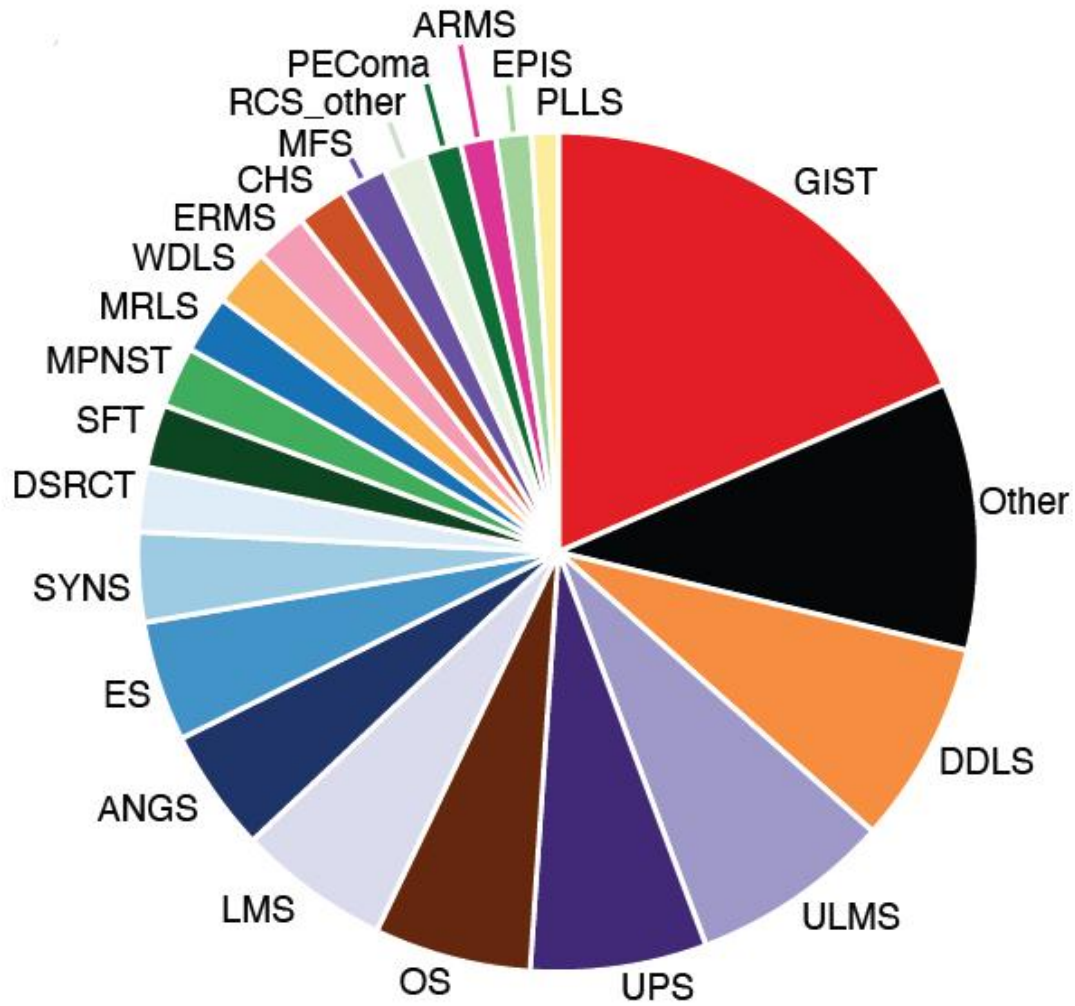


**Figure 1.1: distribution of sarcoma subtypes.** From Nacev et al., 2021 (preprint).

ARMS: alveolar rhabdomyosarcoma; ANGS: angiosarcoma; DSRCT: desmoplastic small round cell tumor; MPNST: malignant peripheral nerve sheath tumor; ULMS: uterine leiomyosarcoma; PLLS: pleomorphic liposarcoma; UPS: undifferentiated pleomorphic sarcoma; LMS: leiomyosarcoma; SYNS: synovial sarcoma; PEComa: perivascular epithelioid cell tumor; OS: osteosarcoma; EPIS: epithelioid sarcoma; SFT: solitary fibrous tumor/hemangiopericytoma; WDLS: well-differentiated liposarcoma; MRLS: myxoid/round cell liposarcoma; DDLS: dedifferentiated liposarcoma; CHS: chondrosarcoma; RCS\_other: round cell sarcoma\_other; MFS: myxofibrosarcoma; ES: Ewing sarcoma; ERMS: embryonal rhabdomyosarcoma; GIST: gastrointestinal stromal tumor.

## 1.2 EPITHELIOID SARCOMA (ES)

Epithelioid sarcoma (ES) is an aggressive and rare mesenchymal tumor first described in 1970 as a peculiar form of soft tissue sarcoma that simulates a necrotizing granuloma or a squamous cell carcinoma (Enzinger, 1970). It accounts for less than 1% of all sarcomas and it affects mostly young and middle-aged adults. The 2020 WHO classification of Tumors of Soft Tissues and Bone describes two different pathological subtypes of ES: the classic or conventional type (C-ES, also called “distal type”) and the proximal type (P-ES, also called “large-cell type”) (WHO, 2020). The first is twice as frequent as the proximal one (Fisher, 2006).

Although the distinction proximal and classic originally referred to the site of origin of the tumor (tendentially more proximal for P-ES and distal for C-ES), these terms are now used uniquely to identify the two histological variants, irrespective of tumor location as P-ES with distal location and C-ES with proximal location may be seen. The differential diagnosis between these two subtypes, which is essentially based on cell morphology, pattern of growth and presence of necrosis, is far from being clear-cut and, indeed, the omission of the distinction of an ES into either variant is not unusual in diagnoses performed in non-specialized centers (WHO, 2020).

C-ES mostly affects adolescents and young adults (20-40 years of age), twice as often in male as in female. The upper extremities of the body (hand, forearm, arm) are the most common site of origin (Spillane et al., 2000). Different from P-ES, a higher degree of heterogeneity is observed in the histological pattern of C-ES. Using a subtype-adapted grading system, Frezza and coll. stratified C-ES into “low-grade” and “high-grade” according to the number of mitoses, the evidence of necrosis and presence of nuclear atypia. This dichotomic grading system significantly correlated with clinical outcome (Frezza et al., 2020).

P-ES affects young to middle-aged adults (20–65 years of age), with a slight preponderance in males (1.6:1). It tends to develop in the axial proximal regions of the body (midline of the trunk, and proximal limbs and limb girdles) and usually develops deeper within the soft tissues compared to C-ES (Guillou et al., 1997). P-ES seems to be associated with a more aggressive clinical behavior as higher rates of recurrences and early metastases have been reported in P-ES (Guillou et al., 1997; Hasegawa et al., 2001).

The involvement of a proximal site is per se an unfavorable prognostic factor in ES. Other negative prognostic elements in ES are older age, male sex, necrosis, larger size, rhabdoid cytomorphology, vascular invasion, depth and inadequate excision (Evans & Baer, 1993; Fisher, 2006; Baratti et al., 2007).

The disease is localized at presentation in about half the cases, but it has a high tendency to give local recurrences. The reported local recurrence rate varies in different series, ranging from 15% to up to 60%. In the advanced disease lymph nodes are usually involved (an uncommon finding in STS) and distant metastases are observed in 30-50% of cases, often involving lungs, scalp, bones, brain, liver (Chase & Enzinger, 1985; Ross et al., 1997; Callister et al., 2001; Baratti et al., 2007; Wolf et al., 2008; Guzzetta et al., 2012; Levy et al., 2014; Pradhan et al., 2017; Outani et al., 2018). The five-year Overall Survival (OS) of ES is about 75% in the cases with localized disease. In detail, in C-ES with low-grade features the OS is about 95% whilst in C-ES with high grade features the OS is similar to that of P-ES, namely 50% and 57%, respectively (Frezza et al., 2020). The OS drops to about 12 months in metastatic cases (Jawad et al., 2009; Thway et al., 2016; Frezza et al., 2018).

### **1.2.1 Pathological and molecular features**

Clinically, C-ES presents as a superficial and slowly growing nodule that causes the formation of chronic nonhealing ulcers whose appearance may resemble a cutaneous squamous cell carcinoma (Lin et al., 2003). Instead, P-ES presents as a deeper mass penetrating soft tissues with evidence of hemorrhage and necrosis (Guillou et al., 1997).

C-ES shows an infiltrative growth pattern that results in an intermingling of tumor cells with surrounding stroma and normal cells. Conversely, P-ES is characterized by a well-defined, multinodular growth pattern (Hornick et al., 2009).

C-ES tumors are characterized by the presence of large polygonal and vacuolated epithelioid cells that gradually give way to plump spindle-shaped cells with eosinophilic cytoplasm, small nucleoli and nuclear atypia. Tumor cells surround a central area of degeneration and/or necrosis, resembling a granulomatous process (Fig. 1.2 A-C) (WHO, 2020). At the ultrastructural level, C-ES cells show desmosome-like intercellular junctions, surface filopodia and cell membranes interdigitated to each other, suggesting epithelial differentiation (C. Fisher, 1988; C. Fisher 1990; C. Fisher, 2006).

Conversely, P-ES tumors are characterized by large and sometimes pleomorphic cells growing in a multinodular and sheet-like pattern (carcinoma-like). In P-ES the presence of necrosis foci does not confer a pseudogranulomatous appearance as in C-ES (Guillou et al., 1997; Hasegawa et al., 2001). Cells showing rhabdoid features are common in P-ES (Guillou et al., 1997). P-ES usually features a higher number of mitosis than C-ES and the neoplastic cells are characterized by the presence of

large nuclei and prominent nucleoli (Fig. 1.2 D-F) (Y. Li et al., 2019). Rare cases of ES showing a hybrid proximal/classic phenotype have been reported (WHO, 2020).

From a cytogenetic standpoint, ES are characterized by a complex karyotype with recurrent deletions at 22q11 (Molenaar et al., 1989; Cordoba et al., 1994; Iwasaki et al., 1996; Sonobe et al., 1997; Dal Cin et al., 1999; Debiec-Rychter et al., 2000).

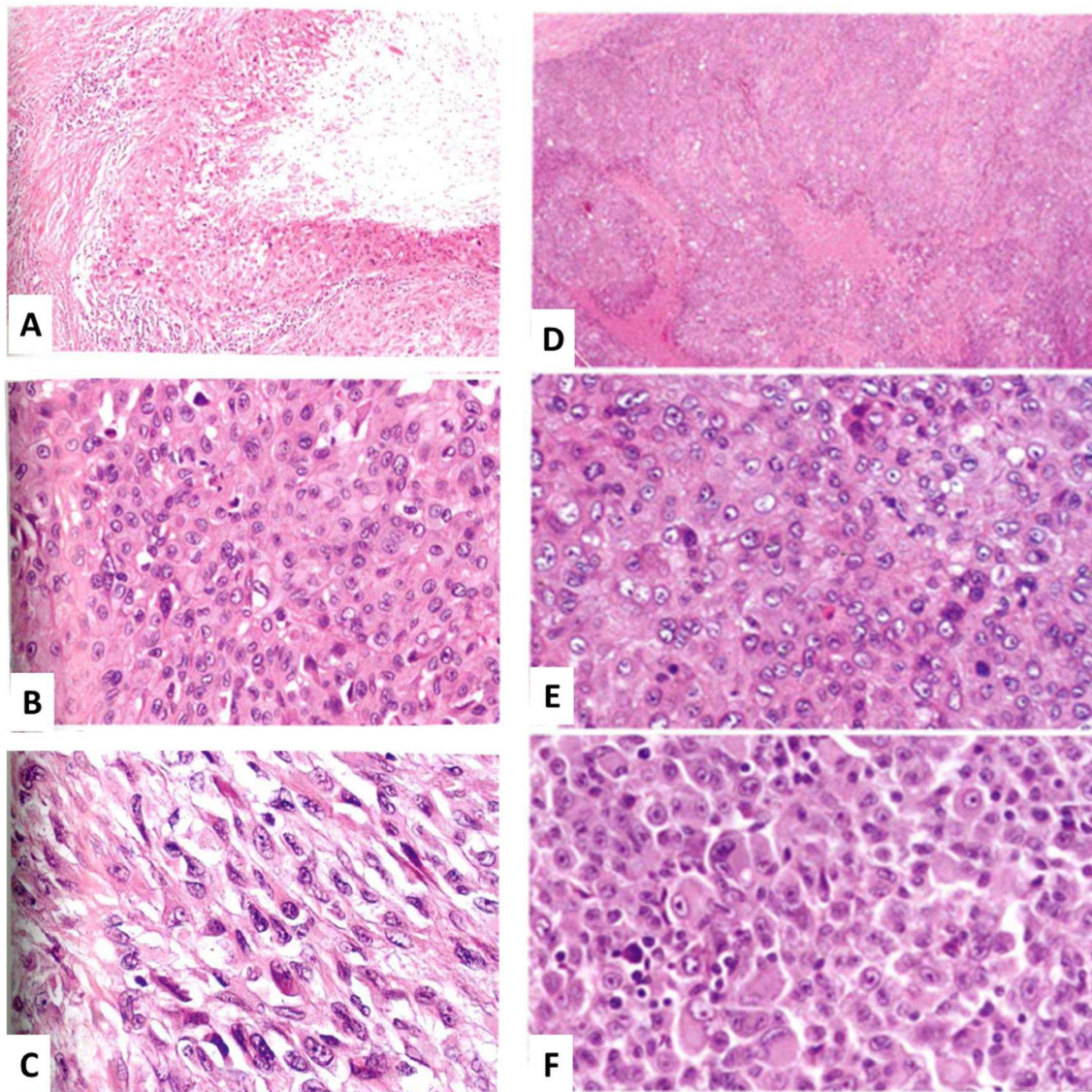


**Figure 1.2: morphology of ES.** Panels A-B-C refer to C-ES, panels D-E-F refer to P-ES.  
A) C-ES cells surrounding a central area of necrosis (pseudogranulomatous growth pattern) in a nodular lesion centred in the dermis. B) ES cells with eosinophilic cytoplasm. C) Plump spindle-shaped cells.  
D) P-ES cells showing a multinodular growth pattern with foci of tumor necrosis. E) Pleomorphic ES cells with deeply eosinophilic cytoplasm and enlarged vesicular nuclei with prominent nucleoli. F) Clusters of rhabdoid cells characterized by intracytoplasmic hyaline inclusions that push the nucleus eccentrically. From WHO, 2020.



From an immunohistochemical standpoint, ES tumors are positive for the expression of the epithelial membrane antigen (EMA) and cytokeratins, namely CK8 and CK19, whereas they are usually negative for CK5/6. Mesenchymal markers, like vimentin, may also be co-expressed (Miettinen et al., 1999; Laskin & Miettinen, 2003). ES tumors are typically negative for S-100, neurofilament protein, factor VIII-related antigen and CD31. Positivity for CD34 is detected in over 50% of the cases, which is helpful in differential diagnosis with carcinomas (Guillou et al., 1997; Miettinen et al., 1999; Fisher, 2006). ERG positivity is detected in 40-67% of cases, mainly in C-ES. Immunoreactivity for ERG may be a source of misclassification with endothelial tumors (Miettinen et al., 2013; Stockman et al., 2014; Kohashi et al., 2015).

Most importantly, ES tumors are characterized by the loss of expression of the SMARCB1 protein (a.k.a. INI1, SNF5 or BAF47) (Fig. 1.3), which represents an essential ES diagnostic marker according to WHO (WHO, 2020). SMARCB1 encodes the protein named SWI/SNF-related matrix-associated actin-dependent regulator of chromatin subfamily B member 1, a core subunit of the mammalian SWItch/Sucrose Non-Fermentable (SWI/SNF) ATP-dependent chromatin remodeling complexes. These chromatin modifiers are ubiquitously expressed in normal cells, where they induce remodeling of the chromatin through nucleosome sliding and eviction. The activity of SWI/SNF complexes is opposed to that of the Polycomb Repressive Complexes 2 (PRC2). In fact EZH2, the catalytic subunit of PRC2, induces the trimethylation of Lysine 27 of histone 3 (H3K27me3) at the promoters of target genes, causing their silencing (Wilson et al., 2010). Through their regulatory activity, the SWI/SNF complexes take part in different biological processes, including cell cycle regulation and maintenance of genomic stability (Medjkane et al., 2004; Vries, 2005; Wang et al., 2014).

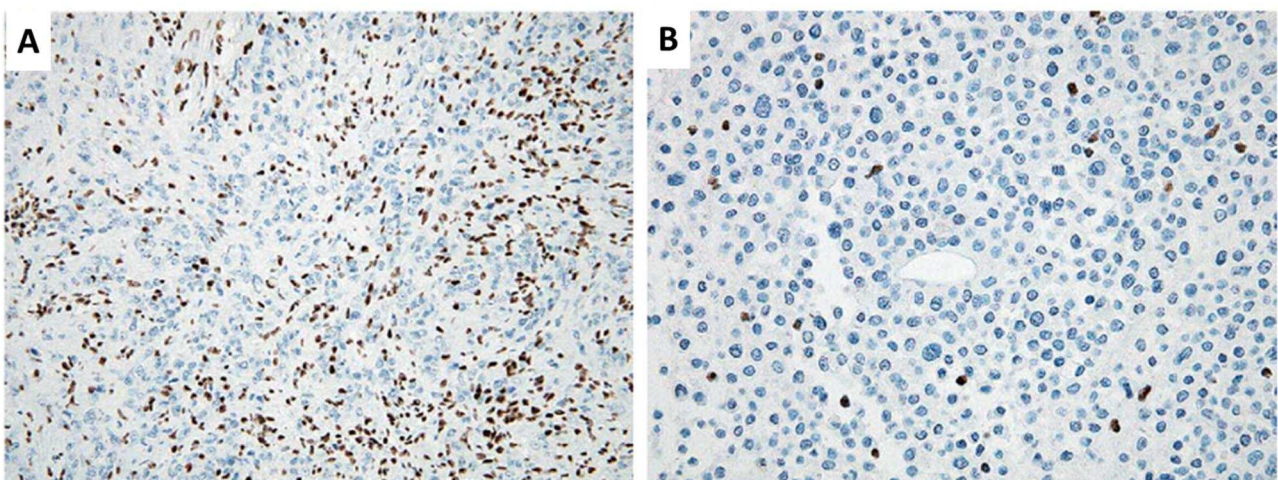


**Figure 1.3: immunostaining for SMARCB1.** A) C-ES and B) P- ES are typified by the loss of INI1/SMARCB1 expression. Positive cells represent intervening stromal lymphocytes. From Hornick et al., 2009.



In a large fraction of cases (up to 90%) the loss of SMARCB1 expression is associated with the deletion of chromosome 22q11 where the SMARCB1 locus is located (Sullivan et al., 2013; Le Loarer et al., 2014).

Epigenetic mechanisms have been also implicated in the loss of SMARCB1 protein expression, particularly in the fraction of cases devoid of SMARCB1 gene deletions. For instance, miR-206, miR-381 and miR-671-5p have been proposed as a possible mechanism of SMARCB1 protein silencing in a fraction of ES (Papp et al., 2014; Sápi et al., 2016).

## **1.2.2 Deregulated pathways in ES**

Given the broad-spectrum role played by chromatin remodeling complexes, the loss of one component is reasonable to result in a perturbation of gene expression as a consequence of genome-wide repositioning of nucleosomes at the chromatin level, with possible impact on oncogenic signaling (Reisman et al., 2009). Nevertheless, the pathways directly affected by SAMRCB1 loss in ES are still to be clarified.

Cascio and colleagues observed high EGFR protein expression levels in 14 of 15 (93%) ES analysed in the absence of evident EGFR gene alterations (Cascio et al., 2010). This finding was confirmed by Xie and colleagues who also provided evidence of expression of the active phosphorylated form of EGFR (pEGFR) in both tumor samples and ES cell lines (VA-ES-BJ and Epi544). Treatment of ES cell lines with EGFR inhibitors caused a reduction in cell proliferation, migration and invasion and increased apoptotic rates. Interestingly, the two cell models were sensitive to mTOR inhibition and the combination of mTOR and EGFR blockade led to a synergistic effect (Xie et al., 2011).

Brenca et al. demonstrated that the ES cell line VA-ES-BJ expresses phosphorylated EGFR and MET, which resulted in AKT and ERK signalling activation. The combination of MET and EGFR blockade resulted in a synergistic effect over cell survival compared to the single agents. Furthermore, the authors demonstrated that the restoration of SMARCB1 expression significantly affected VA-ES-BJ cell proliferation, anchorage-independent growth, and cell migration properties, supporting the tumor suppressor role of this gene and its relevance in ES pathogenesis (Brenca et al., 2013).

Imura et al. besides confirming the dependency of ES cell lines on mTOR pathway, in agreement with Xie's group, demonstrated that the combined targeting of mTOR and c-MET resulted in a major antitumor effect both in vitro and in vivo (Imura et al., 2014).

Loss of E-cadherin and reduced expression of  $\beta$ -catenin have also been reported (Izumi et al., 2006; Sakharpe et al., 2011) but no  $\beta$ -catenin gene mutation was detected (Saito et al., 2001; Sakharpe et al., 2011). Izumi and colleagues suggested a role for dysadherin in E-cadherin downregulation. Dysadherin is a cell membrane glycoprotein that reduces E-cadherin protein expression by functioning as an “anti-adhesion” molecule and favor metastazation (Ino et al., 2002). The authors demonstrated that dysadherin was over-expressed in ES, particularly in P-ES (71% vs. 36%), which correlated with a reduced survival (Izumi et al., 2006).

A pathway that is definitively altered in ES is cell cycle. Jamshidi et al. (Jamshidi et al., 2016) showed that about 37% of ES carries homozygous/heterozygous deletions of CDKN2A which encodes p14/ARF and p16/INK4A, two well known inhibitors of p53 and RB pathways, respectively (Sherr & Roberts, 1995; Stott et al., 1998).

In addition, MYC has been reported to be amplified in ES (Lualdi et al., 2004). Interestingly, MYC activity could be potentiated in ES as a result of SMARCB1 loss. In fact, SMARCB1 was demonstrated to hinder MYC-mediated transcriptional regulation by inhibiting its binding to DNA (Weissmiller et al., 2019).

### **1.2.3 Therapy**

Currently, the treatment of choice for ES patients with localized disease is wide surgical resection. Since ES tumors tend to relapse and metastasize, even after several years since diagnosis, neo-adjuvant or adjuvant treatments (radiotherapy and/or chemotherapy) are often administered, primarily to improve local control rate (Levy et al., 2014; Pradhan et al., 2017).

Patients with advanced ES receive systemic chemotherapy based on anthracycline (A) or anthracycline plus ifosfamide (A/I), obtaining satisfactory palliation, even if its effectiveness is limited in time (Jones et al., 2012).

A study provided evidence of promising activity of the combination of gemcitabine and docetaxel (Pink et al., 2014) and another study indicated that gemcitabine-based regimens may have higher efficacy in C-ES compared to P-ES (RR 30% vs. 22%). Instead, anthracycline-based regimens were more effective in P-ES (RR 26% vs. 19%) (Frezza et al., 2018). Pazopanib had limited efficacy in ES (Frezza et al., 2018).

Overall, the currently employed therapeutic strategies in ES remain unsatisfactory.

Recent studies focused on EZH2 as a possible therapeutic vulnerability in ES. The rationale was that in the absence of antagonism by the SWI/SNF complexes, PRC2 activity could be enhanced and hence represent an ES dependency.

After a phase 1/2 clinical trial (NCT01897571) that reported a favorable safety profile and promising activity in different neoplasms of the EZH2 inhibitor Tazemetostat (Italiano, 2018), a phase 2 trial (NCT02601950) specifically dedicated to SMARCB1-negative tumours (ES and rhabdoid tumors) or relapsed/refractory synovial sarcoma was conducted. Of the ES cohort (62 patients), at 32 weeks of treatment 9 patients (15%) showed durable objective response and 13 (21%) remained progression-free at 1 year. Median progression-free survival was 5.5 months and median overall survival 19.0 months (Gounder et al., 2020).

Based on this data, in January 2020, Tazemetostat received the approval by the Food and Drug Administration (FDA) for the treatment of adults and adolescents older than 16 years old with locally advanced or metastatic ES not eligible to complete surgical resection (Hoy, 2020).

Despite the encouraging results, there is still a proportion of ES that fails to respond to these treatments. A further clinical trial (NCT04204941) is now evaluating the combination of Tazemetostat and Doxorubicin in advanced ES. Ongoing trials are evaluating the role of immunotherapy, immune checkpoint inhibitors in particular, in ES treatment (NCT03190174; NCT03069378).

### 1.3 EPIGENETICS AND SARCOMAS

Growing evidence indicates that alterations in the epigenetic control of gene expression play an important role in sarcoma pathogenesis (Nacev et al., 2020).

The term “epigenetics” literally means over and above (*epi*) the genome, it was coined by Conrad Waddington in 1942 to describe inherited phenotypic changes without genotypic changes (Ch Waddington, 1959; Waddington, 2012). Indeed, with this term we can define changes that, without altering the DNA sequence, impact the transcriptional programmes of genes expression leading to a phenotypic perturbation. Epigenetic mechanisms act at various levels and on various layers, including DNA methylation, histone modification, chromatin remodeling and microRNAs and other noncoding RNAs (Soini, 2016). These mechanisms are physiologically required for the control of gene expression, including those involved in proliferation and developmental processes (Barber & Rastegar, 2010). A deregulation of epigenetic mechanisms may perturb the transcriptional programmes, running in healthy cells, leading to the development of diseases,

including cancer. Recent studies highlight the presence of recurrent somatic mutations in chromatin modifiers in different type of cancers (Forbes et al., 2011; Stratton et al., 2009) and the existence of an aberrant state of epigenetic marks in malignant cells compared to normal ones (Berman et al., 2011). The alterations observed in the cancer epigenome may be due to both non-genetic perturbations and genetic mutations in chromatin modifiers (Nebbio et al., 2018).

The first layer of epigenetic control concerns the state of DNA methylation, which is a natural covalent modification of DNA that, in eukaryotic cells, occurs on the cytosine nucleotide in a CpG dinucleotide and it is catalyzed by the DNA methyltransferase family (DNMT1, DNMT3A, DNMT3B). Alterations in the DNA methylation status were observed in various cancer genomes (Baylin & Jones, 2011), including STSs, where they play a crucial role in the biology and prognosis (Abeshouse et al., 2017). A second layer of epigenetic control of gene expression is associated with modifications of histone proteins, whose genes may be mutated in cancer and that leads to the production of “oncohistones”, which act as oncogenic drivers, like it was observed in paediatric gliomas (Schwartzentruber et al., 2012; Wu et al., 2012). The third layer of epigenetic control is mediated by the enzymatic complexes that “write”, “read” or “erase” the post-translational modifications of histone proteins and they may be mutated in some cancers, as malignant peripheral nerve sheath tumours (W. Lee et al., 2014). The fourth layer of epigenetic regulation involves the chromatin remodeling complexes that mediate the repositioning or the ejection of nucleosomes, but their functions may be altered in cancer, due to a disruption of the complexes themselves, as occurs in synovial sarcoma, malignant rhabdoid tumour and epithelioid sarcoma (Nacev et al., 2020). Finally, the fifth layer of epigenetic control concerns the three-dimensional organization of chromatin, such as chromatin loops and phase separation, that mediate the formation of enhancer regions and their associations with distant genes. Common fusion partners in sarcomas driven by translocations, such as FUS and EWSR1, seem to be involved in these processes (Sawyer et al., 2019; Nacev et al., 2020). A schematic representation of the five layers of epigenetic regulation is given in Fig. 1.4.

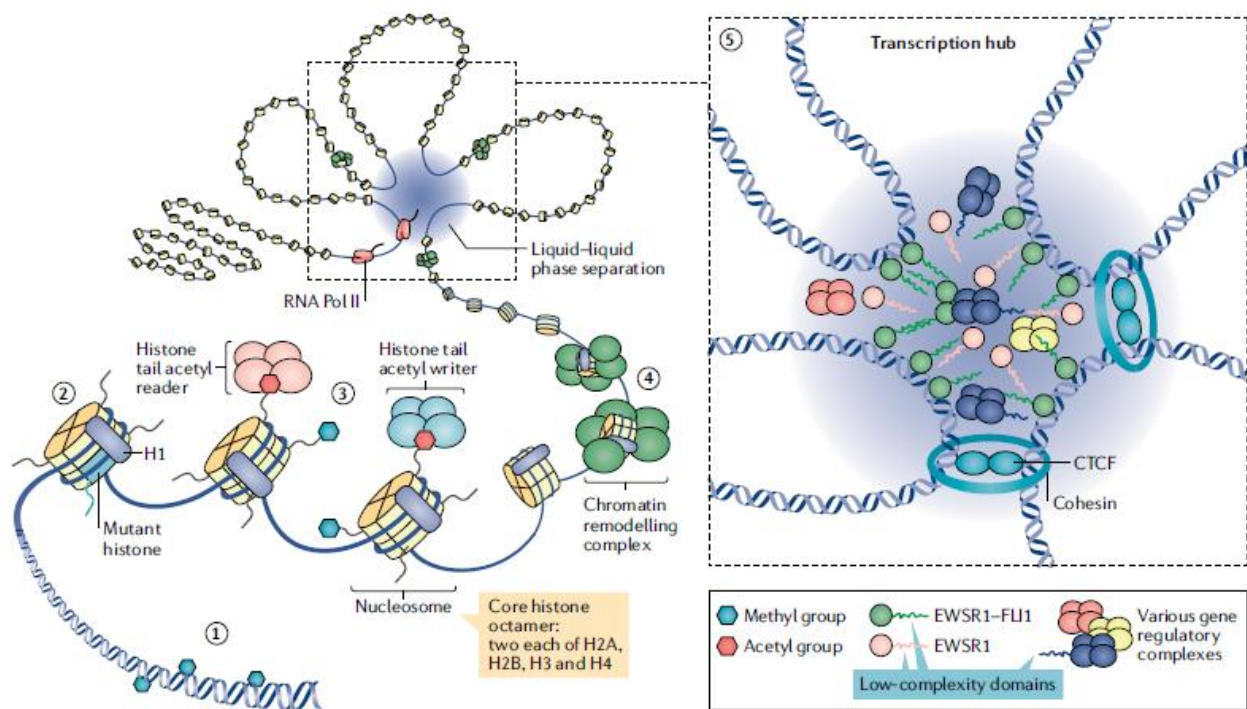


**Figure 1.4: the five layers of epigenetic regulation resulting altered in sarcomas.** 1) The first layer of epigenetic control concerns the state of DNA methylation. 2) The second layer of epigenetic regulation is mediated by histone modifications, but mutations in genes encoding histones may cause the expression of “oncohistones”, that act as oncogenic drivers in sarcomas. 3) The third layer of epigenetic control is based on enzymatic complexes that “write”, “read”, “erase” histone modifications and their loss is observed in some types of sarcomas. 4) The fourth layer of epigenomics is represented by chromatin remodeling complexes, that regulate nucleosome positioning/ejection and result altered in some types of sarcomas. 5) The fifth layer of epigenetic regulation concerns the three-dimensional organization of chromatin, such as chromatin loops and phase separation, that determines the interaction between enhancer elements and spatially distant genes. The generation of novel enhancers through phase separation was described as one of the oncogenic drivers in Ewing sarcoma. CTCF: CCCTC binding factor; EWSR1: Ewing sarcoma breakpoint region 1; FLI1: friend leukaemia virus integration 1; RNA Pol II: RNA polymerase II. From Nacev et al., 2020.

Besides acting at the level of DNA organization/transcription, epigenesis is implicated also in the post-transcriptional control of gene expression. In this context, key epigenetic regulators are microRNAs (miRNAs). miRNAs-mediated regulation of gene expression has been demonstrated to affect a wide range of biological processes including cell cycle regulation, cell growth and differentiation, stress reactions and apoptosis (Iorio et al., 2010; Q. W. Chen et al., 2014; Smolle et al., 2017).

Chromatin remodeling complexes, histone modifiers, and miRNAs will be better detailed below.

### 1.3.1 Chromatin remodeling complexes

In cells, chromatin is wrapped around histone octamers in structures called nucleosomes, whose positioning controls the accessibility of the DNA for replication, transcription, and repair.

Chromatin remodeling complexes are responsible for the repositioning of nucleosomes and the energy required for this process is obtained from ATP hydrolysis. Indeed, all chromatin remodeling complexes have a catalytic subunit belonging to the superfamily 2 helicases, which classifies them into four groups: (1) the SWItch/Sucrose Non-Fermentable (SWI/SNF) family, (2) the Imitation SWItch (ISWI), (3) the Chromodomain Helicase DNA-binding (CHD)/Nucleosome Remodeling Deacetylase (NuRD) and (4) the INOsitol requiring (INO80/SWR1).

1) The SWI/SNF family, also known as BRG1/BRM-associated factor (BAF) complexes, is a central regulator of nucleosome remodelling by promoting sliding or ejection of nucleosomes (Kwon et al., 1994). Mammalian SWI/SNF complexes are classified into three subgroups: canonical BAF (cBAF), polybromo-associated BAF (PBAF), and non-canonical BAF (ncBAF), also called GLTSCR1 or GLTSCR1L-containing and BRD9-containing (GBAF) complex (Fig. 1.5) (Raab et al., 2015; Alpsy & Dykhuizen, 2018). Some subunits (e.g. SMARCC1, SMARCC2, SMARCD1) and ATPases (SMARCA4 or SMARCA2) are shared between all three subfamilies, whereas other subunits are specific for each subgroup.

The cBAF complex is composed by 12 subunits and is characterized by the incorporation of the tandem PHD domain-containing DPF2 subunit and either one AT-rich interaction domain (ARID) containing proteins, ARID1A or ARID1B. The PBAF complex contains a different ARID subunit, ARID2, and uniquely incorporates the PHD-containing subunit PHF10 and the bromodomain-containing subunits PBRM1 and BRD7. Finally, the more recently identified subfamily is the ncBAF complex that is characterized by the incorporation of GLTSCR1/GLTSCR1L and BRD9 subunits in place of ARID and tandem-PHD PHF/DPF subunit. Different from cBAF and PBAF that incorporate SMARCB1, ncBAF is the sole complex that constitutively does not include it (Michel et al., 2018; Centore et al., 2020).

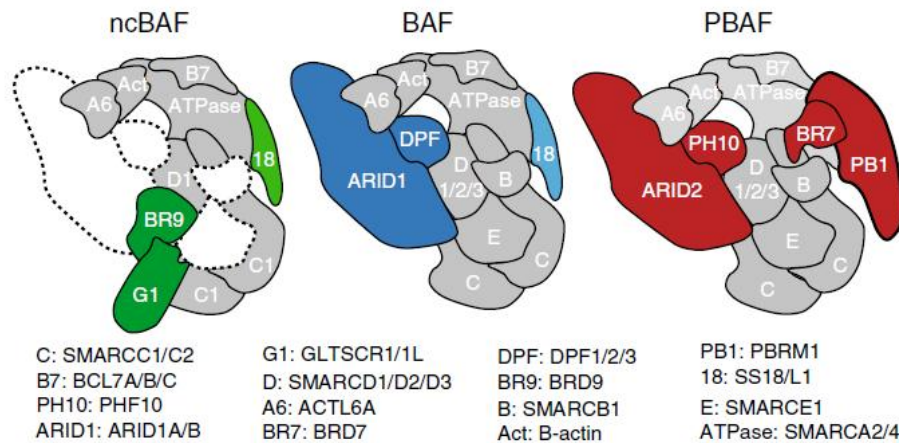


**Figure 1.5: Schematic subunit compositions of mammalian ncBAF, cBAF and PBAF complexes.** From Michel et al., 2018.

SWI/SNF complexes are evolutionarily conserved and involved in the control of cell differentiation and lineage specification. SWI/SNF complexes generally induce activation of gene expression as a result of disruption of DNA/nucleosome contacts, nucleosome sliding, ejection or exchange (Kadoch et al., 2016). However, in some instances they may promote the positioning of nucleosomes to generate a repressive chromatin state or the binding of repressive transcription factors (Rafati et al., 2011). Beyond the regulation of transcription, the SWI/SNF complexes are also involved in DNA damage repair, in which the accessibility to DNA represents an essential element (Park et al., 2006; Kakarougkas et al., 2014; Hodges et al., 2016; Y. Chen et al., 2019).

Among the different chromatin remodelers, the components of the SWI/SNF complexes are those more frequently altered in cancer (about 20% of all cancers) (Kadoch et al., 2013). In particular, loss of SMARCB1 has been reported in ES but also in Malignant Rhabdoid Tumour (MRT), Atypical Teratoid/Rhabdoid Tumours (AT/RT) of the Central Nervous System, Malignant Peripheral Nerve Sheath Tumors (MPNST), chordoma, myoepithelial neoplasms and other tumors (Hollmann & Hornick, 2011; Agaimy, 2014; Margol & Judkins, 2014).

- 2) The ISWI family is composed by 7 main complexes: ACF, CHRAC, WICH, NoRC, CERF, NURF and RSF. Their catalytic subunit is either SMARCA5 (SNF2H) or SMARCA1 (SNF2L), homologs of the *Drosophila* ISWI. These complexes regulate nucleosome assembly, spacing and editing, and are also involved in DNA repair (Tsukiyama et al., 1995). These complexes are very small with only 2-4 subunits. Close homologous of the ISWI family are SMARCAD1 and SMARCA6/HELLS, whose functions are still poorly defined (Neve et al., 2021). The ACF complex is involved in regulating nucleosome spacing and double-strand break repair (Racki et

al., 2009; Klement et al., 2014). The CHRAC complex takes part in chromatin assembly, during which it converts irregular chromatin into chromatin with regularly spaced nucleosomes interacting with the tail of histone H4 (Clapier et al., 2001). The WICH complex is required to remodel chromatin at the sites of transcriptionally active rRNA genes allowing the recruitment of histone acetyltransferases (Dirscherl & Krebs, 2011; Vintermist et al., 2011). The NoRC (Nucleolar remodeling complex) complex favors the transcriptional repression of ribosomal genes and controls nucleosome spacing by interacting with the histone H4 (Strohner et al., 2001). The NURF complex mediates the activation of the transcriptional process by increasing the amount of available DNA after the sliding of histone octamers (Hamiche et al., 2001; H. Li et al., 2006). The CERF complex, together with NURF, is involved in the regulation of neural development (Lazzaro & Picketts, 2001). The CERF complex also plays a central role in the detection and response to DNA damage (Lee et al., 2012).

- 3) The CHD subunits, initially classified as mammalian DNA-binding proteins characterized by a SWI-like helicase domain, are involved in the recruitment of histone demethylase/deacetylase enzymes and in DNA repair (Mills, 2017). CHD1 and CHD2 were shown to participate to DNA repair by interacting with other factors, such as SSRP1 or PARP1 complex (Kelley et al., 1999; Luijsterburg et al., 2016). CHD3, CHD4 or CHD5 are the helicases of the NuRD complex and mediate the interaction with different proteins. Among these, CDK2AP1, SALL1/4, ZMYND8, which can targets the NuRD complex to specific regions, and such as GATAD2A/B, which can favor the recruitment of certain sub-complexes (Leighton & Williams, 2020). Finally, CHD6, CHD7 and CHD8 were observed to bind to the DNA sequences between nucleosomes and then slide them further apart showing distinct binding and remodeling activities (Manning & Yusufzai, 2017). CHD7 and CHD9 can also interact with members of the SWI/SNF family (Bajpai et al., 2010). CHD8 binds different methyltransferase complexes as well as  $\beta$ -catenin and is therefore involved in the regulation of Wnt/ $\beta$ -catenin-dependent gene expression (Nishiyama et al., 2012; Neve et al., 2021).
- 4) The INO80/SWR1 family is composed by three main complexes, each of which contains a specific ATPase subunit (INO80, SRCAP or p400) and two ATP-dependent helicases RUVBL1 and RUVBL2. They are involved in the substitution of canonical histones with alternative histones in a replication-independent manner. These variants generally cause nucleosome instability and are associated with transcriptional activation (Jin et al., 2009). The INO80 complex intervenes in the generation of regularly spaced arrays between nucleosomes,



modulating gene expression in either way, activation or repression (Morrison & Shen, 2009; Gerhold & Gasser, 2014). SRCAP complex can act as a coactivator for many transcription factors (Ruhl et al., 2006). Finally, p400-containing complexes are typically associated with the acetyltransferase TIP60, playing a role in the detection of DNA damaged sites and then in the opening of the chromatin to facilitate the access of the DNA repair machinery (Kusch et al., 2004).

### **1.3.2 Histone modifiers**

Histones are basic proteins that are required for the compaction of genomic DNA in the form of nucleosomes. The nucleosome core is a histone octamer, composed by two copies of H2A, H2B, H3 and H4, around which DNA winds for 146-nucleotide length. Histone H1 acts as a linker between adjacent octamers. Histone proteins are characterized by protruding N-terminal tails, which can be post-translationally modified by methylation, but also by acetylation, citrullination, ubiquitination, sumoylation, ADP-ribosylation and phosphorylation (Allfrey et al., 1964; Rothbart & Strahl, 2014). These modifications represent the so-called “histone code” that, combined with the activity of different chromatin remodelers, modulates the level of accessibility to DNA by the transcription machinery, controls chromatin state and hence gene expression (Strahl & Allis, 2000; Turner, 2000).

Histone methylation occurs mainly on two histone residues, lysine (K) and arginine (R). Histone methylation at lysine residues is mediated by lysine methyltransferases (KMTs), while methylation at arginine residues is catalyzed by protein arginine N-methyltransferases (PRMTs). Methyl groups can be removed by histone demethylases. Each residue is modified by a specific set of enzymes (Fig. 1.6).

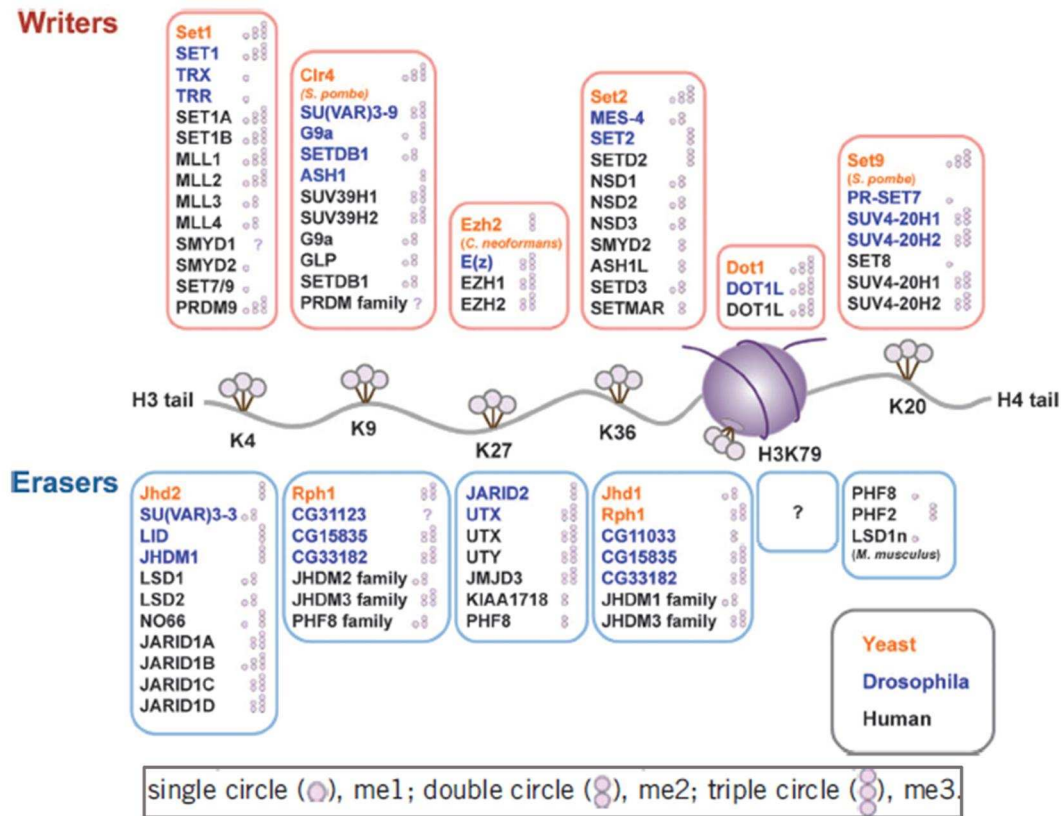


**Figure 1.6: Schematic representation of nucleosome showing main lysine methylation sites on H3 and H4.** Writers (methyltransferases) and erasers (demethylases) are reported in association with their methylation state specificities. From Hyun et al., 2017.

The residue of methylated lysine and the level of methylation (mono-, di-, and tri-methylation) determine the final effect on gene expression. For instance, methylation of K4, K36 or K79 of histone H3 are generally associated with gene activation; conversely H4K20, H3K9 and H3K27 methylation events are linked to gene silencing (Alam et al., 2015). One of the most studied H3K27 methyltransferase is EZH2, which belongs to the PRC2 (Polycomb Repressive Complex 2) complex. The mammalian PRC2 complex contains four core subunits, EZH1/2, SUZ12, EED and RbAp46/48. It can also interact with other accessory proteins, like AEBP2, JARID2 and PCLs (Polycomb-like proteins), which are involved in the regulation of its activity (Kuzmichev et al., 2002; Margueron & Reinberg, 2011; Alekseyenko et al., 2014). PRC2 complexes, by inducing H3K27 methylation, increase the compaction of the chromatin thus mediating transcriptional repression (Margueron & Reinberg, 2011; Kadoch et al., 2017; Schuettengruber et al., 2017). This activity opposes that of SWI/SNF complexes, which are mainly associated with transcriptional activation. The precise balance between these two classes of complexes is fundamental for the maintenance of normal cell homeostasis and members of both SWI/SNF and PRC2 complexes are

often implicated in human diseases, including cancer. For instance, loss of function gene alterations in SUZ12 and EED subunits are reported to occur in MPNST, causing a reduction in the PRC2-dependent H3K27 trimethylation that leads to increase in gene expression (W. Lee et al., 2014).

In Ewing tumors, the typical EWSR1-FLI1 oncogenic fusion protein has been shown to induce EZH2 expression (Riggi et al., 2008; Burdach et al., 2009; Richter et al., 2009).

Moreover, endometrial stromal sarcomas (ESS) may carry a JAZF1-SUZ12 gene fusion that affects PRC2 activity or a EZHIP-MBTD1 fusion that interacts with EZH2 and reduces its methyltransferase activity (Koontz et al., 2001; Piunti et al., 2019).

PRC2 activity may be enhanced in tumors also as a consequence of loss or malfunction of antagonizing complexes. For instance, in SMARCB1-deficient tumors such as MRT, neural and kidney development-associated genes are repressed as a consequence of an increased of PRC2-mediated H3 methylation. The reintroduction of SMARCB1 leads to a displacement of PRC2 complexes at the promoter of these genes, restoring their expression (Nakayama et al., 2017). In synovial sarcoma, the expression of the pathognomonic SS18-SSX fusion protein causes the eviction of SMARCB1 from the SWI/SNF complexes that, as a consequence, gain a different specificity being aberrantly re-targeted to other sites, namely polycomb-target site (Kadoch & Crabtree, 2013).

### **1.3.3 MicroRNAs**

MicroRNAs (miRNAs) belong to the class of small noncoding RNAs that are expressed in different species. Their best characterized function is the negative control of gene expression. This is achieved by the binding of the so-called “seed” region of the miRNA (6-8 bp) at the 5’ end of the miRNA to a complementary sequence, commonly in the 3’ UTR, of target messenger RNA (mRNA) (Bartel, 2009). Some miRNAs seem to be capable of activating gene expression under certain conditions (Vasudevan, 2012).

Initially discovered in *Caenorhabditis elegans* in 1993 (R. C. Lee et al., 1993), the first human miRNA, let-7, was identified in 2000’s (Roush & Slack, 2008). Currently the human genome contains 1917 annotated hairpin precursors, and 2654 mature sequences, as reported in the latest release of the miRbase database (v22, 2019) (Kozomara et al., 2019).

miRNAs can be transcribed from intronic or intergenic regions as single hairpin or clusters of multiple precursors. Most miRNAs are transcribed by RNA Polymerase II as large primary miRNAs (pri-miRNAs) containing one or more stem-loop structures. All canonical pri-miRNAs

present a 5'-cap, whereas the polyadenylation signal in the 3' end can be missing. The pri-miRNAs are initially cleaved in the nucleus with the release of hairpin-shaped precursors of about 70 nucleotides, called pre-miRNAs. This process is mediated by a Microprocessor complex, composed by DROSHA and DGCR8 (Fig. 1.7). After that, pre-miRNAs are exported from the nucleus to the cytoplasm by XPO5 and cleaved by a multiprotein complex including the RNase Dicer, AGO2, and TRBP to form a mature single strand miRNA. Mature miRNAs are finally incorporated into the ribonucleoprotein RISC complex and delivered to the target complementary mRNA molecule (Fig. 1.7). The generation of a double stranded miRNA/mRNA complex determines the degradation of the target mRNA or, in the case of imperfect complementarity, it impairs mRNA translation (Fig. 1.7) (Krol et al., 2010; Ha & Kim, 2014; Akgül & Erdoğan, 2018).

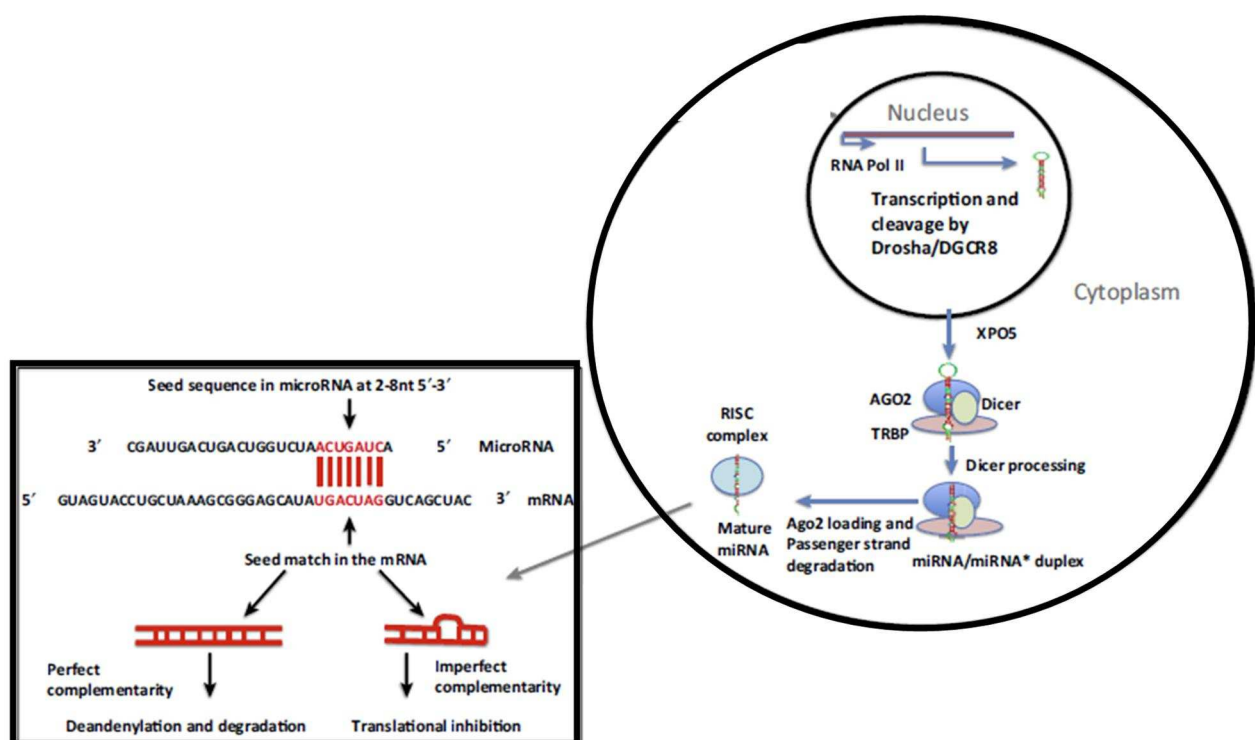


**Figure 1.7: Biogenesis and function of microRNAs.** miRNAs are transcribed by RNA Polymerase II in pri-miRNAs, that are cleaved in the nucleus by a complex involving Drosha and DGCR8 (DGCR8 microprocessor complex subunit), given the pre-miRNAs. After that, pre-miRNAs are exported by XPO5 into the cytoplasm, where are cleaved by a multiprotein complex including the RNase Dicer, AGO2 (Argonaute 2), and TRBP (trans-activation-responsive RNA-binding protein) to form the mature form of miRNAs. These mature forms are incorporated into the RISC complex (RNA-induced silencing complex) and targeted to the 3'-UTR regions of an mRNA molecule: miRNAs with perfect complementarity cause the degradation of the mRNA transcript, whereas miRNAs with imperfect complementarity inhibit translation. Adapted from Hayes et al., 2014.

The number of protein-coding genes controlled by miRNAs, estimated to be about 1/3 of the whole proteome in 2004 (Bartel, 2004), it is continuously increasing. Both physiological and pathological processes appear to be regulated by miRNAs (Friedman et al., 2009). Indeed, miRNAs are

implicated in complex molecular networks, where each mRNA may be targeted by different miRNAs and, at the same time, each miRNA may interact with several transcripts (Fig. 1.8-B, C). Furthermore, different transcription factors (TFs) may control the expression of single miRNA or clusters of miRNAs (Fig. 1.8-D) (Hayes et al., 2014).

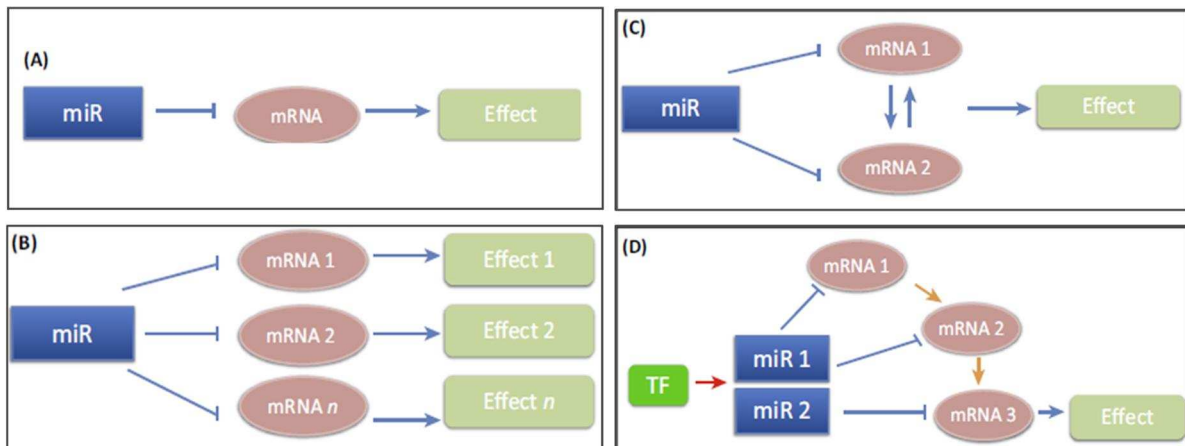


**Figure 1.8: miRNA networks.** A) The basic approach: single miRNA–mRNA interaction, B) The broad approach: one miRNA to many mRNAs, C) The functional approach: one miRNA to many mRNAs, that are also functionally related, D) The pathway-based approach: TFs regulate one or more miRNAs controlling their role at key points in defined pathways. Adapted from Hayes et al., 2014.

Numerous miRNAs are deregulated in human malignancies and may contribute to the different phases of cancer progression (Di Leva et al., 2014). Conventionally, miRNAs are classified as "oncomiRs" or "oncosuppressor miRs", depending on whether they have pro-tumorigenic or anti-tumorigenic activity.

For instance, the oncogenic miR-183 was demonstrated to be overexpressed in rhabdomyosarcomas and synovial sarcomas, leading to the repression of the tumor suppressors EGR1 and PTEN (Sarver et al., 2010). In synovial sarcoma miR-17 is transcriptionally induced by the SS18-SSX oncoprotein and mediates the silencing of the cyclin-dependent kinase inhibitor p21 (CDKN1A) (Minami et al., 2014). In well-differentiated and dedifferentiated liposarcomas, the tumor suppressor miR-143 is significantly down-regulated compared to normal adipose (Ugras et al., 2011).

It must be said that, given the complexity of miRNA/mRNA networks, the oncogenic or tumor suppressive role of a miRNA may not be an intrinsic property of the individual miRNA, but rather a cell context-dependent effect.

## **2. AIM**

The main aim of this work was to shed light on the biology of ES and in particular to gain insights into the molecular features that differentiate the two ES variants, P-ES and C-ES, characterized by a different clinical behavior.

Exploiting the RNA and the microRNA profiling of ES surgical samples, we aimed to identify deregulated genes, miRNAs, and related pathways, that could account for the distinctive clinical and pathological features of the two ES variants. We anticipate that a better knowledge of the molecular characteristic of ES variants may disclose novel diagnostic/prognostic biomarkers and new possible therapeutic vulnerabilities.

# **3. RESULTS**



### 3.1 Transcriptome analysis: whole cohort

A cohort of 22 treatment-naïve ES, 9 P-ES and 13 C-ES, was investigated by RNA-Sequencing analysis (Table 3.1). All tumors included in this analysis were evaluated by the pathologist as having a high tumor cellularity (>60%).

Code	Subtype	Grade	Sex	PT-tumor cellularity >70%
ES25	Proximal	<i>High</i>	F	Y
ES27	Proximal	<i>High</i>	F	Y
ES32	Proximal	<i>High</i>	F	Y
ES62	Proximal	<i>High</i>	F	Y
ES63	Proximal	<i>High</i>	M	Y
ES64	Proximal	<i>High</i>	F	Y
ES66	Proximal	<i>High</i>	F	Y
ES68	Proximal	<i>High</i>	F	Y
ES22	Classic	High	M	N
ES38	Classic	High	M	N
ES40B	Classic	High	F	Y
ES52	Classic (revised)	High	F	Y
ES57	Classic	High	M	Y
ES60	Classic	High	M	Y
ES65	Classic	High	M	Y
ES67	Classic	High	M	Y
ES15	Classic	Low	M	N
ES39	Classic	Low	M	Y
ES41	Classic	Low	M	N
ES55	Classic	Low	F	N
ES59	Classic	Low	M	N
ES61	Classic	Low	M	N

**Table 3.1: the cohort of 22 treatment-naïve ES.**

PT-tumor cellularity: Post-Transcriptome evaluated-tumor cellularity. Y, ≥70%; N <70%

Principal Component Analysis (PCA) (Fig. 3.1) showed a clear separation between P-ES and C-ES along the Principal Component 1 (PC1) axis, except for one P-ES (ES52) that clustered with classic group. This discrepancy led to a histological revision of the sample that resulted in the re-classification of the case as a high-grade C-ES. It is worth emphasizing that the distinction between P-ES and C-ES, and in particular between the high-grade form of C-ES and P-ES, is highly prone to subjectivity as, in the lack of validated biomarkers, is essentially based on morphological features.

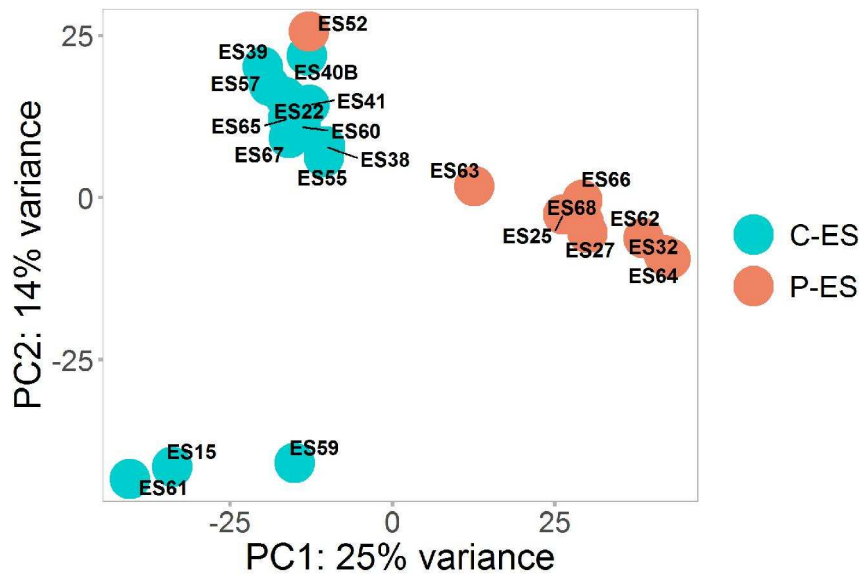


**Figure 3.1: PCA of the transcriptome of the ES whole cohort.** PCA of all the 22 ES cases profiled by RNA-Sequencing labelled by type (salmon: P-ES, cyan: C-ES). PCA was built on the top 1000 genes with highest variance.

Within the C-ES group, three cases (ES15, ES59 and ES61) clustered apart from the other samples (Fig. 3.1). These cases showed a superficial anatomic location on hand and forearm. Despite all samples were carefully macroscopically dissected by the pathologist in order to achieve the highest degree of “purity” in terms of representation of tumor cells of the sections to be used for RNA extraction (ideally >60%), the infiltrative growth pattern that characterizes C-ES (Hornick et al., 2009) makes it hard to completely dissect the tumor from neighboring tissues and non-neoplastic stroma. Bearing this in mind, and given the superficial localization of these tumors, we evaluated the expression of cytokeratin 5 (CK5) which is typically expressed by keratinocytes but negative in ES. The analysis of transcriptome clearly highlighted the presence of CK5 transcripts in the three ES cases that clustered apart in PCA. In addition, immunohistochemical analyses confirmed the intermingling of the tumor with the cutis. Therefore, these three C-ES (ES15, ES59, ES61) were excluded from subsequent analyses in order to be sure that transcriptome data were not affected by the contribution of non-tumoral RNAs.

Four additional C-ES (ES22, ES38, ES41, ES55) were excluded from differential expression analysis based on a degree of contamination from non-neoplastic cells greater than the selected cutoff (30%) (Table 3.1, last column), as assessed by both histological examination and transcriptome data analysis that indicated a residual SMARCB1 expression (SMARCB1 expression is impaired in ES).

Based on these criteria the cohort on which we investigated in deeper detail the transcriptome profile (selected cohort) was composed of 15 ES (8 P-ES and 7 C-ES).

### 3.2 Transcriptome profiling: selected cohort

The net separation in the transcriptome of the two ES variants was confirmed also on the selected cohort of the 15 ES, both in the PCA and in the unsupervised hierarchical clustering (Fig. 3.2). This result supports the diversity of P-ES and C-ES not only at the morphological level but also at the molecular level.

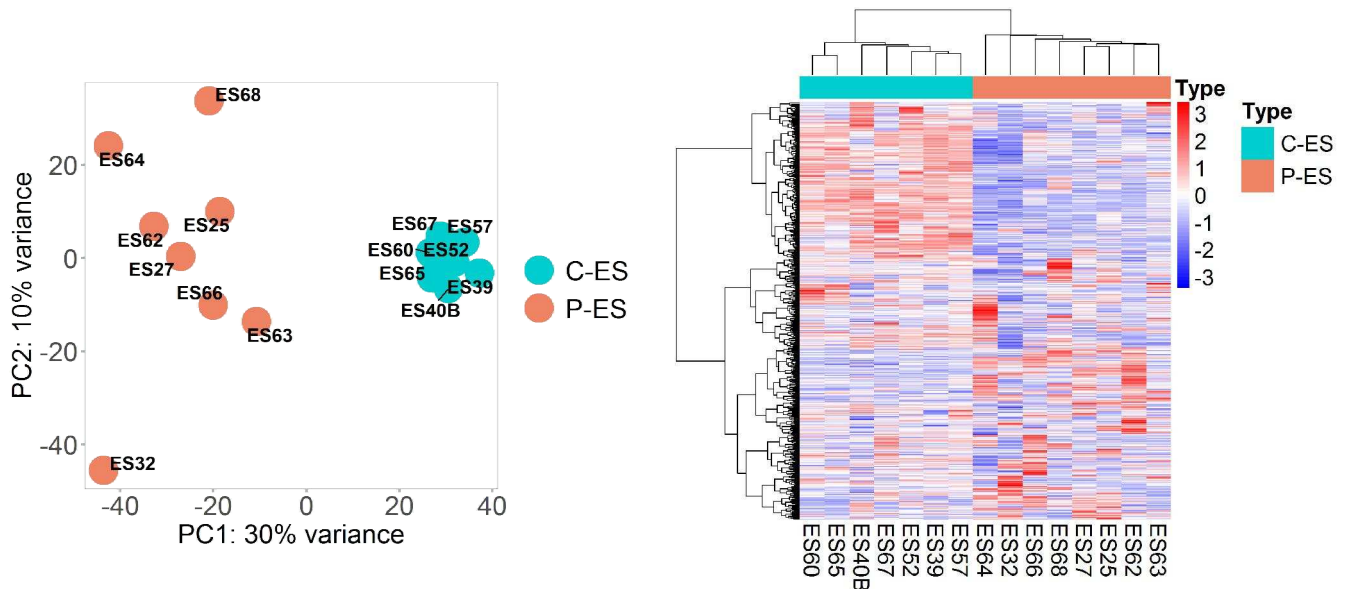


**Figure 3.2: PCA and unsupervised hierarchical clustering of P-ES and C-ES transcriptomes.**

PCA and heatmap with unsupervised hierarchical clustering of the 15 ES selected cases profiled by RNA-Sequencing labelled by type (salmon: P-ES, cyan: C-ES). PCA and heatmap were built on the top 1000 genes with highest variance.

Differential expression analysis of P-ES vs. C-ES identified 1615 differentially expressed genes (DEGs), 696 up-regulated and 919 down-regulated in P-ES ( $\text{abs.log}_2\text{FC} \geq 1$ ;  $\text{padj} \leq 0.05$ ).

Functional enrichment analyses of DEGs were performed using pre-ranked Gene Set Enrichment Analysis (GSEA) and Over Representation Analysis (ORA) run against Gene Ontology Biological Processes (GO-BP) and MSigDB Hallmark gene sets (Hallmarks). GSEA highlighted the enrichment of proliferative signatures in P-ES, like E2F and MYC targets and G2M checkpoint (Fig. 3.3). Accordingly, a higher mitotic rate was confirmed in P-ES (mean mitosis score: 2.3 in P-ES vs 1.4 in C-ES). P-ES also featured an enrichment of signatures related to chromatin remodeling.

Instead, in C-ES GSEA indicated enrichment of TGF- $\beta$  signaling and epithelial-to-mesenchymal transition terms, as well as vessels- and muscle-associated gene sets (Fig. 3.3), suggesting a more mesenchymal phenotype.

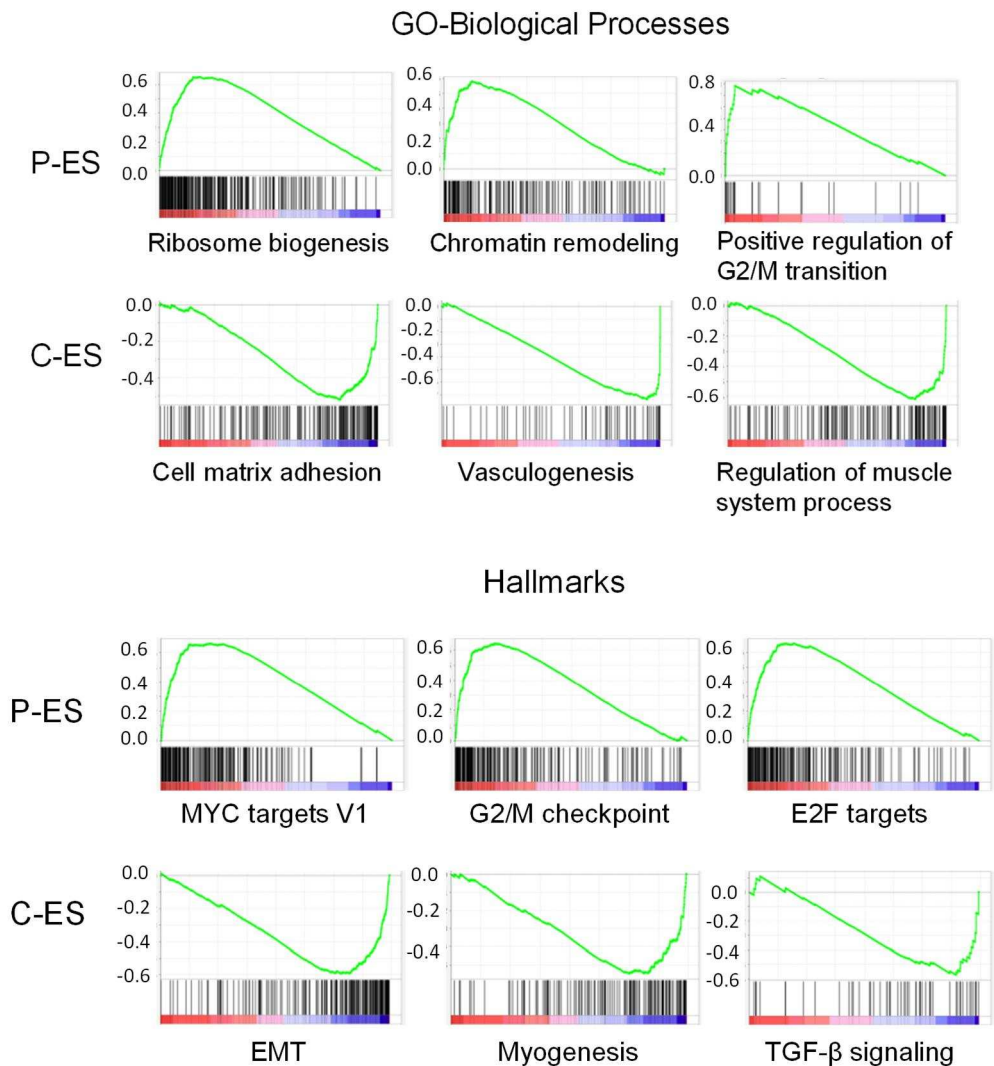


**Figure 3.3: enriched gene sets in P-ES vs. C-ES obtained from GSEA analysis.** A pre-ranked GSEA was run on DEGs against GO-BP (upper panels) and Hallmarks (lower panels) gene sets. Only enrichment plots from the upper quartile (lower FDR) of significantly enriched gene sets (NOM p-val  $\leq 0.05$ , FDR q-val  $\leq 0.05$ ) are reported. The Y axis reports the enrichment score (ES), the X axis shows the differential gene enrichment between P-ES (left) and C-ES (right).

Functional enrichment analyses performed by ORA underlined the presence of two main GO-BP networks in P-ES, namely chromatin metabolism (organization and assembly) and cell cycle regulation, in agreement with GSEA results (Fig. 3.4-A). Instead, in the C-ES group, the resulting clusters of over-represented GO-BP were mostly associated with cell-matrix, cell adhesion and the development of vessels and mesenchymal structures (Fig 3.4-B).

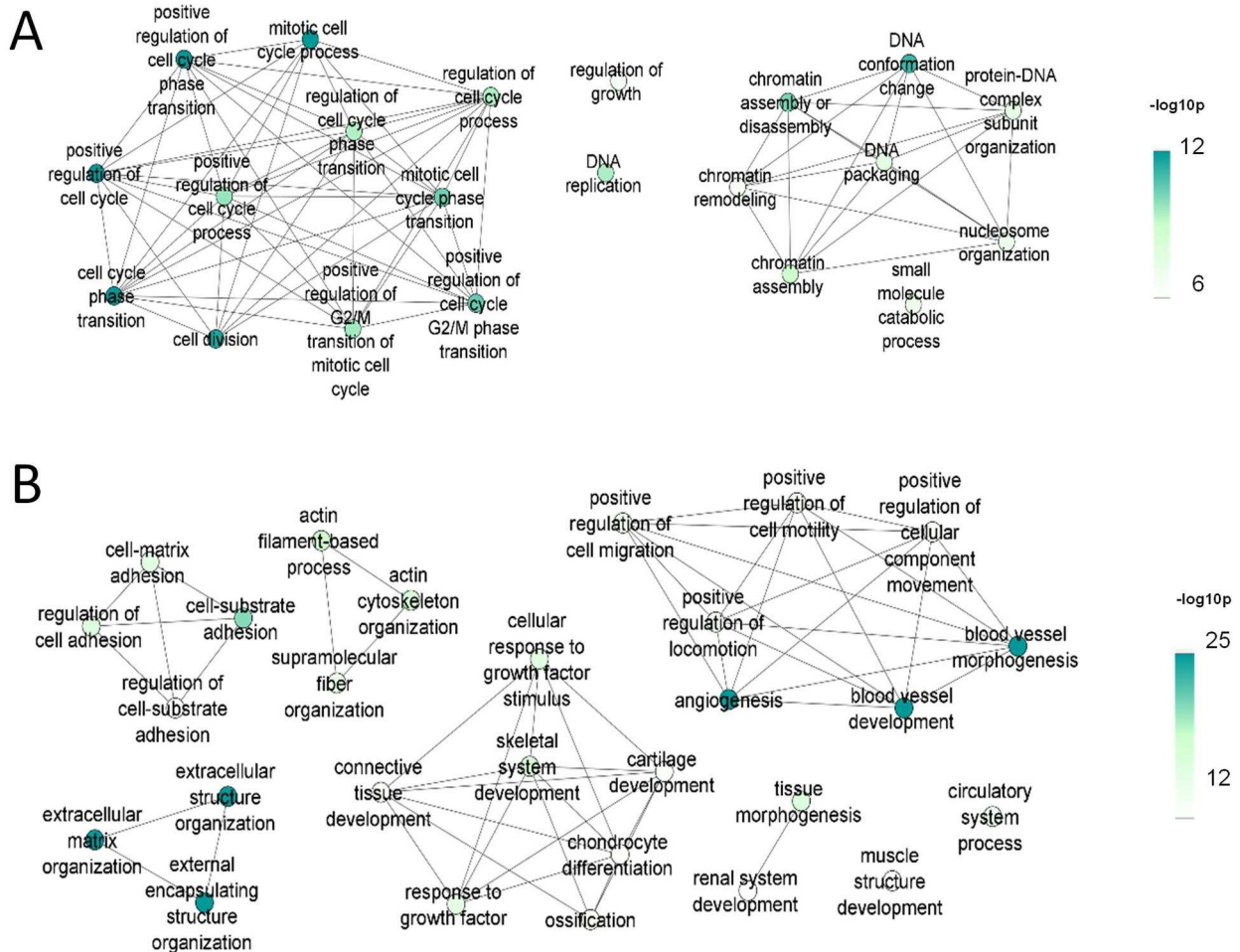


**Figure 3.4: most enriched gene sets in P-ES vs. C-ES obtained from ORA analysis.** A) Up-regulated DEGs were used to perform functional enrichment analysis against GO-BP gene sets to define pathways enriched in P-ES. B) Down-regulated DEGs were used to perform functional enrichment analysis against GO-BP gene sets to identify pathways enriched in C-ES. Dots are coloured according to significance.

This finding suggests that in the mesenchymal-epithelial spectrum of differentiation that characterizes ES, C-ES leans more towards the mesenchymal side compared to P-ES. Accordingly, C-ES typically shows the presence of spindle cells that are essentially absent in P-ES. In addition, a switch in cadherins was observed, with P-ES activating the epithelial E-cadherin (CDH1) and C-ES over-expressing the mesenchymal N-cadherin (CDH2) along with a large set of additional mesenchymal markers such collagen molecules (COL), matrix metalloproteases (MMP) and the EMT inducer SNAI2. C-ES overexpressed also CDK6 (Fig. 3.5 shows a selection of these molecules).

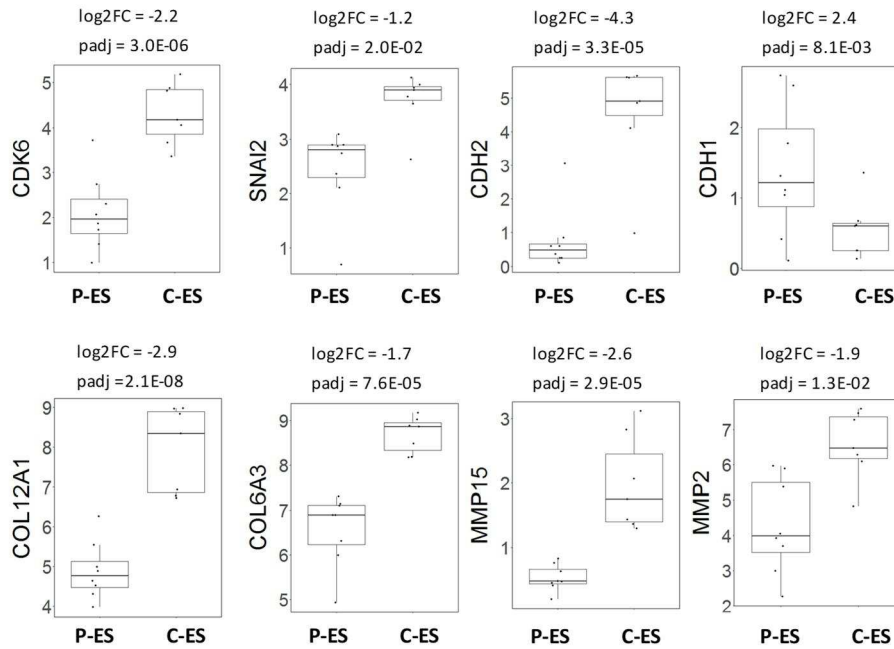


**Figure 3.5: box and whiskers plots showing the expression of genes related to pathways characterizing C-ES.** Plotted data are log2TPM+1 of the genes of interest (Y axis). The log2 Fold Change (log2FC) and adjusted p-value (padj) shown on top of each plot are the values of DESeq2 differential expression analysis. Noteworthy, the up-regulation of CDH2 is paralleled by a down-regulation of CDH1.

Genes up-regulated in P-ES included several proteins involved in the regulation of cell cycle progression (e.g. MYC, CDK4, E2F2, CDC25B; Fig. 3.6), in accordance with the higher proliferative activity showed by this group of tumors.

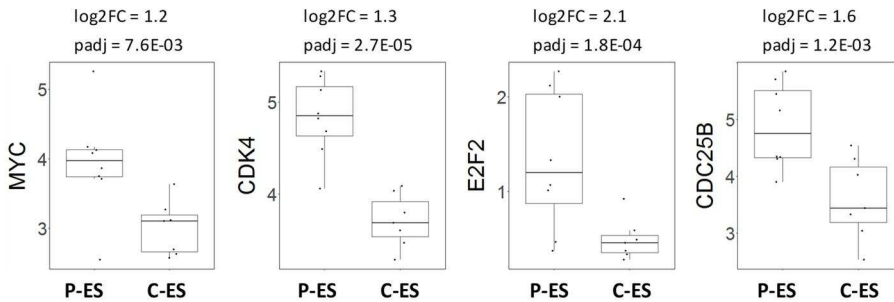


**Figure 3.6: box and whiskers plots showing the expression of genes related to cell cycle progression up-regulated in P-ES.** Plotted data are log2TPM+1 of the genes of interest (Y axis). The log2 Fold Change (log2FC) and adjusted p-value (padj) shown on top of each plot are the values of DESeq2 differential expression analysis.

An interesting finding was the quasi-mutual exclusive expression pattern of CDK4 and CDK6 in the two ES variants with P-ES expressing mostly CDK4, whereas C-ES expressing primarily CDK6 (Fig. 3.7). An intriguing observation was also the marked up-regulation in a subset of P-ES of FGFR2 (Fig. 3.7), a kinase for which targeted treatments are available (Weaver & Bossaer, 2021), and GATA3, a pioneer transcription factor (Fig. 3.7).



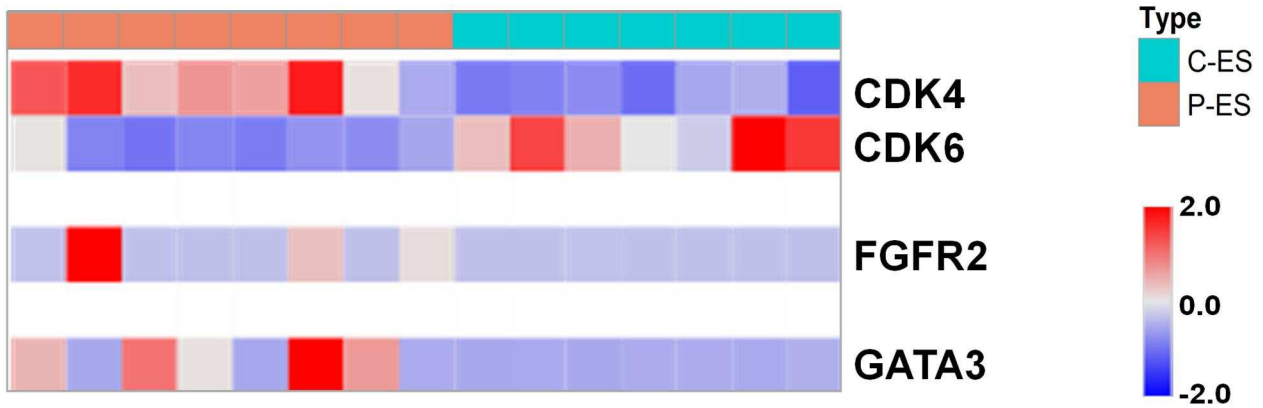


**Figure 3.7: heatmap showing the expression of CDK4/CDK6, FGFR2 and GATA3 in the two ES classes.** The heatmap shows the z-score calculated on TPM of CDK4/CDK6, FGFR2 and GATA3 in the selected cohort.

ES is considered an “epigenetic-driven tumor”, due to the driving role of SMARCB1 loss of expression. Yet, functional annotation indicated an enrichment of chromatin metabolism in P-ES, hinting a more profound involvement of epigenetic deregulation in this ES variant. Indeed, a deeper analysis of the genes up-regulated in P-ES underscored a peculiar up-regulation of several epigenetic regulators, namely the PRC2 components EZH2 and AEBP2; ZMYND8, an EZH2-interactor and histone mark reader; CBX6, a subunit of PRC1 complexes; SMARCD3, a component of cBAF and PBAF complexes; SMARCA1, a member of ISWI complexes; ING2, a mSin3A/HDAC component, and HELLS, a SNF2-family helicase (Fig. 3.8).

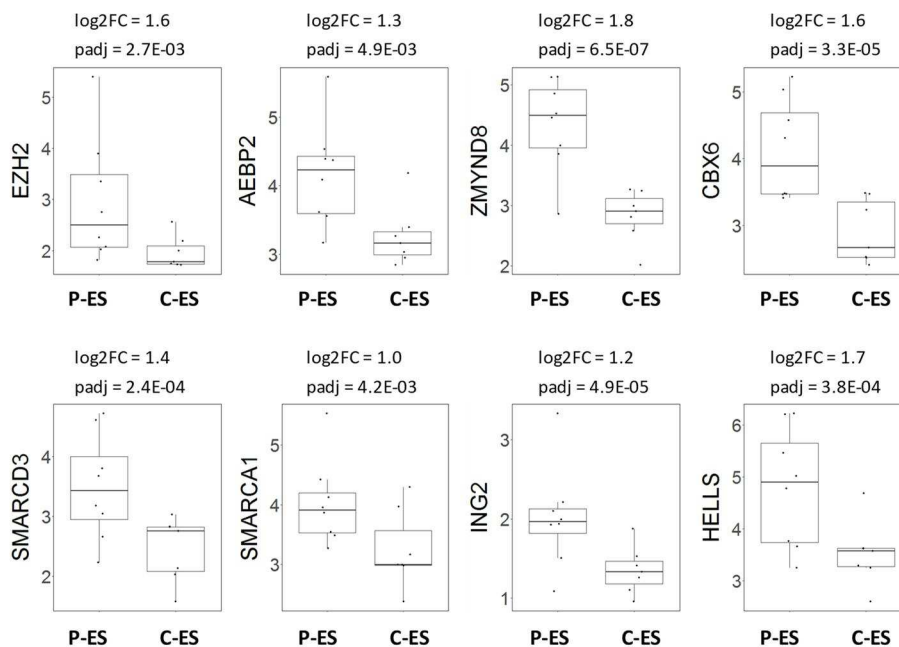


**Figure 3.8: box and whiskers plots showing the expression of differently expressed epigenetic modifiers in the two ES variants.** Plotted data are log<sub>2</sub>TPM+1 of the genes of interest (Y axis). The log<sub>2</sub> Fold Change (log<sub>2</sub>FC) and adjusted p-value (padj) shown on top of each plot are the values of DESeq2 differential expression analysis.

To investigate further the participation of chromatin regulators in ES pathogenesis we interrogated by GSEA two published datasets of epigenetic modifiers, EpiFactors (Medvedeva et al., 2015) and dbEM (Singh Nanda et al., 2016). A clear enrichment of these genes emerged in P-ES (Fig. 3.9), further supporting the altered chromatin metabolism in this ES variant.

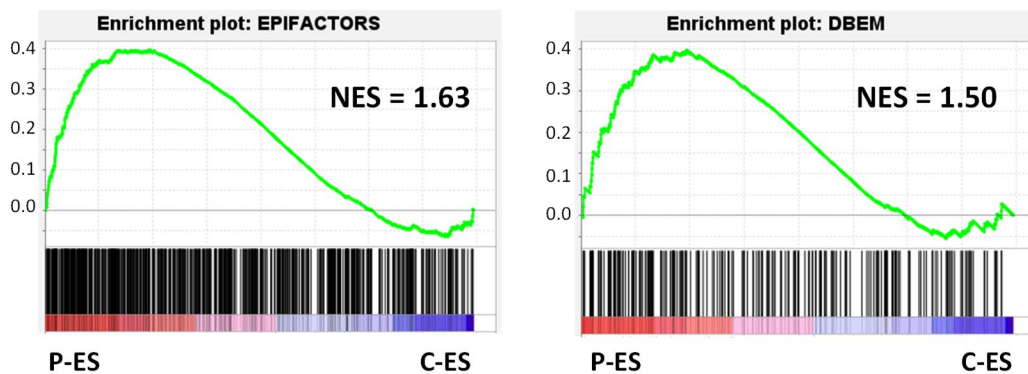


**Figure 3.9: GSEA enrichment results for the epigenetic/chromatin modifiers.** A pre-ranked GSEA was run on DEGs, ranked by significance, against the EpiFactors dataset (on the left) and against the dbEM dataset (on the right). The Y axis reports the enrichment score (ES), the X axis shows the differential gene enrichment between P-ES (left) and C-ES (right). In the figure, NES (Normalized Enrichment Score) is reported.

Based on these results and the known antagonism between SWI/SNF and PRC2 complexes (Wilson et al., 2010), we decided to evaluate different signatures related to PRC2 and EZH2 activity (Fig. 3.10): PRC2\_EZH2\_UP.V1\_UP is a signature composed by genes up-regulated in TIG3 fibroblasts upon knockdown of EZH2 (Bracken et al., 2006), whereas NUYTTEN\_EZH2\_TARGETS\_UP includes genes up-regulated in PC3 prostate cancer cells after knockdown of EZH2 by RNA interference (Nuytten et al., 2008). These analyses pointed out an enrichment of genes up-regulated upon EZH2 knockdown in C-ES, suggesting the presence of a greater activity of EZH2 in the P-ES variant.



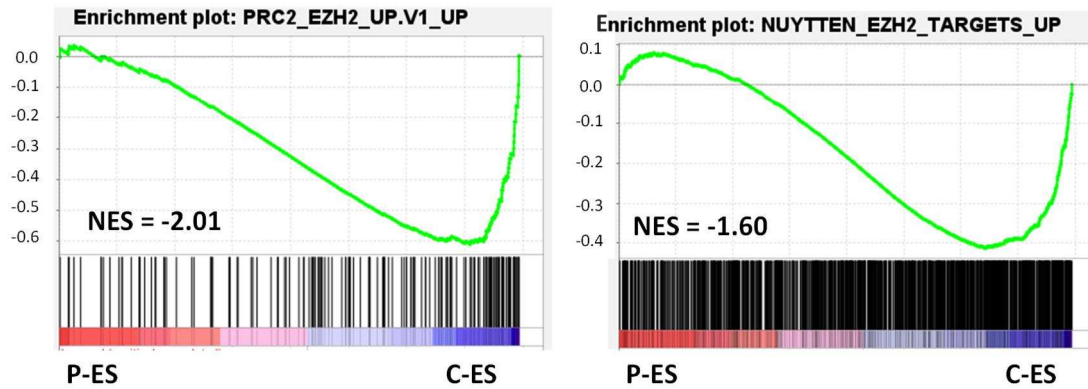


**Figure 3.10: GSEA enrichment results for signatures related to PRC2 and EZH2 activity.** A pre-ranked GSEA was run on DEGs against signatures downloaded from the Broad Institute Molecular Signatures Database. The plots show an enrichment of both signatures in C-ES class. The Y axis reports the enrichment score (ES), the X axis shows the differential gene enrichment between P-ES (left) and C-ES (right). In the figure, NES (Normalized Enrichment Score) is reported.

Overall, these results suggested a greater involvement of epigenetic regulators in sustaining the tumor phenotype of P-ES compared to C-ES.

### 3.3 miRNA profiling: selected cohort

Apart from SMARCB1 alterations, no recurrent gene mutation pattern has been observed in ES that could explain the differences between P-ES and C-ES (Gounder et al., 2020; Del Savio unpublished). Therefore, we sought to evaluate the role of miRNAs in sustaining the different transcriptional pattern observed in the two ES variants. miRNome profiling was generated by miRNA-Sequencing on 12 (7 P-ES and 5 C-ES) of the ES cases previously characterized by RNA-Sequencing.

PCA (Fig. 3.11) showed a trend towards separation between P-ES and C-ES, even though less clear-cut than the one obtained from RNA-Sequencing data.

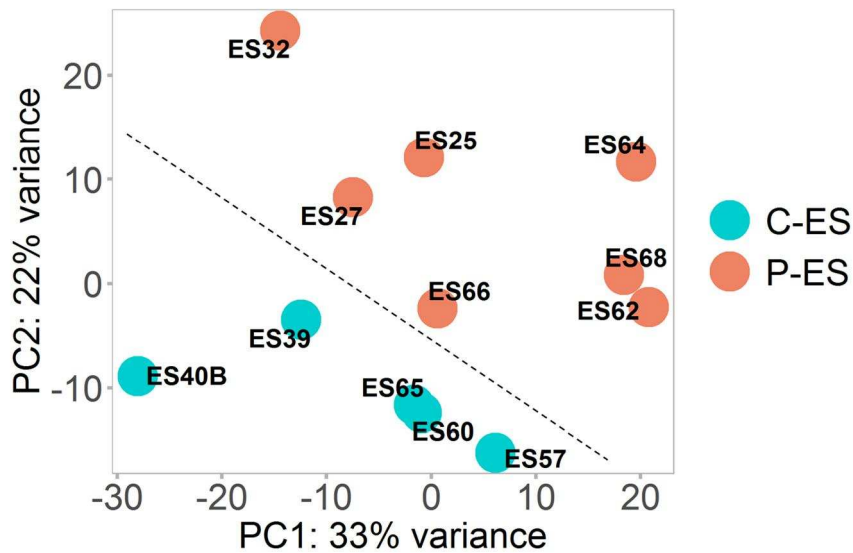


**Figure 3.11: PCA of P-ES and C-ES miRNomes.** PCA of the 12 ES cases profiled by miRNA-Sequencing, labelled by type (salmon: proximal ES, cyan: classic ES). PCA was built on the top 200 miRNAs with highest variance.

The comparison P-ES vs. C-ES identified 109 differentially expressed miRNAs (DEmiRs), 73 up-regulated and 36 down-regulated ( $\text{abs.log}_2\text{FC} \geq 1$ ;  $\text{padj} \leq 0.05$ ). In order to evaluate the possible role of miRNAs in supporting the different tumor biology in the two ES variants, a Spearman correlation analysis was conducted between each DEmiR and the respective target genes obtained from the functional miRNA-target interactions (MTI) dataset of MirTarBase (Huang et al., 2020), under the assumption that the key mechanism of action of miRNAs is to mediate the degradation of target mRNA. MirTarBase is a database containing thousands of MTI. Taking into consideration only MTIs with strong evidence level (validated by reporter assays, qPCR or western blot), 5 down-regulated miRNAs (miR-137, miR-150-5p, miR-152-3p, miR-23a-3p, miR-24-3p) showed a significant anti-correlation (Spearman correlation score  $\leq -0.5$ , p-value  $\leq 0.05$ ) with 7 up-regulated genes in P-ES (MYC, E2F2, CDK4, LDHB, EZH2, VEGFA, PIK3R3) (Fig. 3.12).

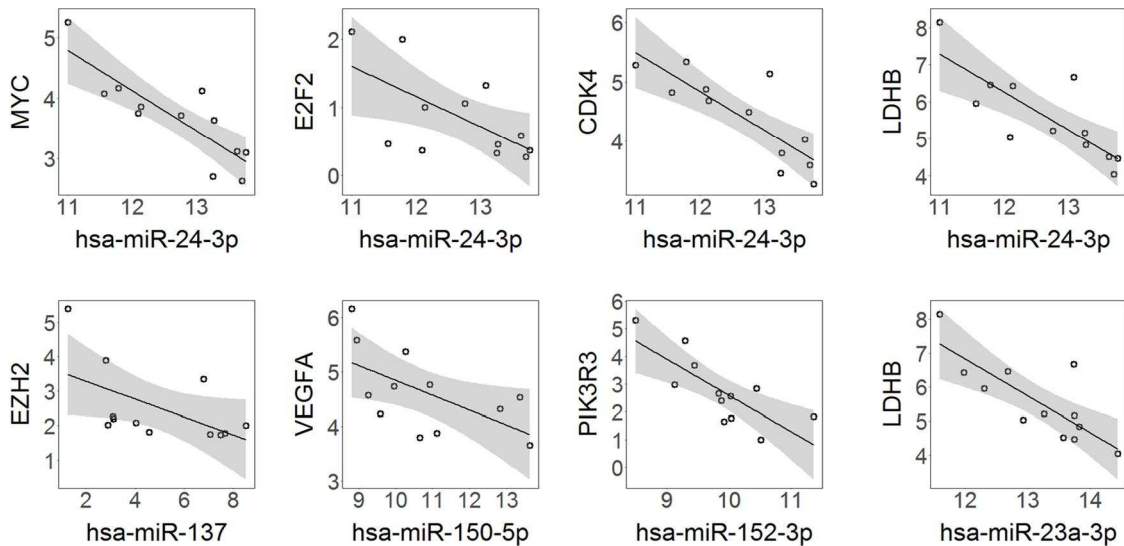


**Figure 3.12: scatter plots showing the expression of the experimentally validated anti-correlated miRNA/gene pairs.** Spearman correlation analysis was conducted on miRNA/target pairs showing strong experimental evidence of interaction according to MirTarBase. Only experimentally validated pairs presenting a significant anti-correlation (Spearman correlation score  $\leq -0.5$ , p-value  $\leq 0.05$ ) are reported. Plotted data are  $\log_2\text{TPM}+1$  of significantly up-regulated genes (Y axis) and  $\log_2\text{CPM}+1$  of significantly down-regulated miRNAs (X axis). The grey area identifies the confidence interval.

Particularly interesting the involvement of miR-24-3p which seems to be able to concomitantly target multiple genes up-regulated in P-ES (MYC, E2F2, CDK4 and LDHB). To further corroborate the relevant role of this miRNA, a GSEA analysis conducted using a dataset of genes down-regulated in cells over-expressing miR-24 (Lal et al., 2009) demonstrated an enrichment of this dataset in P-ES (Fig. 3.13). Additionally, the analysis revealed that the PRC2 component EZH2 that is up-regulated in P-ES was anti-correlated with the expression of a well-known tumor suppressor miRNA, miR-137, whose down-regulation is associated with tumor aggressiveness (Gu et al., 2021).

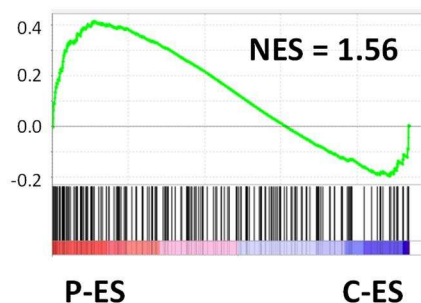


**Figure 3.13: GSEA enrichment results for genes down-regulated in miR-24 over-expressing cells.** A pre-ranked GSEA was run on DEGs, against a dataset of genes down-regulated in cells over-expressing miR-24 from Lal et al., 2009. The Y axis reports the enrichment score (ES), the X axis shows the differential gene enrichment between P-ES (left) and C-ES (right). The False Discovery Rate is 0.016.

The reciprocal analysis (miRNA down-regulated and genes up-regulated in C-ES) demonstrated that 7 miRNAs (miR-196a-5p, miR-203a-3p, miR-29a-3p, miR-29b-3p, miR-337-5p, miR-379-5p, miR-494-3p) anti-correlated with 22 genes up-regulated in C-ES (Fig. 3.14). Particularly intriguing the correlation of miR-29a-3p and miR-29b-3p with multiple components of the extracellular matrix over-expressed in C-ES as well as with CDK6 that seems to replace CDK4 in this ES variant.

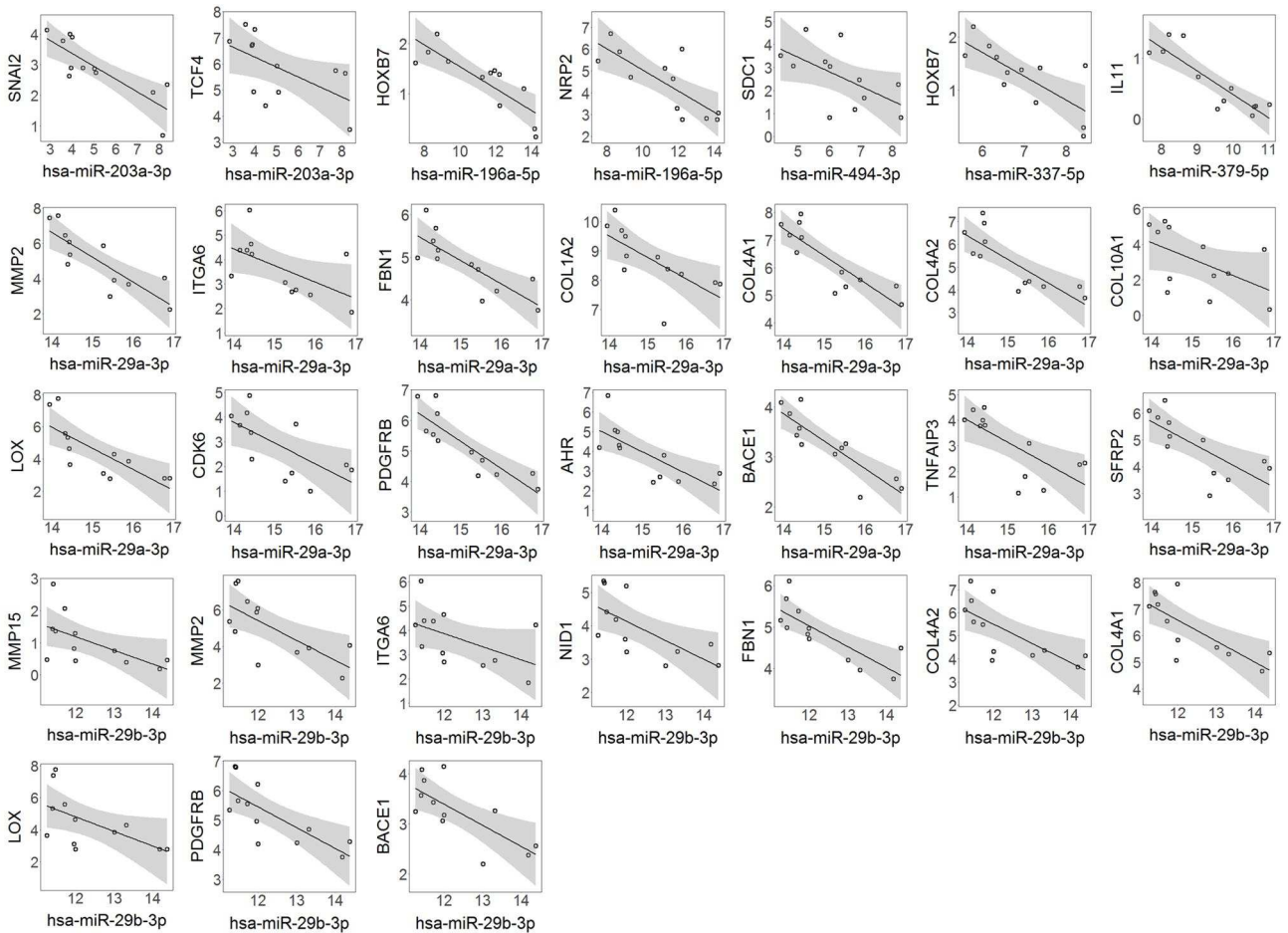


**Figure 3.14: scatter plots showing the expression of the experimentally validated anti-correlated miRNA/gene pairs.** Spearman correlation analysis was conducted on miRNA/target pairs showing strong experimental evidence of interaction according to MirTarBase. Only experimentally validated pairs presenting a significant anti-correlation (Spearman correlation score  $\leq -0.5$ , p-value  $\leq 0.05$ ) are reported. Plotted data are  $\log_2\text{TPM}+1$  of significantly down-regulated genes (Y axis) and  $\log_2\text{CPM}+1$  of significantly up-regulated miRNAs (X axis). The grey area identifies the confidence interval.

Beyond these miRNA/target interactions reported in MirTarBase, we sought to explore the possibility of novel miRNA/gene pairs. To this end, we exploited mirDIP (Tokar et al., 2018), a tool developed by Igor Jurisica (a collaborator of ours) that integrates human miRNA/target predictions from 30 different resources and provides an overall score. For each differentially expressed miRNA, the top 5% of predicted target genes (high confidence predictions) was selected to perform anti-correlation analyses (Spearman correlation score  $\leq -0.5$ , p-value  $\leq 0.05$ ). Target genes

significantly anti-correlated with differentially expressed miRNAs (irrespective of whether these target genes were differentially expressed in RNA-Sequencing analysis) were used as input to perform an ORA analysis. Chromatin remodeling and cell cycle processes on one side and cell motility, adhesion and development of vessels and mesenchymal structures on the other side were the GO-BP associated with the targets of miRNAs down-regulated and miRNAs up-regulated, respectively (Fig. 3.15-A, B).

These results further corroborate the implication of miRNAs in determining different expression profiles in the ES two variants.

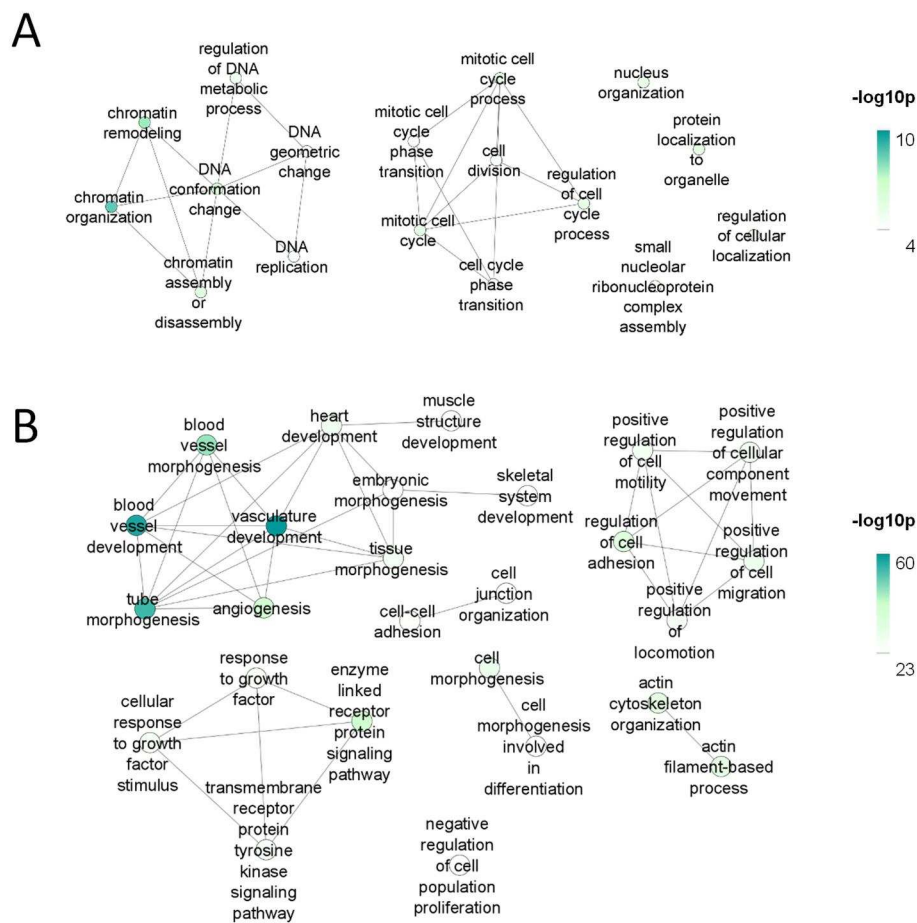


**Figure 3.15: ORA results for DEmiRs anti-correlated target genes.** DEmiRs target genes were predicted using mirDIP 4.1 software. Top 5% of predicted target genes was selected based on the mirDIP integrated score and used to perform a Spearman correlation analysis. Only genes significantly anti-correlated with the cognate DEmiRs were used as input to perform an ORA against GO-BP, separating genes inversely correlated with down-regulated (A) or up-regulated (B) DEmiRs. Dots are coloured according to significance.

Several of the predicted targets of miRNAs down-regulated in P-ES were indeed significantly up-regulated in this ES subtype (Table 3.2) and several were associated with cell cycle and chromatin remodeling. Among these, BAHD1, CDC25B, and HMGA1 were predicted to be targeted by the very same miRNA, miR-874-5p. Instead, AEBP2 and HELLS genes were predicted to be targeted by miR-23a-3p and miR-24-3p, respectively, two miRNAs that belong to the same cluster and are transcribed as a unique pri-miRNA.

<b>Gene</b>		<b>miRNA</b>		<b>P-value</b>	<b>Rho</b>
<b>AEBP2</b>	↑	hsa-miR-23a-3p	↓	6.60E-03	-0.76
<b>HELLS</b>	↑	hsa-miR-24-3p	↓	2.04E-02	-0.67
<b>SMARCD3</b>	↑	hsa-miR-1287-5p	↓	2.22E-02	-0.66
<b>CDC25B</b>	↑	hsa-miR-874-5p	↓	0.00E+00	-0.91
<b>BAHD1</b>	↑	hsa-miR-874-5p	↓	5.25E-03	-0.77
<b>HMGA1</b>	↑	hsa-miR-874-5p	↓	1.88E-02	-0.68

**Table 3.2: selected anti-correlated mirDIP-predicted target genes of down-regulated DEmiRs.** For each DEmiR, significantly anti-correlated mirDIP-predicted target genes were functionally annotated (ORA) separating between up- and down-regulated miRNAs. Genes involved in the main pathways enriched in P-ES class and having more significant anti-correlation score were selected for further investigations.

### 3.4 miRNA targeting validation

Based on the results obtained so far that point to chromatin remodeling and cell cycle as processes significantly enriched in P-ES, we sought to start our validation from miRNA/gene pairs belonging to these pathways.

We started by verifying whether, as previously demonstrated in other tumor settings (Lal et al., 2009; Sun et al., 2015; S.-H. Lee et al., 2016; Gu et al., 2021), miR-137 and miR-24-3p actually targeted EZH2 and MYC also in the context of ES.

To this end, the ES cell line HS-ES-2R was transfected with miRNA mimics for miR-137, miR-24-3p and control (NC#1) and evaluated 48h and 72h post-transfection by RT-qPCR. miR-137 and miR-24-3p mimics induced a significant reduction in the mRNA levels of their cognate genes (Fig. 3.16), supporting a role for these miRNAs in the modulation of EZH2 and MYC within ES.

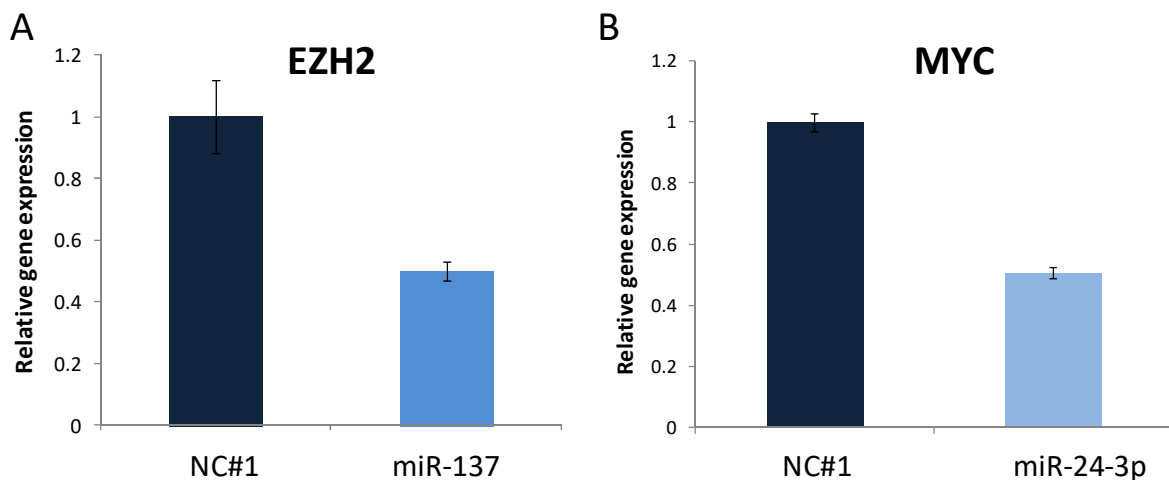


**Figure 3.16: EZH2 and MYC mRNA levels after miRNA mimics transfection in HS-ES-2R.** HS-ES-2R were plated at a seeding density of 200'000 cells/well, transfected with DharmaFECT 4 transfection reagent and miRNA mimics (final concentration: 30nM), then cells were collected 48h and 72h post-transfection. RT-qPCR showing EZH2 (A) and MYC (B) mRNA levels 72h post-transfection with mimics. EZH2 and MYC expression were normalized on the expression of 2 housekeeping genes (GAPDH and SF3A1), and plots show expression values relative to NC#1-transfected samples. Standard deviations were calculated on the technical replicates.

The plot reports the result of one representative experiment. The results were confirmed in at least 2 independent experiments and the same trend was observed at 48h.

NC#1: mirVana Negative Control #1.



We then focus on HELLS, which was predicted with a high confidence score to be targeted by miR-24-3p according to mirDIP. By using the same approach as above, transfection of the miR-24-3p mimic yielded a significant reduction in HELLS expression levels, both at mRNA (Fig. 3.17-A) and protein levels (Fig. 3.17-B). Although predicted to target HELLS with a moderate prediction score, also the mimics for miR-137 induced HELLS down-regulation.

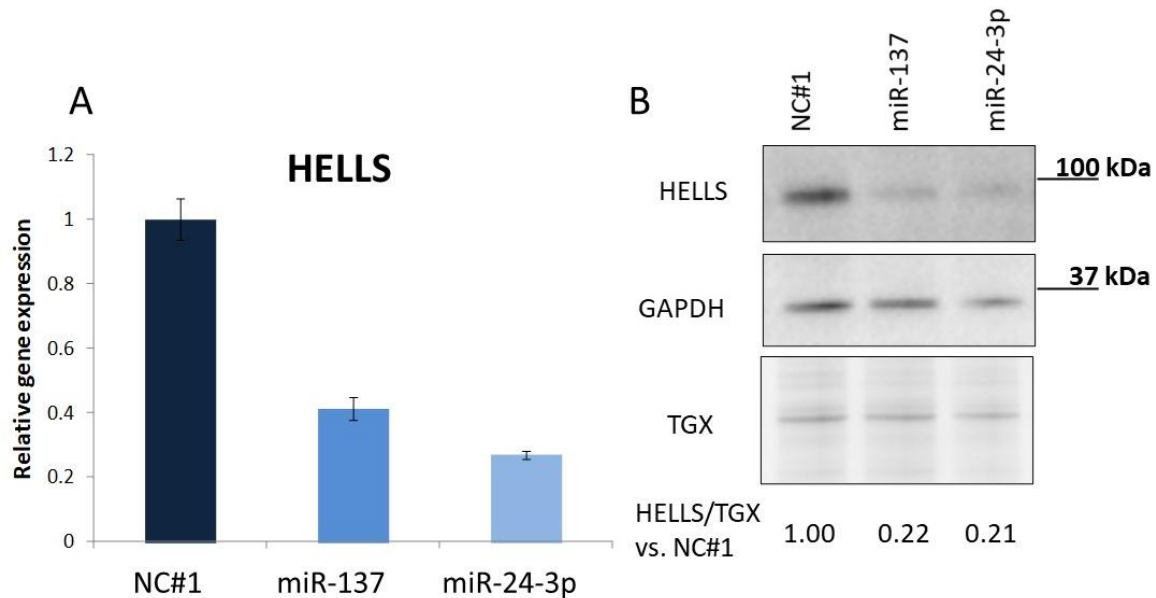


**Figure 3.17: HELLS mRNA and protein levels after miRNA mimics transfection in HS-ES-2R.** A-B) Mimics transfection and cells collection were performed as described above. The figure shows HELLS mRNA and protein levels 72h post-transfection. RT-qPCR showing HELLS mRNA level (A) normalized on the expression of 2 housekeeping genes (GAPDH and SF3A1) and relative to NC#1-transfected samples. Standard deviations were calculated on the technical replicates. Blot showing HELLS protein level (B) normalized on TGX gel staining and relative to NC#1-transfected samples. The plot reports the result of one representative experiment. The results were confirmed in at least 2 independent experiments and the same trend was observed at 48h. NC #1: mirVana Negative Control #1.



# 4. DISCUSSION

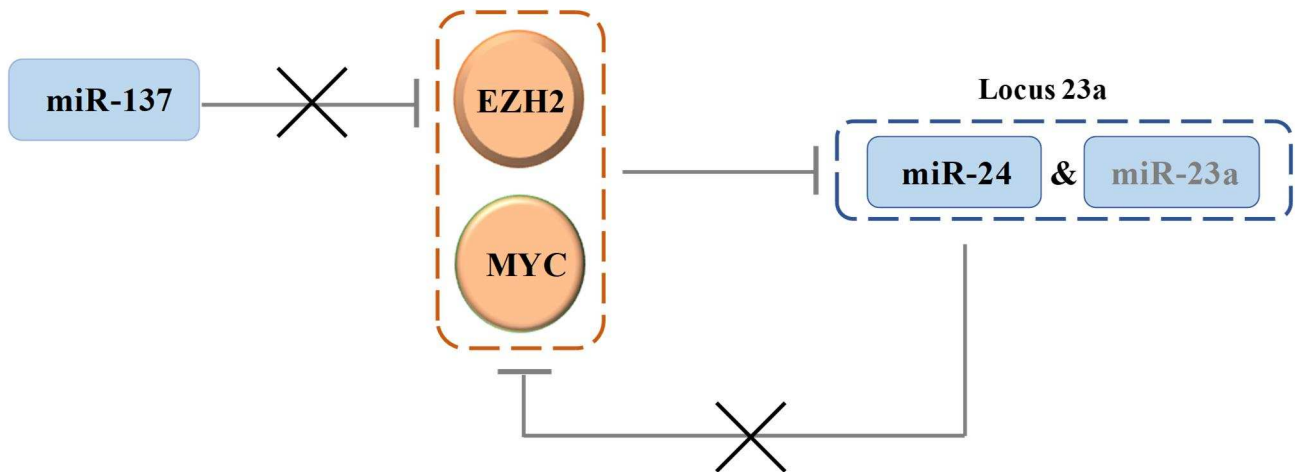
Although ES is overall considered a slow growing tumor, its histological and morphological characteristics define two subtypes, P-ES and C-ES, with significantly different prognosis: P-ES pursues a more aggressive clinical course whilst C-ES is more indolent and less prone to local and distal spreading. Both ES variants share loss of the SWI/SNF component SMARCB1/INI1 as the major genetic abnormality. Thus, what are the molecular basis for the biological diversity of the two ES subtypes is currently unknown. To fill this gap, we performed a comprehensive transcriptional profiling, both RNA and miRNA profiling, of a sizable series of this very rare sarcoma.

The comparison P-ES vs. C-ES indicated that C-ES seemed to display a more mesenchymal phenotype, associated with the up-regulation of several cell matrix and adhesion molecules, as well as EMT-related factors. The reduced expression of a set of miRNAs, namely miR-203a-3p, miR-29a-3p and miR-29b-3p, could contribute at least in part to this phenotype. In fact, miR-203a-3p targets SNAI2 and TCF4; miR-29a-3p and miR-29b-3p target several matrix and cell adhesion molecules.

More interestingly, the comparison of transcriptome and miRNome of P-ES and C-ES indicated that chromatin remodeling and cell cycle signatures were enriched in the more aggressive P-ES subtype. In fact, P-ES featured up-regulation of several chromatin remodelling factors, including EZH2. This finding is particularly intriguing not only in the light of the known antagonism between the SWI/SNF complex and the PRC2 complex (Wilson et al., 2010), but also considering the promising activity observed in a subset of ES treated with the EZH2 inhibitor Tazemetostat (Gounder et al., 2020). What ES variant belonged the tumors that responded to Tazemetostat and whether they over-expressed EZH2 was not stated in the paper reporting the trial results. It will be interesting assess whether EZH2 expression may serve as a predictive marker for patient stratification to this treatment.

The analysis of the miRNome indicated that miR-137, which has been reported to target EZH2 (Sun et al., 2015; Gu et al., 2021), is down-regulated in P-ES compared to C-ES. Thus, loss of miR-137 could unleash EZH2 expression in this ES variant. EZH2 has been shown to collaborate with MYC to negatively regulate the expression of a number of pro-EMT genes (Rao et al., 2015). Interestingly, also MYC is over-expressed in P-ES, thus reinforcing this negative control on EMT by EZH2. Among the targets of EZH2/MYC alliance there is the miR-23a cluster that includes miR-23a, miR-27a and miR-24 (Rao et al., 2015). Accordingly, both miR-23a and miR-24 were down-regulated in P-ES.

miR-23a is predicted to target the PRC2 component AEBP2; instead, miR-24 targets MYC (Lal et al., 2009). Taken together, these results suggest the existence in P-ES of a feed-forward loop where the loss of miR-137 expression induces EZH2 up-regulation that, in combination with MYC, induces down-regulation of miR-23a and miR-24. In turn, the reduced expression of miR-24 relieves the negative control exerted by this miRNA on MYC, further boosting the circuit (see scheme below).



The MYC/EZH2 cross talk seems to be supported also by the evidences that EZH2 transcriptionally up-regulates C-MYC in glioblastoma thereby contributing to cancer stem cell maintenance (Suvà et al., 2009). Intriguingly, MYC-mediated gene expression was demonstrated to be negatively regulated by the interaction with SMARCB1, whose loss would instead favor MYC-dependent transcription (Weissmiller et al., 2019; Msaouel et al., 2020).

Also HELLS was up-regulated in P-ES, and we here provided evidence that HELLS is regulated by miR-24-3p, in turn repressed in P-ES. HELLS is a SNF2-related ATPase capable of both inhibiting gene expression in combination with DNMT and HDAC (Zhu et al., 2006; Myant & Stancheva, 2008; Han et al., 2020) and mediating gene activation. In particular, HELLS was shown to interact with and potentiate MYC and E2F3 transcriptional activity (Zhang et al., 2019; Zocchi et al., 2020). Thus, the up-regulation of HELLS in P-ES, possibly as a result of miR-24-3p down-regulation, could contribute to the hyper-activation of MYC and E2F signaling observed in P-ES.

Interestingly, P-ES and C-ES seem to rely on different G1 kinases, with P-ES expressing high levels of CDK4 and C-ES high levels of CDK6. miRNAs could play a role in determining this switch as miR-24-3p, which targets CDK4, was down-regulated in P-ES class and miR-29a-3p, which targets CDK6, was down-regulated in C-ES. The different usage of CDK4 and CDK6 in the

two ES variants might be relevant both from a diagnostic and from a therapeutic standpoint. In the lack of robust biomarker that differentiated P-ES from C-ES the distinction is essentially based on morphological criteria. Provided the different dependency on CDK4 and CDK6 is confirmed, this could reveal as a useful tool in differential diagnosis between P-ES and C-ES. Moreover, CDK4/CDK6 inhibitors are currently under clinical testing in the sarcoma setting (e.g. clinical trial NCT01209598) (Dickson et al., 2016) and these inhibitors show different affinity towards the two kinases (Pack et al., 2021). Thus, this result could help in stratifying ES patients for this type of treatment.

An additionally interesting and potentially clinically relevant finding is the marked up-regulation of FGFR2 in a subset of P-ES. FGFR inhibitors are also under clinical evaluation in patients with advanced tumors (e.g. FIGHT-101 trial, NCT02393248) and gained accelerated approval for a subset of malignancies (Weaver & Bossaer, 2021). The elevated expression of FGFR2 in a subset of P-ES suggests a possible eligibility of these patients to the treatment with FGFR inhibitors.

Also GATA3 is up-regulated in a subset of P-ES. Intriguingly, its expression was associated with a higher mitotic count and shorter disease-free and overall survival in patients with soft tissue sarcomas (Haraguchi et al., 2016). Therefore, GATA3 could represent a useful marker in differential diagnosis between P-ES and C-ES and could identify a subset of more aggressive malignancies.

Overall, our work demonstrated that ES comprises a heterogeneous group of tumors in which two variants identified based on morphological characteristics actually display a significantly different molecular make-up. Moreover, the integration of transcriptome and miRNome profiling unveiled important biological and molecular characteristics that may reveal novel diagnostic/prognostic markers and possibly novel therapeutic approaches.

# **5. MATERIAL AND METHODS**

## **5.1 Epithelioid sarcoma samples**

This study was conducted as a translational part of the retrospective/prospective observational EpiSObs study (NCT03099681), coordinated by the Italian Sarcoma Group (ISG). Informed consent was obtained from all enrolled patients. Samples from a total of 22 treatment-naïve ES patients were available for molecular investigations (Table 3.1). Only cases immunohistochemically negative for SMARCB1 protein expression were included in the study.

Formalin-fixed paraffin-embedded (FFPE) sections selected for RNA extraction were carefully macroscopically dissected by the pathologist in order to achieve the highest degree of “purity” in terms of representation of tumor cells (ideally >60%).

## **5.2 RNA extraction**

FFPE tissues were dewaxed using the QIAGEN deparaffinization solution and total RNA was extracted using the Ambion RecoverAll Nucleic Acid isolation kit for FFPE, according to the manufacturer’s instructions. RNA concentration was measured using a fluorimetric-based assay (Qubit RNA HS Assay kit, ThermoFisher Scientific), and its quality was evaluated by Agilent 2200 TapeStation electrophoresis (RNA Assay Kit, Agilent Technologies).

RNA extraction from cell lines was performed with the miRNeasy Mini Kit (QIAGEN) following manufacturer’s instructions, including the step of genomic DNA digestion with DNase I (QIAGEN). The concentration of extracted RNA was measured with the Qubit RNA HS Assay kit (ThermoFisher Scientific).

## **5.3 RNA-Sequencing and data processing**

RNA sequencing libraries were prepared from 100ng to 500ng of total RNA using TruSeq stranded total RNA kit (Illumina), according to the manufacturer’s instructions. Briefly, RNA was treated with RiboZero Deplete reagents to remove ribosomal RNA (rRNA), then it was converted into double-stranded cDNA with the incorporation of dUTP in place of dTTP during the synthesis of the second strand. cDNA fragments were adenylated at the 3’ end and adapter indices were ligated, then the products were amplified using PCR. During the amplification reaction, the presence of dUTP in the second strand of the cDNA quenched its amplification, leading to the production of a stranded cDNA library representing the first strand. The concentration of the obtained libraries was measured using the fluorimetric-based assay Qubit dsDNA High Sensitivity Assay Kit (ThermoFisher Scientific). The quality of the libraries in term of both size and purity was evaluated

by Agilent 2200 TapeStation electrophoresis (D1000 Assay Kit, Agilent Technologies). The final product should have a dimension of 260 base pairs.

Libraries passing this quality check were diluted to the same concentration and pooled together to a final concentration of 2 nM. Finally, pools of libraries were run on Illumina HiSeq 1000 instrument to obtain an average of 60 million 50 base paired-end reads per sample. The quality of the raw data obtained from the sequencing run was assessed with the FastQC software (version 0.11.9) using default settings. Reads were then trimmed, aligned and quantified using Trimmomatic (version 0.39) (Bolger et al., 2014), STAR (version 2.7.3a) (Dobin et al., 2013) and RSEM (version 1.3.1) (B. Li & Dewey, 2011) tools, respectively. The reference genome used was the Genome Research Consortium human build 38 (GRCh38, hg38). The annotation related to the reference genome was collected from the GENCODE project, specifically Release 33 (January 2020).

Tximport v. 1.20.0 (Soneson et al., 2015) was used to summarize transcript data to gene level and to import them into the DESeq2 package (Love et al., 2014) under R environment (version 4.1.0) to perform the differential expression analysis comparing P-ES vs. C-ES. Low-expressed genes, defined as having less than 10 counts in the smaller class of the comparison, were excluded from the differential expression analysis. Differentially expressed genes (DEGs) were defined as having  $\text{abs.log}_2\text{FoldChange} \geq 1$  and adjusted  $p\text{-value} \leq 0.05$  ( $\text{abs.log}_2\text{FC} \geq 1$  and  $\text{padj} \leq 0.05$ ).

## 5.4 miRNA-Sequencing and data processing

Libraries for miRNA profiling were prepared using QIAseq® miRNA Library Kit (QIAGEN), according to the manufacturer's instructions, starting from 100ng of total RNA. Briefly, a pre-adenylated DNA adapter and an RNA adapter were respectively ligated to the 3' ends and to the 5' ends of mature miRNAs. These adapter-ligated miRNAs were converted into cDNA using a reverse transcription primer that contained Unique Molecular Index (UMI), that marked univocally every miRNA molecule. After cDNA purification, libraries were amplified using PCR with which a unique index was concomitantly added to each sample. The quantity of the obtained libraries was measured using the fluorimetric-based assay Qubit dsDNA High Sensitivity Assay Kit (ThermoFisher Scientific), while their quality was evaluated by Agilent 2200 TapeStation electrophoresis (D1000 Assay Kit, Agilent Technologies). A miRNA-sized library should be approximately 180 base pairs. Libraries passing this quality check were diluted to the same concentration and pooled together to a final concentration of 2nM. Finally, pools of libraries were run on Illumina HiSeq 1000 instrument to obtain an average of 12 million 75 base single-end reads per sample. FastQ files obtained from the sequencing were processed using nextflow smRNA-seq

pipeline (<https://github.com/nf-core/smrnaseq>). Alignment was performed using the Genome Reference Consortium Human Built 38 (GRCh38, hg38) and miRbase 22. The raw reads obtained from the alignment were processed using DESeq2 in R to perform the differential expression analysis comparing P-ES vs. C-ES. miRNAs showing less than 10 counts in the smaller class of the comparison were excluded. Differentially expressed miRNAs (DEmiRs) were defined as having  $\text{abs.log}_2\text{FC} \geq 1$  and  $\text{padj} \leq 0.05$ .

## 5.5 Graphical representation of data

Principal Component Analysis (PCA), hierarchical clustering and heatmap generation were performed on data transformed using the Variance Stabilizing Transformation (VST) implemented in DESeq2. PCA plots and heatmaps were built on the top genes/miRNAs with the highest variance (top 1000 for RNA-Sequencing; top 200 for miRNA-Sequencing) using the DESeq2 and the Pheatmap packages, respectively.

Box and whiskers plots showing the expression of genes of interest were drawn using the inbuilt R function, plotting  $\log_2\text{TPM}+1$ , where TPM indicates the Transcripts Per Million obtained with Tximport (see above). In the box and whiskers plot, the upper (Q3) and lower (Q1) quartile delimitate the box; the median value (Q2, middle quartile) is the inner line. The inter-quartile range (IQR) is the distance between upper and lower quartile. Upper and lower fences are calculated as:  $Q3 + (1.5 * \text{IQR})$  and  $Q1 - (1.5 * \text{IQR})$ , respectively. Whiskers mark the minimum and maximum observation inside fences.

The heatmap for genes of interest was built on the z-score of TPM using Morpheus (<https://software.broadinstitute.org/morpheus>).

## 5.6 Functional annotation analyses

Functional annotation of RNA-Sequencing data was carried out using Gene Set Enrichment Analysis (GSEA) (Mootha et al., 2003; Subramanian et al., 2005) and Over Representation Analysis (ORA).

GSEA was run in the pre-ranked mode using the broad institute GSEA desktop app (version 4.1.0) and a ranked list obtained ranking genes according to the  $-\log_{10}(\text{p-value}) * (\text{sign of } \log_2(\text{Fold-Change}))$  obtained from DESeq2 analysis comparing P-ES vs. C-ES (Plaisier et al., 2010).

Analysis was conducted with default options, including number of permutations=1000, enrichment statistic=weighted.



The following modifications to the default parameters were applied: Min size=5, Max size=2000, collapse/emap to gene symbols=no collapse.

GSEA was run against Gene Ontology-Biological Process (GO-BP) (c5.GP.BP.v7.4), hallmark (h.v7.4), PRC2\_EZH2\_UP.V1\_UP (Bracken et al., 2006) and NUYTEN\_EZH2\_TARGETS\_UP (Nuytten et al., 2008) gene sets downloaded from the Broad Institute Molecular Signatures Database (MSigDB v7.4). Other signatures evaluated by pre-ranked GSEA were built from literature datasets, including the published datasets EpiFactors (Medvedeva et al., 2015) and dbEM (Singh Nanda et al., 2016), and a dataset of genes down-regulated in cells over-expressing miR-24 (Lal et al., 2009).

ORA on GO-BP was carried out separately for genes significantly up- and down-regulated between P-ES and C-ES samples by using Metascape (version 3.8.2) (Zhou et al., 2019), which also provided the cytoscape networks of enriched terms.

Differentially expressed miRNAs were used as input for a search in the Functional MTI dataset of MirTarBase (Huang et al., 2020) to identify targets experimentally validated with strong evidence. Anti-correlation analysis was performed between CPM (Counts Per Million) values for each DE miR and TPM values for the identified respective targets by the Spearman rank correlation test using the R core package function cor.

MirDIP 4.1 database (Tokar et al., 2018) was employed to predict novel target genes for DE miRs. To this end, miRNA/target pairs annotated in MiRTarBase as experimentally validated with strong evidence were first removed from mirDIP database. On the remaining pairs, the mirDIP integrated rank was used to select the top 5% predicted target genes for each DE miR, and the resulting miRNA/target gene pairs were used to perform anti-correlation analysis as described above. Only genes having Spearman correlation scores  $\leq -0.5$  and p-values  $\leq 0.05$  with their predicted targeting DE miR were functionally annotated by ORA in Metascape against the GO-BP dataset. The analysis was conducted separately for genes anti-correlated with up-regulated and down-regulated DE miRs.

## **5.7 Cell cultures and miRNA mimics transfection**

The human epithelioid sarcoma cell line HS-ES-2R (RRID: CVCL\_8715) was purchased from RIKEN. Cells were cultured in high glucose Dulbecco's Modified Eagle's Medium (Gibco, ThermoFisher Scientific) supplemented with 10% Fetal Bovine Serum (FBS) (Gibco, ThermoFisher Scientific) and maintained at 37°C with 5% CO<sub>2</sub>. Transfection with mirVana miRNA mimics or Negative Control #1 (ThermoFisher Scientific) was performed with DharmaFECT 4 siRNA Transfection Reagent (Horizon Discovery) following manufacturer's instructions. Cells were

seeded in 6-well plates at a seeding density of 200'000 cells/well, transfected with miRNA mimics or NC#1 at a final concentration of 30nM, grown under standard conditions and harvested 48-72h post-transfection.

## 5.8 Quantitative Real-Time PCR

Total RNA (500ng) was reverse-transcribed into cDNA using the Superscript III reverse transcriptase following manufacturer's instructions (ThermoFisher Scientific). Quantitative Real-Time PCR was performed on cDNA using SsoFast Evagreen Supermix (Biorad) following product's protocol. The expression of the genes of interest was calculated using the Bio-Rad CFX manager software ( $\Delta\Delta C_t$  calculation) normalizing their expression on two housekeeping genes (GAPDH and SF3A1). Primers used are listed in table 5.1.

Target gene	Forward primer	Reverse primer
<b>GAPDH</b>	TCACCAGGGCTGCTTTTAAC	TGACAAGCTTCCCGTTCTCA
<b>SF3A1</b>	TTGTTGACAAGACTGCCAGC	TAGCTTCAAATTCAGGCCCGT
<b>EZH2</b>	CTGCTTCCTACATCGTAAGTGC	TGTTGGGTGTTGCATGAAAAGAATA
<b>MYC</b>	GTAGTGGAAAACCAGCAGCCT	CGAGTCGTAGTCGAGGTCAT
<b>HELLS</b>	TTGTCTGTGGCCCTTTGTCT	TTGACGTTCCCTCCTGGGTTTC

**Table 5.1: primers used in RT-qPCR.**

GAPDH: glyceraldehyde 3-phosphate dehydrogenase, SF3A1: Splicing Factor 3a Subunit 1, EZH2: Enhancer Of Zeste 2 Polycomb Repressive Complex 2 Subunit, MYC: MYC Proto-Oncogene, BHLH Transcription Factor, HELLS: Helicase, Lymphoid Specific

## 5.9 Western blotting

Cells were lysed in 1X Laemmli sample buffer. Samples were separated by SDS-polyacrylamide gel electrophoresis on 4-15% TGX stain-free gels (BioRad) and transferred onto nitrocellulose membranes (Sartorius Stedim Biotech GmbH). Membranes were incubated with the following primary antibodies: anti-HELLS (sc-46665, Santa Cruz Biotechnology), anti-GAPDH (sc-32233 Santa Cruz Biotechnology). Primary antibodies were detected with anti-mouse HRP-conjugated antibodies (Perkin Elmer). Blots were visualized by enhanced Chemiluminescence (Western Lightning Plus-ECL reagent, Perkin Elmer) and imaged on a Chemidoc XRS+ Imaging System (BioRad). The Image-Lab software was employed to for the densitometric analysis and image output (BioRad).

## **6. REFERENCES**

- Abeshouse, A., Adebamowo, C., Adebamowo, S. N., Akbani, R., Akeredolu, T., Ally, A., Anderson, M. L., Anur, P., Appelbaum, E. L., Armenia, J., Auman, J. T., Bailey, M. H., Baker, L., Balasundaram, M., Balu, S., Barthel, F. P., Bartlett, J., Baylin, S. B., Behera, M., ... Zmuda, E. (2017). Comprehensive and Integrated Genomic Characterization of Adult Soft Tissue Sarcomas. *Cell*, *171*(4), 950–965.e28. <https://doi.org/10.1016/j.cell.2017.10.014>
- Agaimy, A. (2014). The expanding family of SMARCB1(INI1)-deficient neoplasia: Implications of phenotypic, biological, and molecular heterogeneity. *Advances in Anatomic Pathology*, *21*(6), 394–410. <https://doi.org/10.1097/PAP.0000000000000038>
- Akgül, B., & Erdoğan, İ. (2018). Intracytoplasmic Re-localization of miRISC Complexes. *Frontiers in Genetics*, *9*, 403. <https://doi.org/10.3389/fgene.2018.00403>
- Alam, H., Gu, B., & Lee, M. G. (2015). Histone methylation modifiers in cellular signaling pathways. *Cellular and Molecular Life Sciences*, *72*(23), 4577–4592. <https://doi.org/10.1007/s00018-015-2023-y>
- Alekseyenko, A. A., Gorchakov, A. A., Kharchenko, P. V., & Kuroda, M. I. (2014). Reciprocal interactions of human C10orf12 and C17orf96 with PRC2 revealed by BioTAP-XL cross-linking and affinity purification. *Proceedings of the National Academy of Sciences of the United States of America*, *111*(7), 2488–2493. <https://doi.org/10.1073/pnas.1400648111>
- Allfrey, V. G., Faulkner, R., & Mirsky, A. E. (1964). ACETYLATION AND METHYLATION OF HISTONES AND THEIR POSSIBLE ROLE IN THE REGULATION OF RNA SYNTHESIS. *Proceedings of the National Academy of Sciences of the United States of America*, *51*, 786–794. <https://doi.org/10.1073/pnas.51.5.786>
- Alpsoy, A., & Dykhuizen, E. C. (2018). Glioma tumor suppressor candidate region gene 1 (GLTSCR1) and its paralog GLTSCR1-like form SWI/SNF chromatin remodeling subcomplexes. *The Journal of Biological Chemistry*, *293*(11), 3892–3903. <https://doi.org/10.1074/jbc.RA117.001065>
- Bajpai, R., Chen, D. A., Rada-Iglesias, A., Zhang, J., Xiong, Y., Helms, J., Chang, C.-P., Zhao, Y., Swigut, T., & Wysocka, J. (2010). CHD7 cooperates with PBAF to control multipotent neural crest formation. *Nature*, *463*(7283), 958–962. <https://doi.org/10.1038/nature08733>
- Baratti, D., Pennacchioli, E., Casali, P. G., Bertulli, R., Lozza, L., Olmi, P., Collini, P., Radaelli, S., Fiore, M., & Gronchi, A. (2007). Epithelioid sarcoma: Prognostic factors and survival in a series of patients treated at a single institution. *Annals of Surgical Oncology*, *14*(12), 3542–3551. <https://doi.org/10.1245/s10434-007-9628-9>
- Barber, B. A., & Rastegar, M. (2010). Epigenetic control of Hox genes during neurogenesis, development, and disease. *Annals of Anatomy = Anatomischer Anzeiger: Official Organ of the Anatomische Gesellschaft*, *192*(5), 261–274. <https://doi.org/10.1016/j.aanat.2010.07.009>
- Bartel, D. P. (2004). MicroRNAs: Genomics, biogenesis, mechanism, and function. *Cell*, *116*(2), 281–297. [https://doi.org/10.1016/s0092-8674\(04\)00045-5](https://doi.org/10.1016/s0092-8674(04)00045-5)
- Bartel, D. P. (2009). MicroRNAs: Target Recognition and Regulatory Functions. *Cell*, *136*(2), 215–233. <https://doi.org/10.1016/j.cell.2009.01.002>
- Baylin, S. B., & Jones, P. A. (2011). A decade of exploring the cancer epigenome—Biological and translational implications. *Nature Reviews. Cancer*, *11*(10), 726–734. <https://doi.org/10.1038/nrc3130>
- Berman, B. P., Weisenberger, D. J., Aman, J. F., Hinoue, T., Ramjan, Z., Liu, Y., Noushmehr, H., Lange, C. P. E., van Dijk, C. M., Tollenaar, R. A. E. M., Van Den Berg, D., & Laird, P. W. (2011). Regions of focal DNA hypermethylation and long-range hypomethylation in colorectal cancer coincide with nuclear lamina-associated domains. *Nature Genetics*, *44*(1), 40–46. <https://doi.org/10.1038/ng.969>

- Bolger, A. M., Lohse, M., & Usadel, B. (2014). Trimmomatic: A flexible trimmer for Illumina sequence data. *Bioinformatics (Oxford, England)*, *30*(15), 2114–2120. <https://doi.org/10.1093/bioinformatics/btu170>
- Bracken, A. P., Dietrich, N., Pasini, D., Hansen, K. H., & Helin, K. (2006). Genome-wide mapping of Polycomb target genes unravels their roles in cell fate transitions. *Genes & Development*, *20*(9), 1123–1136. <https://doi.org/10.1101/gad.381706>
- Brenca, M., Rossi, S., Lorenzetto, E., Piccinin, E., Piccinin, S., Rossi, F. M., Giuliano, A., Dei Tos, A. P., Maestro, R., & Modena, P. (2013). *SMARCB1 / INI1* Genetic Inactivation Is Responsible for Tumorigenic Properties of Epithelioid Sarcoma Cell Line VAESBJ. *Molecular Cancer Therapeutics*, *12*(6), 1060–1072. <https://doi.org/10.1158/1535-7163.MCT-13-0005>
- Burdach, S., Plehm, S., Unland, R., Dirksen, U., Borkhardt, A., Staeger, M. S., Müller-Tidow, C., & Richter, G. H. S. (2009). Epigenetic maintenance of stemness and malignancy in peripheral neuroectodermal tumors by EZH2. *Cell Cycle (Georgetown, Tex.)*, *8*(13), 1991–1996. <https://doi.org/10.4161/cc.8.13.8929>
- Callister, M. D., Ballo, M. T., Pisters, P. W., Patel, S. R., Feig, B. W., Pollock, R. E., Benjamin, R. S., & Zagars, G. K. (2001). Epithelioid sarcoma: Results of conservative surgery and radiotherapy. *International Journal of Radiation Oncology, Biology, Physics*, *51*(2), 384–391. [https://doi.org/10.1016/s0360-3016\(01\)01646-7](https://doi.org/10.1016/s0360-3016(01)01646-7)
- Cascio, M. J., O'Donnell, R. J., & Horvai, A. E. (2010). Epithelioid sarcoma expresses epidermal growth factor receptor but gene amplification and kinase domain mutations are rare. *Modern Pathology*, *23*(4), 574–580. <https://doi.org/10.1038/modpathol.2010.2>
- Centore, R. C., Sandoval, G. J., Soares, L. M. M., Kadoch, C., & Chan, H. M. (2020). Mammalian SWI/SNF Chromatin Remodeling Complexes: Emerging Mechanisms and Therapeutic Strategies. *Trends in Genetics*, *36*(12), 936–950. <https://doi.org/10.1016/j.tig.2020.07.011>
- Ch, W. (1959). Canalization of development and genetic assimilation of acquired characters. *Nature*, *183*(4676). <https://doi.org/10.1038/1831654a0>
- Chase, D. R., & Enzinger, F. M. (1985). Epithelioid sarcoma. Diagnosis, prognostic indicators, and treatment. *The American Journal of Surgical Pathology*, *9*(4), 241–263.
- Chen, Q. W., Zhu, X. Y., Li, Y. Y., & Meng, Z. Q. (2014). Epigenetic regulation and cancer (Review). *ONCOLOGY REPORTS*, *10*.
- Chen, Y., Zhang, H., Xu, Z., Tang, H., Geng, A., Cai, B., Su, T., Shi, J., Jiang, C., Tian, X., Seluanov, A., Huang, J., Wan, X., Jiang, Y., Gorbunova, V., & Mao, Z. (2019). A PARP1-BRG1-SIRT1 axis promotes HR repair by reducing nucleosome density at DNA damage sites. *Nucleic Acids Research*, *47*(16), 8563–8580. <https://doi.org/10.1093/nar/gkz592>
- Clapier, C. R., Längst, G., Corona, D. F., Becker, P. B., & Nightingale, K. P. (2001). Critical role for the histone H4 N terminus in nucleosome remodeling by ISWI. *Molecular and Cellular Biology*, *21*(3), 875–883. <https://doi.org/10.1128/MCB.21.3.875-883.2001>
- Cordoba, J. C., Parham, D. M., Meyer, W. H., & Douglass, E. C. (1994). A new cytogenetic finding in an epithelioid sarcoma, t(8;22)(q22;q11). *Cancer Genetics and Cytogenetics*, *72*(2), 151–154. [https://doi.org/10.1016/0165-4608\(94\)90132-5](https://doi.org/10.1016/0165-4608(94)90132-5)
- Dal Cin, P., Van den Berghe, H., & Pauwels, P. (1999). Epithelioid sarcoma of the proximal type with complex karyotype including i(8q). *Cancer Genetics and Cytogenetics*, *114*(1), 80–82. [https://doi.org/10.1016/s0165-4608\(99\)00034-5](https://doi.org/10.1016/s0165-4608(99)00034-5)
- Debiec-Rychter, M., Sciot, R., & Hagemeyer, A. (2000). Common chromosome aberrations in the proximal type of epithelioid sarcoma. *Cancer Genetics and Cytogenetics*, *123*(2), 133–136. [https://doi.org/10.1016/s0165-4608\(00\)00320-4](https://doi.org/10.1016/s0165-4608(00)00320-4)

- Di Leva, G., Garofalo, M., & Croce, C. M. (2014). MicroRNAs in Cancer. *Annual Review of Pathology: Mechanisms of Disease*, 9(1), 287–314. <https://doi.org/10.1146/annurev-pathol-012513-104715>
- Dickson, M. A., Schwartz, G. K., Keohan, M. L., D'Angelo, S. P., Gounder, M. M., Chi, P., Antonescu, C. R., Landa, J., Qin, L.-X., Crago, A. M., Singer, S., Koff, A., & Tap, W. D. (2016). Progression-Free Survival Among Patients With Well-Differentiated or Dedifferentiated Liposarcoma Treated With CDK4 Inhibitor Palbociclib: A Phase 2 Clinical Trial. *JAMA Oncology*, 2(7), 937–940. <https://doi.org/10.1001/jamaoncol.2016.0264>
- Dirscherl, S. S., & Krebs, J. E. (2011). Functional diversity of ISWI complexes. *Biochemistry and Cell Biology*. <https://doi.org/10.1139/o04-044>
- Dobin, A., Davis, C. A., Schlesinger, F., Drenkow, J., Zaleski, C., Jha, S., Batut, P., Chaisson, M., & Gingeras, T. R. (2013). STAR: Ultrafast universal RNA-seq aligner. *Bioinformatics (Oxford, England)*, 29(1), 15–21. <https://doi.org/10.1093/bioinformatics/bts635>
- Enzinger, F. M. (1970). Epithelioid sarcoma. A sarcoma simulating a granuloma or a carcinoma. *Cancer*, 26(5), 1029–1041. [https://doi.org/10.1002/1097-0142\(197011\)26:5<1029::aid-cncr2820260510>3.0.co;2-r](https://doi.org/10.1002/1097-0142(197011)26:5<1029::aid-cncr2820260510>3.0.co;2-r)
- Evans, H. L., & Baer, S. C. (1993). Epithelioid sarcoma: A clinicopathologic and prognostic study of 26 cases. *Seminars in Diagnostic Pathology*, 10(4), 286–291.
- Fisher, C. (1988). Epithelioid sarcoma: The spectrum of ultrastructural differentiation in seven immunohistochemically defined cases. *Human Pathology*, 19(3), 265–275. [https://doi.org/10.1016/s0046-8177\(88\)80519-7](https://doi.org/10.1016/s0046-8177(88)80519-7)
- Fisher, C. (1990). The value of electronmicroscopy and immunohistochemistry in the diagnosis of soft tissue sarcomas: A study of 200 cases. *Histopathology*, 16(5), 441–454. <https://doi.org/10.1111/j.1365-2559.1990.tb01543.x>
- Fisher, C. (2006). Epithelioid sarcoma of Enzinger. *Advances in Anatomic Pathology*, 13(3), 114–121. <https://doi.org/10.1097/00125480-200605000-00002>
- Forbes, S. A., Bindal, N., Bamford, S., Cole, C., Kok, C. Y., Beare, D., Jia, M., Shepherd, R., Leung, K., Menzies, A., Teague, J. W., Campbell, P. J., Stratton, M. R., & Futreal, P. A. (2011). COSMIC: Mining complete cancer genomes in the Catalogue of Somatic Mutations in Cancer. *Nucleic Acids Research*, 39(Database issue), D945-950. <https://doi.org/10.1093/nar/gkq929>
- Frezza, A. M., Jones, R. L., Lo Vullo, S., Asano, N., Lucibello, F., Ben-Ami, E., Ratan, R., Teterycz, P., Boye, K., Brahmi, M., Palmerini, E., Fedenko, A., Vincenzi, B., Brunello, A., Desai, I. M. E., Benjamin, R. S., Blay, J. Y., Broto, J. M., Casali, P. G., ... Stacchiotti, S. (2018). Anthracycline, Gemcitabine, and Pazopanib in Epithelioid Sarcoma: A Multi-institutional Case Series. *JAMA Oncology*, 4(9), e180219. <https://doi.org/10.1001/jamaoncol.2018.0219>
- Frezza, A. M., Sbaraglia, M., Lo Vullo, S., Baldi, G. G., Simeone, N., Frenos, F., Campanacci, D., Stacchiotti, S., Pasquali, S., Callegaro, D., Gambarotti, M., Barisella, M., Palomba, A., Mariani, L., Casali, P. G., Dei Tos, A. P., & Gronchi, A. (2020). The natural history of epithelioid sarcoma. A retrospective multicentre case-series within the Italian Sarcoma Group. *European Journal of Surgical Oncology: The Journal of the European Society of Surgical Oncology and the British Association of Surgical Oncology*. <https://doi.org/10.1016/j.ejso.2020.03.215>
- Friedman, R. C., Farh, K. K.-H., Burge, C. B., & Bartel, D. P. (2009). Most mammalian mRNAs are conserved targets of microRNAs. *Genome Research*, 19(1), 92–105. <https://doi.org/10.1101/gr.082701.108>

- Gerhold, C. B., & Gasser, S. M. (2014). INO80 and SWR complexes: Relating structure to function in chromatin remodeling. *Trends in Cell Biology*, 24(11), 619–631. <https://doi.org/10.1016/j.tcb.2014.06.004>
- Gounder, M., Schöffski, P., Jones, R. L., Agulnik, M., Cote, G. M., Villalobos, V. M., Attia, S., Chugh, R., Chen, T. W.-W., Jahan, T., Loggers, E. T., Gupta, A., Italiano, A., Demetri, G. D., Ratan, R., Davis, L. E., Mir, O., Dileo, P., Van Tine, B. A., ... Stacchiotti, S. (2020). Tazemetostat in advanced epithelioid sarcoma with loss of INI1/SMARCB1: An international, open-label, phase 2 basket study. *The Lancet Oncology*, 21(11), 1423–1432. [https://doi.org/10.1016/S1470-2045\(20\)30451-4](https://doi.org/10.1016/S1470-2045(20)30451-4)
- Grünewald, T. G., Alonso, M., Avnet, S., Banito, A., Burdach, S., Cidre-Aranaz, F., Di Pompo, G., Distel, M., Dorado-Garcia, H., Garcia-Castro, J., González-González, L., Grigoriadis, A. E., Kasan, M., Koelsche, C., Krumbholz, M., Lecanda, F., Lemma, S., Longo, D. L., Madrigal-Esquível, C., ... Heymann, D. (2020). Sarcoma treatment in the era of molecular medicine. *EMBO Molecular Medicine*, 12(11). <https://doi.org/10.15252/emmm.201911131>
- Gu, J., Wang, J., You, A., Li, J., Zhang, Y., Rao, G., Ge, X., Zhang, K., Liu, X., & Wang, D. (2021). MiR-137 inhibits the proliferation, invasion and migration of glioma via targeting to regulate EZH2. *Genes & Genomics*, 43(10), 1157–1165. <https://doi.org/10.1007/s13258-021-01117-9>
- Guillou, L., Wadden, C., Coindre, J. M., Krausz, T., & Fletcher, C. D. (1997). “Proximal-type” epithelioid sarcoma, a distinctive aggressive neoplasm showing rhabdoid features. Clinicopathologic, immunohistochemical, and ultrastructural study of a series. *The American Journal of Surgical Pathology*, 21(2), 130–146. <https://doi.org/10.1097/00000478-199702000-00002>
- Guzzetta, A. A., Montgomery, E. A., Lyu, H., Hooker, C. M., Meyer, C. F., Loeb, D. M., Frassica, D., Weber, K. L., & Ahuja, N. (2012). Epithelioid sarcoma: One institution’s experience with a rare sarcoma. *The Journal of Surgical Research*, 177(1), 116–122. <https://doi.org/10.1016/j.jss.2012.04.030>
- Ha, M., & Kim, V. N. (2014). Regulation of microRNA biogenesis. *Nature Reviews. Molecular Cell Biology*, 15(8), 509–524. <https://doi.org/10.1038/nrm3838>
- Hamiche, A., Kang, J.-G., Dennis, C., Xiao, H., & Wu, C. (2001). Histone tails modulate nucleosome mobility and regulate ATP-dependent nucleosome sliding by NURF. *Proceedings of the National Academy of Sciences*, 98(25), 14316–14321. <https://doi.org/10.1073/pnas.251421398>
- Han, M., Li, J., Cao, Y., Huang, Y., Li, W., Zhu, H., Zhao, Q., Han, J.-D. J., Wu, Q., Li, J., Feng, J., & Wong, J. (2020). A role for LSH in facilitating DNA methylation by DNMT1 through enhancing UHRF1 chromatin association. *Nucleic Acids Research*, 48(21), 12116–12134. <https://doi.org/10.1093/nar/gkaa1003>
- Haraguchi, T., Miyoshi, H., Hiraoka, K., Yokoyama, S., Ishibashi, Y., Hashiguchi, T., Matsuda, K., Hamada, T., Okawa, T., Shiba, N., & Ohshima, K. (2016). GATA3 Expression Is a Poor Prognostic Factor in Soft Tissue Sarcomas. *PloS One*, 11(6), e0156524. <https://doi.org/10.1371/journal.pone.0156524>
- Hasegawa, T., Matsuno, Y., Shimoda, T., Umeda, T., Yokoyama, R., & Hirohashi, S. (2001). Proximal-Type Epithelioid Sarcoma: A Clinicopathologic Study of 20 Cases. *Modern Pathology*, 14(7), 655–663. <https://doi.org/10.1038/modpathol.3880368>
- Hayes, J., Peruzzi, P. P., & Lawler, S. (2014). MicroRNAs in cancer: Biomarkers, functions and therapy. *Trends in Molecular Medicine*, 20(8), 460–469. <https://doi.org/10.1016/j.molmed.2014.06.005>

- Hodges, C., Kirkland, J. G., & Crabtree, G. R. (2016). The Many Roles of BAF (mSWI/SNF) and PBAF Complexes in Cancer. *Cold Spring Harbor Perspectives in Medicine*, 6(8). <https://doi.org/10.1101/cshperspect.a026930>
- Hollmann, T. J., & Hornick, J. L. (2011). INI1-deficient tumors: Diagnostic features and molecular genetics. *The American Journal of Surgical Pathology*, 35(10), e47-63. <https://doi.org/10.1097/PAS.0b013e31822b325b>
- Hornick, J. L., Dal Cin, P., & Fletcher, C. D. M. (2009). Loss of INI1 Expression is Characteristic of Both Conventional and Proximal-type Epithelioid Sarcoma. *American Journal of Surgical Pathology*, 33(4), 542–550. <https://doi.org/10.1097/PAS.0b013e3181882c54>
- Hoy, S. M. (2020). Tazemetostat: First Approval. *Drugs*, 80(5), 513–521. <https://doi.org/10.1007/s40265-020-01288-x>
- Huang, H.-Y., Lin, Y.-C.-D., Li, J., Huang, K.-Y., Shrestha, S., Hong, H.-C., Tang, Y., Chen, Y.-G., Jin, C.-N., Yu, Y., Xu, J.-T., Li, Y.-M., Cai, X.-X., Zhou, Z.-Y., Chen, X.-H., Pei, Y.-Y., Hu, L., Su, J.-J., Cui, S.-D., ... Huang, H.-D. (2020). miRTarBase 2020: Updates to the experimentally validated microRNA-target interaction database. *Nucleic Acids Research*, 48(D1), D148–D154. <https://doi.org/10.1093/nar/gkz896>
- Hyun, K., Jeon, J., Park, K., & Kim, J. (2017). Writing, erasing and reading histone lysine methylations. *Experimental & Molecular Medicine*, 49(4), e324. <https://doi.org/10.1038/emm.2017.11>
- Imura, Y., Yasui, H., Outani, H., Wakamatsu, T., Hamada, K., Nakai, T., Yamada, S., Myoui, A., Araki, N., Ueda, T., Itoh, K., Yoshikawa, H., & Naka, N. (2014). Combined targeting of mTOR and c-MET signaling pathways for effective management of epithelioid sarcoma. *Molecular Cancer*, 13(1), 185. <https://doi.org/10.1186/1476-4598-13-185>
- Ino, Y., Gotoh, M., Sakamoto, M., Tsukagoshi, K., & Hirohashi, S. (2002). Dysadherin, a cancer-associated cell membrane glycoprotein, down-regulates E-cadherin and promotes metastasis. *Proceedings of the National Academy of Sciences of the United States of America*, 99(1), 365–370. <https://doi.org/10.1073/pnas.012425299>
- Iorio, M. V., Piovan, C., & Croce, C. M. (2010). Interplay between microRNAs and the epigenetic machinery: An intricate network. *Biochimica Et Biophysica Acta*, 1799(10–12), 694–701. <https://doi.org/10.1016/j.bbagr.2010.05.005>
- Italiano, A. (2018). *Tazemetostat, an EZH2 inhibitor, in relapsed or refractory B-cell non-Hodgkin lymphoma and advanced solid tumours: A first-in-human, open-label, phase I study*. 19, 11.
- Iwasaki, H., Ohjimi, Y., Ishiguro, M., Isayama, T., Kaneko, Y., Yoh, S., Emoto, G., & Kikuchi, M. (1996). Epithelioid sarcoma with an 18q aberration. *Cancer Genetics and Cytogenetics*, 91(1), 46–52. [https://doi.org/10.1016/s0165-4608\(95\)00315-0](https://doi.org/10.1016/s0165-4608(95)00315-0)
- Izumi, T., Oda, Y., Hasegawa, T., Nakanishi, Y., Iwasaki, H., Sonobe, H., Goto, H., Kusakabe, H., Takahira, T., Kobayashi, C., Kawaguchi, K., Saito, T., Yamamoto, H., Tamiya, S., Iwamoto, Y., & Tsuneyoshi, M. (2006). Prognostic significance of dysadherin expression in epithelioid sarcoma and its diagnostic utility in distinguishing epithelioid sarcoma from malignant rhabdoid tumor. *Modern Pathology*, 19(6), 820–831. <https://doi.org/10.1038/modpathol.3800599>
- Jamshidi, F., Bashashati, A., Shumansky, K., Dickson, B., Gokgoz, N., Wunder, J. S., Andrulis, I. L., Lazar, A. J., Shah, S. P., Huntsman, D. G., & Nielsen, T. O. (2016). The genomic landscape of epithelioid sarcoma cell lines and tumours. *The Journal of Pathology*, 238(1), 63–73. <https://doi.org/10.1002/path.4636>
- Jawad, M. U., Extein, J., Min, E. S., & Scully, S. P. (2009). Prognostic factors for survival in patients with epithelioid sarcoma: 441 cases from the SEER database. *Clinical Orthopaedics and Related Research*, 467(11), 2939–2948. <https://doi.org/10.1007/s11999-009-0749-2>



- Jin, C., Zang, C., Wei, G., Cui, K., Peng, W., Zhao, K., & Felsenfeld, G. (2009). H3.3/H2A.Z double variant-containing nucleosomes mark “nucleosome-free regions” of active promoters and other regulatory regions. *Nature Genetics*, *41*(8), 941–945. <https://doi.org/10.1038/ng.409>
- Jones, R. L., Constantinidou, A., Olmos, D., Thway, K., Fisher, C., Al-Muderis, O., Scurr, M., & Judson, I. R. (2012). Role of palliative chemotherapy in advanced epithelioid sarcoma. *American Journal of Clinical Oncology*, *35*(4), 351–357. <https://doi.org/10.1097/COC.0b013e3182118cf7>
- Kadoch, C., Copeland, R. A., & Keilhack, H. (2016). PRC2 and SWI/SNF Chromatin Remodeling Complexes in Health and Disease. *Biochemistry*, *55*(11), 1600–1614. <https://doi.org/10.1021/acs.biochem.5b01191>
- Kadoch, C., & Crabtree, G. R. (2013). Reversible disruption of mSWI/SNF (BAF) complexes by the SS18-SSX oncogenic fusion in synovial sarcoma. *Cell*, *153*(1), 71–85. <https://doi.org/10.1016/j.cell.2013.02.036>
- Kadoch, C., Hargreaves, D. C., Hodges, C., Elias, L., Ho, L., Ranish, J., & Crabtree, G. R. (2013). Proteomic and bioinformatic analysis of mammalian SWI/SNF complexes identifies extensive roles in human malignancy. *Nature Genetics*, *45*(6), 592–601. <https://doi.org/10.1038/ng.2628>
- Kadoch, C., Williams, R. T., Calarco, J. P., Miller, E. L., Weber, C. M., Braun, S. M. G., Pulice, J. L., Chory, E. J., & Crabtree, G. R. (2017). Dynamics of BAF-Polycomb complex opposition on heterochromatin in normal and oncogenic states. *Nature Genetics*, *49*(2), 213–222. <https://doi.org/10.1038/ng.3734>
- Kakarougkas, A., Ismail, A., Chambers, A. L., Riballo, E., Herbert, A. D., Künzel, J., Löbrich, M., Jeggo, P. A., & Downs, J. A. (2014). Requirement for PBAF in transcriptional repression and repair at DNA breaks in actively transcribed regions of chromatin. *Molecular Cell*, *55*(5), 723–732. <https://doi.org/10.1016/j.molcel.2014.06.028>
- Kelley, D. E., Stokes, D. G., & Perry, R. P. (1999). CHD1 interacts with SSRP1 and depends on both its chromodomain and its ATPase/helicase-like domain for proper association with chromatin. *Chromosoma*, *108*(1), 10–25. <https://doi.org/10.1007/s004120050347>
- Klement, K., Luijsterburg, M. S., Pinder, J. B., Cena, C. S., Del Nero, V., Wintersinger, C. M., Dellaire, G., van Attikum, H., & Goodarzi, A. A. (2014). Opposing ISWI- and CHD-class chromatin remodeling activities orchestrate heterochromatic DNA repair. *Journal of Cell Biology*, *207*(6), 717–733. <https://doi.org/10.1083/jcb.201405077>
- Kohashi, K., Yamada, Y., Hotokebuchi, Y., Yamamoto, H., Taguchi, T., Iwamoto, Y., & Oda, Y. (2015). ERG and SALL4 expressions in SMARCB1/INI1-deficient tumors: A useful tool for distinguishing epithelioid sarcoma from malignant rhabdoid tumor. *Human Pathology*, *46*(2), 225–230. <https://doi.org/10.1016/j.humpath.2014.10.010>
- Koontz, J. I., Soreng, A. L., Nucci, M., Kuo, F. C., Pauwels, P., van Den Berghe, H., Dal Cin, P., Fletcher, J. A., & Sklar, J. (2001). Frequent fusion of the JAZF1 and JJAZ1 genes in endometrial stromal tumors. *Proceedings of the National Academy of Sciences of the United States of America*, *98*(11), 6348–6353. <https://doi.org/10.1073/pnas.101132598>
- Kozomara, A., Birgaoanu, M., & Griffiths-Jones, S. (2019). miRBase: From microRNA sequences to function. *Nucleic Acids Research*, *47*(Database issue), D155–D162. <https://doi.org/10.1093/nar/gky1141>
- Krol, J., Loedige, I., & Filipowicz, W. (2010). The widespread regulation of microRNA biogenesis, function and decay. *Nature Reviews Genetics*, *11*(9), 597–610. <https://doi.org/10.1038/nrg2843>
- Kusch, T., Florens, L., MacDonald, W. H., Swanson, S. K., Glaser, R. L., Yates, J. R., Abmayr, S. M., Washburn, M. P., & Workman, J. L. (2004). Acetylation by Tip60 Is Required for

- Selective Histone Variant Exchange at DNA Lesions. *Science*, 306(5704), 2084–2087. <https://doi.org/10.1126/science.1103455>
- Kuzmichev, A., Nishioka, K., Erdjument-Bromage, H., Tempst, P., & Reinberg, D. (2002). Histone methyltransferase activity associated with a human multiprotein complex containing the Enhancer of Zeste protein. *Genes & Development*, 16(22), 2893–2905. <https://doi.org/10.1101/gad.1035902>
- Kwon, H., Imbalzano, A. N., Khavari, P. A., Kingston, R. E., & Green, M. R. (1994). Nucleosome disruption and enhancement of activator binding by a human SW1/SNF complex. *Nature*, 370(6489), 477–481. <https://doi.org/10.1038/370477a0>
- Lal, A., Navarro, F., Maher, C. A., Maliszewski, L. E., Yan, N., O'Day, E., Chowdhury, D., Dykxhoorn, D. M., Tsai, P., Hofmann, O., Becker, K. G., Gorospe, M., Hide, W., & Lieberman, J. (2009). MiR-24 Inhibits cell proliferation by targeting E2F2, MYC, and other cell-cycle genes via binding to “seedless” 3'UTR microRNA recognition elements. *Molecular Cell*, 35(5), 610–625. <https://doi.org/10.1016/j.molcel.2009.08.020>
- Laskin, W. B., & Miettinen, M. (2003). Epithelioid sarcoma: New insights based on an extended immunohistochemical analysis. *Archives of Pathology & Laboratory Medicine*, 127(9), 1161–1168. [https://doi.org/10.1043/1543-2165\(2003\)127<1161:ESNIBO>2.0.CO;2](https://doi.org/10.1043/1543-2165(2003)127<1161:ESNIBO>2.0.CO;2)
- Lazzaro, M. A., & Picketts, D. J. (2001). Cloning and characterization of the murine Imitation Switch (ISWI) genes: Differential expression patterns suggest distinct developmental roles for Snf2h and Snf2l. *Journal of Neurochemistry*, 77(4), 1145–1156. <https://doi.org/10.1046/j.1471-4159.2001.00324.x>
- Le Loarer, F., Zhang, L., Fletcher, C. D., Ribeiro, A., Singer, S., Italiano, A., Neuville, A., Houlier, A., Chibon, F., Coindre, J.-M., & Antonescu, C. R. (2014). Consistent SMARCB1 homozygous deletions in epithelioid sarcoma and in a subset of myoepithelial carcinomas can be reliably detected by FISH in archival material. *Genes, Chromosomes & Cancer*, 53(6), 475–486. <https://doi.org/10.1002/gcc.22159>
- Lee, R. C., Feinbaum, R. L., & Ambros, V. (1993). The *C. elegans* heterochronic gene *lin-4* encodes small RNAs with antisense complementarity to *lin-14*. *Cell*, 75(5), 843–854. [https://doi.org/10.1016/0092-8674\(93\)90529-y](https://doi.org/10.1016/0092-8674(93)90529-y)
- Lee, S.-H., Chen, T.-Y., Dhar, S. S., Gu, B., Chen, K., Kim, Y. Z., Li, W., & Lee, M. G. (2016). A feedback loop comprising PRMT7 and miR-24-2 interplays with Oct4, Nanog, Klf4 and c-Myc to regulate stemness. *Nucleic Acids Research*, 44(22), 10603–10618. <https://doi.org/10.1093/nar/gkw788>
- Lee, S.-K., Park, E.-J., Lee, H.-S., Lee, Y. S., & Kwon, J. (2012). Genome-wide screen of human bromodomain-containing proteins identifies *Cecr2* as a novel DNA damage response protein. *Molecules and Cells*, 34(1), 85–91. <https://doi.org/10.1007/s10059-012-0112-4>
- Lee, W., Teckie, S., Wiesner, T., Ran, L., Prieto Granada, C. N., Lin, M., Zhu, S., Cao, Z., Liang, Y., Sboner, A., Tap, W. D., Fletcher, J. A., Huberman, K. H., Qin, L.-X., Viale, A., Singer, S., Zheng, D., Berger, M. F., Chen, Y., ... Chi, P. (2014). PRC2 is recurrently inactivated through EED or SUZ12 loss in malignant peripheral nerve sheath tumors. *Nature Genetics*, 46(11), 1227–1232. <https://doi.org/10.1038/ng.3095>
- Leighton, G., & Williams, D. C. (2020). The Methyl-CpG-Binding Domain 2 and 3 Proteins and Formation of the Nucleosome Remodeling and Deacetylase Complex. *Journal of Molecular Biology*, 432(6), 1624–1639. <https://doi.org/10.1016/j.jmb.2019.10.007>
- Levy, A., Le Péchoux, C., Terrier, P., Bouaita, R., Domont, J., Mir, O., Coppola, S., Honoré, C., Le Cesne, A., & Bonvalot, S. (2014). Epithelioid sarcoma: Need for a multimodal approach to maximize the chances of curative conservative treatment. *Annals of Surgical Oncology*, 21(1), 269–276. <https://doi.org/10.1245/s10434-013-3247-4>

- Li, B., & Dewey, C. N. (2011). RSEM: Accurate transcript quantification from RNA-Seq data with or without a reference genome. *BMC Bioinformatics*, *12*, 323. <https://doi.org/10.1186/1471-2105-12-323>
- Li, H., Ilin, S., Wang, W., Duncan, E. M., Wysocka, J., Allis, C. D., & Patel, D. J. (2006). Molecular basis for site-specific read-out of histone H3K4me3 by the BPTF PHD finger of NURF. *Nature*, *442*(7098), 91–95. <https://doi.org/10.1038/nature04802>
- Li, Y., Cao, G., Tao, X., Guo, J., Wu, S., & Tao, Y. (2019). Clinicopathologic features of epithelioid sarcoma: Report of seventeen cases and review of literature. *International Journal of Clinical and Experimental Pathology*, *12*(8), 3042–3048.
- Lin, L., Skacel, M., Sigel, J. E., Bergfeld, W. F., Montgomery, E., Fisher, C., & Goldblum, J. R. (2003). Epithelioid sarcoma: An immunohistochemical analysis evaluating the utility of cytokeratin 5/6 in distinguishing superficial epithelioid sarcoma from spindled squamous cell carcinoma. *Journal of Cutaneous Pathology*, *30*(2), 114–117. <https://doi.org/10.1034/j.1600-0560.2002.00040.x>
- Love, M. I., Huber, W., & Anders, S. (2014). Moderated estimation of fold change and dispersion for RNA-seq data with DESeq2. *Genome Biology*, *15*(12), 550. <https://doi.org/10.1186/s13059-014-0550-8>
- Lualdi, E., Modena, P., Debiec-Rychter, M., Pedeutour, F., Teixeira, M. R., Facchinetti, F., Dagrada, G. P., Pilotti, S., & Sozzi, G. (2004). Molecular cytogenetic characterization of proximal-type epithelioid sarcoma. *Genes, Chromosomes & Cancer*, *41*(3), 283–290. <https://doi.org/10.1002/gcc.20086>
- Luijsterburg, M. S., de Krijger, I., Wiegant, W. W., Shah, R. G., Smeenk, G., de Groot, A. J. L., Pines, A., Vertegaal, A. C. O., Jacobs, J. J. L., Shah, G. M., & van Attikum, H. (2016). PARP1 Links CHD2-Mediated Chromatin Expansion and H3.3 Deposition to DNA Repair by Non-homologous End-Joining. *Molecular Cell*, *61*(4), 547–562. <https://doi.org/10.1016/j.molcel.2016.01.019>
- Manning, B. J., & Yusufzai, T. (2017). The ATP-dependent chromatin remodeling enzymes CHD6, CHD7, and CHD8 exhibit distinct nucleosome binding and remodeling activities. *Journal of Biological Chemistry*, *292*(28), 11927–11936. <https://doi.org/10.1074/jbc.M117.779470>
- Margol, A. S., & Judkins, A. R. (2014). Pathology and diagnosis of SMARCB1-deficient tumors. *Cancer Genetics*, *207*(9), 358–364. <https://doi.org/10.1016/j.cancergen.2014.07.004>
- Margueron, R., & Reinberg, D. (2011). The Polycomb complex PRC2 and its mark in life. *Nature*, *469*(7330), 343–349. <https://doi.org/10.1038/nature09784>
- Medjkane, S., Novikov, E., Versteeg, I., & Delattre, O. (2004). The tumor suppressor hSNF5/INI1 modulates cell growth and actin cytoskeleton organization. *Cancer Research*, *64*(10), 3406–3413. <https://doi.org/10.1158/0008-5472.CAN-03-3004>
- Medvedeva, Y. A., Lennartsson, A., Ehsani, R., Kulakovskiy, I. V., Vorontsov, I. E., Panahandeh, P., Khimulya, G., Kasukawa, T., FANTOM Consortium, & Drabløs, F. (2015). EpiFactors: A comprehensive database of human epigenetic factors and complexes. *Database: The Journal of Biological Databases and Curation*, *2015*, bav067. <https://doi.org/10.1093/database/bav067>
- Michel, B. C., D’Avino, A. R., Cassel, S. H., Mashtalir, N., McKenzie, Z. M., McBride, M. J., Valencia, A. M., Zhou, Q., Bocker, M., Soares, L. M. M., Pan, J., Remillard, D. I., Lareau, C. A., Zullo, H. J., Fortoul, N., Gray, N. S., Bradner, J. E., Chan, H. M., & Kadoch, C. (2018). A non-canonical SWI/SNF complex is a synthetic lethal target in cancers driven by BAF complex perturbation. *Nature Cell Biology*, *20*(12), 1410–1420. <https://doi.org/10.1038/s41556-018-0221-1>
- Miettinen, M., Fanburg-Smith, J. C., Virolainen, M., Shmookler, B. M., & Fetsch, J. F. (1999). Epithelioid sarcoma: An immunohistochemical analysis of 112 classical and variant cases

- and a discussion of the differential diagnosis. *Human Pathology*, 30(8), 934–942. [https://doi.org/10.1016/s0046-8177\(99\)90247-2](https://doi.org/10.1016/s0046-8177(99)90247-2)
- Miettinen, M., Wang, Z., Sarlomo-Rikala, M., Abdullaev, Z., Pack, S. D., & Fetsch, J. F. (2013). ERG expression in epithelioid sarcoma: A diagnostic pitfall. *The American Journal of Surgical Pathology*, 37(10), 1580–1585. <https://doi.org/10.1097/PAS.0b013e31828de23a>
- Mills, A. A. (2017). The Chromodomain Helicase DNA-Binding Chromatin Remodelers: Family Traits that Protect from and Promote Cancer. *Cold Spring Harbor Perspectives in Medicine*, 7(4). <https://doi.org/10.1101/cshperspect.a026450>
- Minami, Y., Kohsaka, S., Tsuda, M., Yachi, K., Hatori, N., Tanino, M., Kimura, T., Nishihara, H., Minami, A., Iwasaki, N., & Tanaka, S. (2014). SS18-SSX-regulated miR-17 promotes tumor growth of synovial sarcoma by inhibiting p21WAF1/CIP1. *Cancer Science*, 105(9), 1152–1159. <https://doi.org/10.1111/cas.12479>
- Molenaar, W. M., DeJong, B., Dam-Meiring, A., Postma, A., DeVries, J., & Hoekstra, H. J. (1989). Epithelioid sarcoma or malignant rhabdoid tumor of soft tissue? Epithelioid immunophenotype and rhabdoid karyotype. *Human Pathology*, 20(4), 347–351. [https://doi.org/10.1016/0046-8177\(89\)90044-0](https://doi.org/10.1016/0046-8177(89)90044-0)
- Mootha, V. K., Lindgren, C. M., Eriksson, K.-F., Subramanian, A., Sihag, S., Lehar, J., Puigserver, P., Carlsson, E., Ridderstråle, M., Laurila, E., Houstis, N., Daly, M. J., Patterson, N., Mesirov, J. P., Golub, T. R., Tamayo, P., Spiegelman, B., Lander, E. S., Hirschhorn, J. N., ... Groop, L. C. (2003). PGC-1 $\alpha$ -responsive genes involved in oxidative phosphorylation are coordinately downregulated in human diabetes. *Nature Genetics*, 34(3), 267–273. <https://doi.org/10.1038/ng1180>
- Morrison, A. J., & Shen, X. (2009). Chromatin remodelling beyond transcription: The INO80 and SWR1 complexes. *Nature Reviews Molecular Cell Biology*, 10(6), 373–384. <https://doi.org/10.1038/nrm2693>
- Msaouel, P., Malouf, G. G., Su, X., Yao, H., Tripathi, D. N., Soeung, M., Gao, J., Rao, P., Coarfa, C., Creighton, C. J., Bertocchio, J.-P., Kunnimalaiyaan, S., Multani, A. S., Blando, J., He, R., Shapiro, D. D., Perelli, L., Srinivasan, S., Carbone, F., ... Tannir, N. M. (2020). Comprehensive Molecular Characterization Identifies Distinct Genomic and Immune Hallmarks of Renal Medullary Carcinoma. *Cancer Cell*, 37(5), 720-734.e13. <https://doi.org/10.1016/j.ccell.2020.04.002>
- Myant, K., & Stancheva, I. (2008). LSH cooperates with DNA methyltransferases to repress transcription. *Molecular and Cellular Biology*, 28(1), 215–226. <https://doi.org/10.1128/MCB.01073-07>
- Nacev, B. A., Jones, K. B., Intlekofer, A. M., Yu, J. S. E., Allis, C. D., Tap, W. D., Ladanyi, M., & Nielsen, T. O. (2020). The epigenomics of sarcoma. *Nature Reviews Cancer*, 20(10), 608–623. <https://doi.org/10.1038/s41568-020-0288-4>
- Nacev, B. A., Sanchez-Vega, F., Smith, S. A., Antonescu, C. R., Rosenbaum, E., Shi, H., Tang, C., Socci, N. D., Rana, S., Gularte-Mérida, R., Zehir, A., Gounder, M. M., Bowler, T. G., Luthra, A., Jadeja, B., Okada, A., Strong, J. A., Stoller, J., Chan, J. E., ... Tap, W. D. (2021). Clinical sequencing of soft tissue and bone sarcomas delineates diverse genomic landscapes and potential therapeutic targets. *MedRxiv*, 2021.10.28.21265587. <https://doi.org/10.1101/2021.10.28.21265587>
- Nakayama, R. T., Pulice, J. L., Valencia, A. M., McBride, M. J., McKenzie, Z. M., Gillespie, M. A., Ku, W. L., Teng, M., Cui, K., Williams, R. T., Cassel, S. H., Qing, H., Widmer, C. J., Demetri, G. D., Irizarry, R. A., Zhao, K., Ranish, J. A., & Kadoch, C. (2017). SMARCB1 is required for widespread BAF complex-mediated activation of enhancers and bivalent promoters. *Nature Genetics*, 49(11), 1613–1623. <https://doi.org/10.1038/ng.3958>

- Nebbioso, A., Tambaro, F. P., Dell'Aversana, C., & Altucci, L. (2018). Cancer epigenetics: Moving forward. *PLOS Genetics*, *14*(6), e1007362. <https://doi.org/10.1371/journal.pgen.1007362>
- Neve, B., Jonckheere, N., Vincent, A., & Van Seuning, I. (2021). Long non-coding RNAs: The tentacles of chromatin remodeler complexes. *Cellular and Molecular Life Sciences*, *78*(4), 1139–1161. <https://doi.org/10.1007/s00018-020-03646-0>
- Nishiyama, M., Skoultchi, A. I., & Nakayama, K. I. (2012). Histone H1 Recruitment by CHD8 Is Essential for Suppression of the Wnt- $\beta$ -Catenin Signaling Pathway. *Molecular and Cellular Biology*, *32*(2), 501–512. <https://doi.org/10.1128/MCB.06409-11>
- Nuytten, M., Beke, L., Van Eynde, A., Ceulemans, H., Beullens, M., Van Hummelen, P., Fuks, F., & Bollen, M. (2008). The transcriptional repressor NIPP1 is an essential player in EZH2-mediated gene silencing. *Oncogene*, *27*(10), 1449–1460. <https://doi.org/10.1038/sj.onc.1210774>
- Outani, H., Imura, Y., Tanaka, T., Takenaka, S., Oshima, K., Hamada, K., Kakunaga, S., Joyama, S., Naka, N., Kudawara, I., Ueda, T., Araki, N., & Yoshikawa, H. (2018). Clinical outcomes of patients with epithelioid sarcomas: Impact and management of nodal metastasis. *International Journal of Clinical Oncology*, *23*(1), 181–188. <https://doi.org/10.1007/s10147-017-1179-x>
- Pack, L. R., Daigh, L. H., Chung, M., & Meyer, T. (2021). Clinical CDK4/6 inhibitors induce selective and immediate dissociation of p21 from cyclin D-CDK4 to inhibit CDK2. *Nature Communications*, *12*(1), 3356. <https://doi.org/10.1038/s41467-021-23612-z>
- Papp, G., Krausz, T., Stricker, T. P., Szendrői, M., & Sági, Z. (2014). *SMARCB1* expression in epithelioid sarcoma is regulated by miR-206, miR-381, and miR-671-5p on Both mRNA and protein levels: *Smarcb1* Regulation By Mirnas In Epithelioid Sarcoma. *Genes, Chromosomes and Cancer*, *53*(2), 168–176. <https://doi.org/10.1002/gcc.22128>
- Park, J.-H., Park, E.-J., Lee, H.-S., Kim, S. J., Hur, S.-K., Imbalzano, A. N., & Kwon, J. (2006). Mammalian SWI/SNF complexes facilitate DNA double-strand break repair by promoting gamma-H2AX induction. *The EMBO Journal*, *25*(17), 3986–3997. <https://doi.org/10.1038/sj.emboj.7601291>
- Pink, D., Richter, S., Gerdes, S., Andreou, D., Tunn, P.-U., Busemann, C., Ehninger, G., Reichardt, P., & Schuler, M. K. (2014). Gemcitabine and Docetaxel for Epithelioid Sarcoma: Results from a Retrospective, Multi-Institutional Analysis. *Oncology*, *87*(2), 95–103. <https://doi.org/10.1159/000362602>
- Piunti, A., Smith, E. R., Morgan, M. A. J., Ugarenko, M., Khaltyan, N., Helmin, K. A., Ryan, C. A., Murray, D. C., Rickels, R. A., Yilmaz, B. D., Rendleman, E. J., Savas, J. N., Singer, B. D., Bulun, S. E., & Shilatifard, A. (2019). CATACOMB: An endogenous inducible gene that antagonizes H3K27 methylation activity of Polycomb repressive complex 2 via an H3K27M-like mechanism. *Science Advances*, *5*(7), eaax2887. <https://doi.org/10.1126/sciadv.aax2887>
- Plaisier, S. B., Taschereau, R., Wong, J. A., & Graeber, T. G. (2010). Rank-rank hypergeometric overlap: Identification of statistically significant overlap between gene-expression signatures. *Nucleic Acids Research*, *38*(17), e169. <https://doi.org/10.1093/nar/gkq636>
- Pradhan, A., Grimer, R. J., Abudu, A., Tillman, R. M., Carter, S. R., Jeys, L., Ferguson, P. C., Griffin, A. M., & Wunder, J. S. (2017). Epithelioid sarcomas: How important is loco-regional control? *European Journal of Surgical Oncology*, *43*(9), 1746–1752. <https://doi.org/10.1016/j.ejso.2017.07.002>
- Raab, J. R., Resnick, S., & Magnuson, T. (2015). Genome-Wide Transcriptional Regulation Mediated by Biochemically Distinct SWI/SNF Complexes. *PLoS Genetics*, *11*(12), e1005748. <https://doi.org/10.1371/journal.pgen.1005748>

- Racki, L. R., Yang, J. G., Naber, N., Partensky, P. D., Acevedo, A., Purcell, T. J., Cooke, R., Cheng, Y., & Narlikar, G. J. (2009). The chromatin remodeller ACF acts as a dimeric motor to space nucleosomes. *Nature*, *462*(7276), 1016–1021. <https://doi.org/10.1038/nature08621>
- Rafati, H., Parra, M., Hakre, S., Moshkin, Y., Verdin, E., & Mahmoudi, T. (2011). Repressive LTR Nucleosome Positioning by the BAF Complex Is Required for HIV Latency. *PLOS Biology*, *9*(11), e1001206. <https://doi.org/10.1371/journal.pbio.1001206>
- Rao, R. A., Dhele, N., Cheemadan, S., Ketkar, A., Jayandharan, G. R., Palakodeti, D., & Rampalli, S. (2015). Ezh2 mediated H3K27me3 activity facilitates somatic transition during human pluripotent reprogramming. *Scientific Reports*, *5*, 8229. <https://doi.org/10.1038/srep08229>
- Reisman, D., Glaros, S., & Thompson, E. A. (2009). The SWI/SNF complex and cancer. *Oncogene*, *28*(14), 1653–1668. <https://doi.org/10.1038/onc.2009.4>
- Richter, G. H. S., Plehm, S., Fasan, A., Rössler, S., Unland, R., Bennani-Baiti, I. M., Hotfilder, M., Löwel, D., von Luettichau, I., Mossbrugger, I., Quintanilla-Martinez, L., Kovar, H., Staeger, M. S., Müller-Tidow, C., & Burdach, S. (2009). EZH2 is a mediator of EWS/FLI1 driven tumor growth and metastasis blocking endothelial and neuro-ectodermal differentiation. *Proceedings of the National Academy of Sciences of the United States of America*, *106*(13), 5324–5329. <https://doi.org/10.1073/pnas.0810759106>
- Riggi, N., Suvà, M.-L., Suvà, D., Cironi, L., Provero, P., Tercier, S., Joseph, J.-M., Stehle, J.-C., Baumer, K., Kindler, V., & Stamenkovic, I. (2008). EWS-FLI-1 expression triggers a Ewing's sarcoma initiation program in primary human mesenchymal stem cells. *Cancer Research*, *68*(7), 2176–2185. <https://doi.org/10.1158/0008-5472.CAN-07-1761>
- Ross, H. M., Lewis, J. J., Woodruff, J. M., & Brennan, M. F. (1997). Epithelioid sarcoma: Clinical behavior and prognostic factors of survival. *Annals of Surgical Oncology*, *4*(6), 491–495. <https://doi.org/10.1007/BF02303673>
- Rothbart, S. B., & Strahl, B. D. (2014). Interpreting the language of histone and DNA modifications. *Biochimica et Biophysica Acta (BBA) - Gene Regulatory Mechanisms*, *1839*(8), 627–643. <https://doi.org/10.1016/j.bbagr.2014.03.001>
- Roush, S., & Slack, F. J. (2008). The let-7 family of microRNAs. *Trends in Cell Biology*, *18*(10), 505–516. <https://doi.org/10.1016/j.tcb.2008.07.007>
- Ruhl, D. D., Jin, J., Cai, Y., Swanson, S., Florens, L., Washburn, M. P., Conaway, R. C., Conaway, J. W., & Chrivia, J. C. (2006). Purification of a Human SRCAP Complex That Remodels Chromatin by Incorporating the Histone Variant H2A.Z into Nucleosomes. *Biochemistry*, *45*(17), 5671–5677. <https://doi.org/10.1021/bi060043d>
- Saito, T., Oda, Y., Itakura, E., Shiratsuchi, H., Kinoshita, Y., Oshiro, Y., Tamiya, S., Hachitanda, Y., Iwamoto, Y., & Tsuneyoshi, M. (2001). Expression of intercellular adhesion molecules in epithelioid sarcoma and malignant rhabdoid tumor. *Pathology International*, *51*(7), 532–542. <https://doi.org/10.1046/j.1440-1827.2001.01232.x>
- Sakharpe, A., Lahat, G., Gulamhusein, T., Liu, P., Bolshakov, S., Nguyen, T., Zhang, P., Belousov, R., Young, E., Xie, X., Rao, P., Hornick, J. L., Lazar, A. J., Pollock, R. E., & Lev, D. (2011). Epithelioid sarcoma and unclassified sarcoma with epithelioid features: Clinicopathological variables, molecular markers, and a new experimental model. *The Oncologist*, *16*(4), 512–522. <https://doi.org/10.1634/theoncologist.2010-0174>
- Sápi, Z., Papp, G., Szendrői, M., Pápai, Z., Plótár, V., Krausz, T., & Fletcher, C. D. M. (2016). Epigenetic regulation of SMARCB1 By miR-206, -381 and -671-5p is evident in a variety of SMARCB1 immunonegative soft tissue sarcomas, while miR-765 appears specific for epithelioid sarcoma. A miRNA study of 223 soft tissue sarcomas. *Genes, Chromosomes & Cancer*, *55*(10), 786–802. <https://doi.org/10.1002/gcc.22379>

- Sarver, A. L., Li, L., & Subramanian, S. (2010). MicroRNA miR-183 functions as an oncogene by targeting the transcription factor EGR1 and promoting tumor cell migration. *Cancer Research*, *70*(23), 9570–9580. <https://doi.org/10.1158/0008-5472.CAN-10-2074>
- Sawyer, I. A., Bartek, J., & Dundr, M. (2019). Phase separated microenvironments inside the cell nucleus are linked to disease and regulate epigenetic state, transcription and RNA processing. *Seminars in Cell & Developmental Biology*, *90*, 94–103. <https://doi.org/10.1016/j.semcdb.2018.07.001>
- Sbaraglia, M., Bellan, E., & Dei Tos, A. P. (2020). The 2020 WHO Classification of Soft Tissue Tumours: News and perspectives. *Pathologica*, 1–15. <https://doi.org/10.32074/1591-951X-213>
- Schaefer, I.-M., Cote, G. M., & Hornick, J. L. (2018). Contemporary Sarcoma Diagnosis, Genetics, and Genomics. *Journal of Clinical Oncology*, *36*(2), 101–110. <https://doi.org/10.1200/JCO.2017.74.9374>
- Schuettengruber, B., Bourbon, H.-M., Di Croce, L., & Cavalli, G. (2017). Genome Regulation by Polycomb and Trithorax: 70 Years and Counting. *Cell*, *171*(1), 34–57. <https://doi.org/10.1016/j.cell.2017.08.002>
- Schwartzentruber, J., Korshunov, A., Liu, X.-Y., Jones, D. T. W., Pfaff, E., Jacob, K., Sturm, D., Fontebasso, A. M., Quang, D.-A. K., Tönjes, M., Hovestadt, V., Albrecht, S., Kool, M., Nantel, A., Konermann, C., Lindroth, A., Jäger, N., Rausch, T., Ryzhova, M., ... Jabado, N. (2012). Driver mutations in histone H3.3 and chromatin remodelling genes in paediatric glioblastoma. *Nature*, *482*(7384), 226–231. <https://doi.org/10.1038/nature10833>
- Sherr, C. J., & Roberts, J. M. (1995). Inhibitors of mammalian G1 cyclin-dependent kinases. *Genes & Development*, *9*(10), 1149–1163. <https://doi.org/10.1101/gad.9.10.1149>
- Singh Nanda, J., Kumar, R., & Raghava, G. P. S. (2016). dbEM: A database of epigenetic modifiers curated from cancerous and normal genomes. *Scientific Reports*, *6*, 19340. <https://doi.org/10.1038/srep19340>
- Smolle, M. A., Leithner, A., Posch, F., Szkandera, J., Liegl-Atzwanger, B., & Pichler, M. (2017). MicroRNAs in Different Histologies of Soft Tissue Sarcoma: A Comprehensive Review. *International Journal of Molecular Sciences*, *18*(9), 1960. <https://doi.org/10.3390/ijms18091960>
- Soini, Y. (2016). Epigenetic and genetic changes in soft tissue sarcomas: A review. *APMIS*, *124*(11), 925–934. <https://doi.org/10.1111/apm.12600>
- Soneson, C., Love, M. I., & Robinson, M. D. (2015). Differential analyses for RNA-seq: Transcript-level estimates improve gene-level inferences. *F1000Research*, *4*, 1521. <https://doi.org/10.12688/f1000research.7563.2>
- Sonobe, H., Ohtsuki, Y., Sugimoto, T., & Shimizu, K. (1997). Involvement of 8q, 22q, and monosomy 21 in an epithelioid sarcoma. *Cancer Genetics and Cytogenetics*, *96*(2), 178–180. [https://doi.org/10.1016/s0165-4608\(96\)00412-8](https://doi.org/10.1016/s0165-4608(96)00412-8)
- Spillane, A. J., Thomas, J. M., & Fisher, C. (2000). Epithelioid sarcoma: The clinicopathological complexities of this rare soft tissue sarcoma. *Annals of Surgical Oncology*, *7*(3), 218–225. <https://doi.org/10.1007/bf02523657>
- Stiller, C. A., Trama, A., Serraino, D., Rossi, S., Navarro, C., Chirlaque, M. D., Casali, P. G., & RARECARE Working Group. (2013). Descriptive epidemiology of sarcomas in Europe: Report from the RARECARE project. *European Journal of Cancer (Oxford, England: 1990)*, *49*(3), 684–695. <https://doi.org/10.1016/j.ejca.2012.09.011>
- Stockman, D. L., Hornick, J. L., Deavers, M. T., Lev, D. C., Lazar, A. J., & Wang, W.-L. (2014). ERG and FLI1 protein expression in epithelioid sarcoma. *Modern Pathology: An Official Journal of the United States and Canadian Academy of Pathology, Inc*, *27*(4), 496–501. <https://doi.org/10.1038/modpathol.2013.161>

- Stott, F. J., Bates, S., James, M. C., McConnell, B. B., Starborg, M., Brookes, S., Palmero, I., Ryan, K., Hara, E., Vousden, K. H., & Peters, G. (1998). The alternative product from the human CDKN2A locus, p14(ARF), participates in a regulatory feedback loop with p53 and MDM2. *The EMBO Journal*, *17*(17), 5001–5014. <https://doi.org/10.1093/emboj/17.17.5001>
- Strahl, B. D., & Allis, C. D. (2000). The language of covalent histone modifications. *Nature*, *403*(6765), 41–45. <https://doi.org/10.1038/47412>
- Stratton, M. R., Campbell, P. J., & Futreal, P. A. (2009). The cancer genome. *Nature*, *458*(7239), 719–724. <https://doi.org/10.1038/nature07943>
- Strohner, R., Nemeth, A., Jansa, P., Hofmann-Rohrer, U., Santoro, R., Längst, G., & Grummt, I. (2001). NoRC—a novel member of mammalian ISWI-containing chromatin remodeling machines. *The EMBO Journal*, *20*(17), 4892–4900. <https://doi.org/10.1093/emboj/20.17.4892>
- Subramanian, A., Tamayo, P., Mootha, V. K., Mukherjee, S., Ebert, B. L., Gillette, M. A., Paulovich, A., Pomeroy, S. L., Golub, T. R., Lander, E. S., & Mesirov, J. P. (2005). Gene set enrichment analysis: A knowledge-based approach for interpreting genome-wide expression profiles. *Proceedings of the National Academy of Sciences*, *102*(43), 15545–15550. <https://doi.org/10.1073/pnas.0506580102>
- Sullivan, L. M., Folpe, A. L., Pawel, B. R., Judkins, A. R., & Biegel, J. A. (2013). Epithelioid sarcoma is associated with a high percentage of SMARCB1 deletions. *Modern Pathology*, *26*(3), 385–392. <https://doi.org/10.1038/modpathol.2012.175>
- Sun, J., Zheng, G., Gu, Z., & Guo, Z. (2015). MiR-137 inhibits proliferation and angiogenesis of human glioblastoma cells by targeting EZH2. *Journal of Neuro-Oncology*, *122*(3), 481–489. <https://doi.org/10.1007/s11060-015-1753-x>
- Suvà, M.-L., Riggi, N., Janiszewska, M., Radovanovic, I., Provero, P., Stehle, J.-C., Baumer, K., Le Bitoux, M.-A., Marino, D., Cironi, L., Marquez, V. E., Clément, V., & Stamenkovic, I. (2009). EZH2 is essential for glioblastoma cancer stem cell maintenance. *Cancer Research*, *69*(24), 9211–9218. <https://doi.org/10.1158/0008-5472.CAN-09-1622>
- Taylor, B. S., Barretina, J., Maki, R. G., Antonescu, C. R., Singer, S., & Ladanyi, M. (2011). Advances in sarcoma genomics and new therapeutic targets. *Nature Reviews Cancer*, *11*(8), 541–557. <https://doi.org/10.1038/nrc3087>
- Thway, K., Jones, R. L., Noujaim, J., & Fisher, C. (2016). Epithelioid Sarcoma: Diagnostic Features and Genetics. *Advances in Anatomic Pathology*, *23*(1), 41–49. <https://doi.org/10.1097/PAP.000000000000102>
- Tokar, T., Pastrello, C., Rossos, A. E. M., Abovsky, M., Hauschild, A.-C., Tsay, M., Lu, R., & Jurisica, I. (2018). mirDIP 4.1—Integrative database of human microRNA target predictions. *Nucleic Acids Research*, *46*(D1), D360–D370. <https://doi.org/10.1093/nar/gkx1144>
- Tsukiyama, T., Daniel, C., Tamkun, J., & Wu, C. (1995). ISWI, a member of the SWI2/SNF2 ATPase family, encodes the 140 kDa subunit of the nucleosome remodeling factor. *Cell*, *83*(6), 1021–1026. [https://doi.org/10.1016/0092-8674\(95\)90217-1](https://doi.org/10.1016/0092-8674(95)90217-1)
- Turner, B. M. (2000). Histone acetylation and an epigenetic code. *BioEssays: News and Reviews in Molecular, Cellular and Developmental Biology*, *22*(9), 836–845. [https://doi.org/10.1002/1521-1878\(200009\)22:9<836::AID-BIES9>3.0.CO;2-X](https://doi.org/10.1002/1521-1878(200009)22:9<836::AID-BIES9>3.0.CO;2-X)
- Ugras, S., Brill, E., Jacobsen, A., Hafner, M., Socci, N. D., Decarolis, P. L., Khanin, R., O'Connor, R., Mihailovic, A., Taylor, B. S., Sheridan, R., Gimble, J. M., Viale, A., Crago, A., Antonescu, C. R., Sander, C., Tuschl, T., & Singer, S. (2011). Small RNA sequencing and functional characterization reveals MicroRNA-143 tumor suppressor activity in liposarcoma. *Cancer Research*, *71*(17), 5659–5669. <https://doi.org/10.1158/0008-5472.CAN-11-0890>



- Vasudevan, S. (2012). Posttranscriptional upregulation by microRNAs. *Wiley Interdisciplinary Reviews. RNA*, 3(3), 311–330. <https://doi.org/10.1002/wrna.121>
- Vintermist, A., Böhm, S., Sadeghifar, F., Louvet, E., Mansén, A., Percipalle, P., & Farrants, A.-K. Ö. (2011). The Chromatin Remodelling Complex B-WICH Changes the Chromatin Structure and Recruits Histone Acetyl-Transferases to Active rRNA Genes. *PLOS ONE*, 6(4), e19184. <https://doi.org/10.1371/journal.pone.0019184>
- Vries, R. G. J. (2005). Cancer-associated mutations in chromatin remodeler hSNF5 promote chromosomal instability by compromising the mitotic checkpoint. *Genes & Development*, 19(6), 665–670. <https://doi.org/10.1101/gad.335805>
- Waddington, C. H. (2012). The epigenotype. 1942. *International Journal of Epidemiology*, 41(1), 10–13. <https://doi.org/10.1093/ije/dyr184>
- Wang, X., Haswell, J. R., & Roberts, C. W. M. (2014). Molecular pathways: SWI/SNF (BAF) complexes are frequently mutated in cancer—mechanisms and potential therapeutic insights. *Clinical Cancer Research: An Official Journal of the American Association for Cancer Research*, 20(1), 21–27. <https://doi.org/10.1158/1078-0432.CCR-13-0280>
- Weaver, A., & Bossaer, J. B. (2021). Fibroblast growth factor receptor (FGFR) inhibitors: A review of a novel therapeutic class. *Journal of Oncology Pharmacy Practice: Official Publication of the International Society of Oncology Pharmacy Practitioners*, 27(3), 702–710. <https://doi.org/10.1177/1078155220983425>
- Weissmiller, A. M., Wang, J., Lorey, S. L., Howard, G. C., Martinez, E., Liu, Q., & Tansey, W. P. (2019). Inhibition of MYC by the SMARCB1 tumor suppressor. *Nature Communications*, 10(1), 2014. <https://doi.org/10.1038/s41467-019-10022-5>
- WHO, W. C. of T. E. B. (2020). *Soft Tissue and Bone Tumours* (5th ed., Vol. 3).
- Wilson, B. G., Wang, X., Shen, X., McKenna, E. S., Lemieux, M. E., Cho, Y.-J., Koellhoffer, E. C., Pomeroy, S. L., Orkin, S. H., & Roberts, C. W. M. (2010). Epigenetic antagonism between polycomb and SWI/SNF complexes during oncogenic transformation. *Cancer Cell*, 18(4), 316–328. <https://doi.org/10.1016/j.ccr.2010.09.006>
- Wolf, P. S., Flum, D. R., Tanas, M. R., Rubin, B. P., & Mann, G. N. (2008). Epithelioid sarcoma: The University of Washington experience. *American Journal of Surgery*, 196(3), 407–412. <https://doi.org/10.1016/j.amjsurg.2007.07.029>
- Wu, G., Broniscer, A., McEachron, T. A., Lu, C., Paugh, B. S., Beckfort, J., Qu, C., Ding, L., Huether, R., Parker, M., Zhang, J., Gajjar, A., Dyer, M. A., Mullighan, C. G., Gilbertson, R. J., Mardis, E. R., Wilson, R. K., Downing, J. R., Ellison, D. W., ... St. Jude Children's Research Hospital–Washington University Pediatric Cancer Genome Project. (2012). Somatic histone H3 alterations in pediatric diffuse intrinsic pontine gliomas and non-brainstem glioblastomas. *Nature Genetics*, 44(3), 251–253. <https://doi.org/10.1038/ng.1102>
- Xie, X., Ghadimi, M. P. H., Young, E. D., Belousov, R., Zhu, Q., Liu, J., Lopez, G., Colombo, C., Peng, T., Reynoso, D., Hornick, J. L., Lazar, A. J., & Lev, D. (2011). Combining EGFR and mTOR Blockade for the Treatment of Epithelioid Sarcoma. *Clinical Cancer Research*, 17(18), 5901–5912. <https://doi.org/10.1158/1078-0432.CCR-11-0660>
- Zhang, G., Dong, Z., Prager, B. C., Kim, L. J., Wu, Q., Gimple, R. C., Wang, X., Bao, S., Hamerlik, P., & Rich, J. N. (2019). Chromatin remodeler HELLS maintains glioma stem cells through E2F3 and MYC. *JCI Insight*, 4(7), 126140. <https://doi.org/10.1172/jci.insight.126140>
- Zhou, Y., Zhou, B., Pache, L., Chang, M., Khodabakhshi, A. H., Tanaseichuk, O., Benner, C., & Chanda, S. K. (2019). Metascape provides a biologist-oriented resource for the analysis of systems-level datasets. *Nature Communications*, 10(1), 1523. <https://doi.org/10.1038/s41467-019-09234-6>

- Zhu, H., Geiman, T. M., Xi, S., Jiang, Q., Schmidtman, A., Chen, T., Li, E., & Muegge, K. (2006). Lsh is involved in de novo methylation of DNA. *The EMBO Journal*, 25(2), 335–345. <https://doi.org/10.1038/sj.emboj.7600925>
- Zocchi, L., Mehta, A., Wu, S. C., Wu, J., Gu, Y., Wang, J., Suh, S., Spitale, R. C., & Benavente, C. A. (2020). Chromatin remodeling protein HELLS is critical for retinoblastoma tumor initiation and progression. *Oncogenesis*, 9(2), 1–15. <https://doi.org/10.1038/s41389-020-0210-7>

# **7. ACKNOWLEDGMENTS**

This work was possible thanks to the valuable contribution of: Dr. Prof. Angelo P. Dei Tos (University of Padua School of Medicine, Padua, Italy); Dr. Marta Sbaraglia (Azienda Ospedale Università Padova, Padua, Italy) and Dr. Anna Maria Frezza (Istituto Nazionale Tumori, Milan, Italy).

I would like to thank my supervisor Dr. Roberta Maestro for her guidance and scientific advice during these three years. I would also like to thank my co-supervisor Dr. Luca Sigalotti for his time, patience, and for sharing his knowledge with me during this period.

I would like to thank Dr. Davide Baldazzi for his fundamental support in the management and analysis of bioinformatics data. I am also deeply grateful to all the people who I have met in these three years in the Unit of Oncogenetics and Functional Oncogenomics for their valuable suggestions and their kind help. Special thanks to Dr. Beatrice Valenti, whose support and encouragement helped me to overcome even the most difficult moments.







To conclude, I cannot forget to thank my parents and my dear Davide G. for all the unconditional support they have shown me in these three years.

# **8. PUBLISHED ARTICLES**

During my PhD I had the chance to collaborate with other members of the Unit of Oncogenetics and Functional Oncogenomics at the CRO Aviano National Cancer Institute. In particular, I contributed to the evaluation of the sensitivity to tyrosine kinase inhibitors of a cell model recapitulating a KIT mutation identified in a rare case of hereditary GIST.

Case Report

# A Novel Kindred with Familial Gastrointestinal Stromal Tumors Caused by a Rare *KIT* Germline Mutation (N655K): Clinico-Pathological Presentation and TKI Sensitivity

Mara Fornasarig <sup>1,†</sup> , Daniela Gasparotto <sup>2,†</sup>, Luisa Foltran <sup>3,†</sup>, Michele Campigotto <sup>4</sup> , Sara Lombardi <sup>2</sup>, Elisa Del Savio <sup>2</sup>, Angela Buonadonna <sup>3</sup> , Fabio Puglisi <sup>3,5</sup> , Sandro Sulfaro <sup>6</sup>, Vincenzo Canzonieri <sup>4,7</sup> , Renato Cannizzaro <sup>1</sup>  and Roberta Maestro <sup>2,\*</sup>

<sup>1</sup> Unit of Oncological Gastroenterology, Centro di Riferimento Oncologico di Aviano (CRO Aviano), IRCCS, 33081 Aviano, Italy; mforasarig@cro.it (M.F.); rcannizzaro@cro.it (R.C.)

<sup>2</sup> Unit of Oncogenetics and Functional Oncogenomics, Centro di Riferimento Oncologico di Aviano (CRO Aviano), IRCCS, 33081 Aviano, Italy; dgasparotto@cro.it (D.G.); os1@cro.it (S.L.); elisa.delsavio@cro.it (E.D.S.)

<sup>3</sup> Unit of Medical Oncology and Cancer Prevention, Centro di Riferimento Oncologico di Aviano (CRO Aviano), IRCCS, 33081 Aviano, Italy; luisa.foltran@cro.it (L.F.); abunadonna@cro.it (A.B.); fabio.puglisi@cro.it (F.P.)

<sup>4</sup> Department of Medical, Surgical and Health Sciences, University of Trieste, 34127 Trieste, Italy; campigottomichele@gmail.com (M.C.); vcanzonieri@cro.it (V.C.)

<sup>5</sup> Department of Medicine, University of Udine, 3310 Udine, Italy

<sup>6</sup> Unit of Pathology, Santa Maria Degli Angeli General Hospital, 33170 Pordenone, Italy; sandro.sulfaro@asfo.sanita.fvg.it

<sup>7</sup> Unit of Pathology, Centro di Riferimento Oncologico di Aviano (CRO Aviano), IRCCS, 33081 Aviano, Italy

\* Correspondence: maestro@cro.it

† These authors contributed equally to this work.

Received: 16 October 2020; Accepted: 14 November 2020; Published: 17 November 2020



**Abstract:** Gastrointestinal stromal tumors (GISTs), the most common mesenchymal tumors of the gastrointestinal tract, are characterized by activating mutations in *KIT* or *PDGFRA* genes. The vast majority of GISTs are sporadic, but rare hereditary forms have been reported, often featuring multifocality and younger age of onset. We here report the identification of a novel kindred affected by familial GIST caused by a *KIT* germline mutation in exon 13 (N655K). No family affected by hereditary GIST due to this *KIT* variant has been reported in literature so far. We were able to track the mutation in three members of the family (proband, mother, and second-degree cousin), all affected by multiple GISTs. Due to its rarity, the N655K variant is poorly characterized. We conducted in vitro drug sensitivity assays that indicated that most tyrosine kinase inhibitors (TKIs) currently included in the therapeutic armamentarium for GISTs have a limited inhibitory activity toward this mutation. However, when compared to a classical imatinib-resistant *KIT* mutation (T670I), N655K was slightly more sensitive to imatinib, and encouraging responses were observed with last-generation TKIs.

**Keywords:** GIST; gastrointestinal stromal tumors; familial GIST; *KIT*; germline mutation

## 1. Introduction

Gastrointestinal stromal tumors (GISTs) are the most common mesenchymal tumors of the gastrointestinal tract and are thought to arise from the interstitial cells of Cajal (ICCs) [1,2]. The majority of GISTs (about 75%) harbor activating mutations in the *KIT* gene, most commonly in exon 11 and 9. Mutations in *PDGFRA* are detected in about 10–15% of GISTs. The fraction of GISTs devoid of *KIT* or *PDGFRA* mutations (~15%) is driven by rarer genetic alterations [1–4].

GISTs are essentially sporadic tumors, but rare familial forms associated with germline GIST-predisposing mutations have been reported. Among these are inactivating alterations of the *NF1* gene, responsible for type I neurofibromatosis, or defects in the genes encoding the succinate dehydrogenase complex (SDH), typically associated with the Carney–Stratakis GIST/paraganglioma syndrome [2,4–6].

Hereditary GISTs due to *KIT* or *PDGFRA* germline mutations are extremely rare, with very few cases reported so far. Tumor location and histology are similar to sporadic forms, but hereditary GISTs are often of early onset, multifocal, and associated with ICC hyperplasia. Other clinical manifestations include dysphagia, cutaneous hyperpigmentation, increased numbers of nevi, and mast-cell disorders [2,5,6].

We here report a case of a familial GIST syndrome due to a *KIT* exon 13 N655K germline mutation. The sensitivity of this rare *KIT* mutation to tyrosine kinase inhibitors (TKIs) currently approved or under trial for GISTs treatment was evaluated in vitro.

## 2. Materials and Methods

### 2.1. Histology and Immunohistochemistry

Formalin-fixed paraffin embedded (FFPE) surgical specimens were stained with hematoxylin and eosin (H&E). Immunohistochemical staining was performed by an automated immunostainer (Ventana, Roche, Basel, Switzerland) using the following antibodies: *KIT*/CD117 (polyclonal; 1:200; DAKO, Agilent, Santa Clara, CA, USA), CD34 (QEnd 10, 1:1; DAKO), S100 protein (polyclonal; 1:2000; DAKO), alpha-smooth muscle actin (SMA) (1A4; 1:400; DAKO), Ki-67 (MIB-1; 1:200; DAKO), DOG1 (SP31; 1:100; Cell Marque, Merck, Darmstadt, Germany), and desmin (DE-R-11, 1:100; DAKO).

### 2.2. Molecular Analysis

DNA was extracted from FFPE tumor specimens by QIAamp DNA FFPE Tissue Kit (QIAGEN, Hilden, Germany). DNA from peripheral blood mononuclear cells was extracted with an EZ1 biorobot (QIAGEN).

Next generation sequencing (NGS) libraries were prepared with a TruSeq Custom Amplicon Low-Input kit (Illumina, San Diego, CA, USA) targeting the coding sequence of the *KIT*, *PDGFRA*, *BRAF*, *SDHA*, *SDHB*, *SDHC*, *SDHD*, *HRAS*, *KRAS*, *NRAS*, *SPRED1*, *NF1*, *NF2*, and *TP53*, as described [4]. Libraries were sequenced on an MiSeq platform (Illumina) using a v3 kit, 2 × 150 cycles. Data were analyzed with the Miseq Reporter software (v2.6.2), using the custom amplicon workflow and somatic variant caller. Mean amplicon coverage was 3200. Variants were analyzed with the VariantStudio 3.0 software (Illumina) and filtered by coverage > 50 and frequency ≥ 20%. Mutations detected by NGS were validated by Sanger sequencing on an ABI PRISM 3100 Genetic Analyzer (Thermo Fisher Scientific, Waltham, MA, USA).

### 2.3. Engineering of Ba/F3 Cells for the Expression of *KIT* Mutants

The murine interleukin-3 (IL-3) dependent Ba/F3 cell line is a cell model widely used in kinase studies. In fact, when ectopically expressed, certain tyrosine kinases can relieve Ba/F3 cells from IL-3 dependency, while tyrosine kinase inhibitors antagonize this effect [7,8].

Ba/F3 cells (ATCC, Manassas, VA, USA) were cultured in RPMI medium supplemented with murine interleukin-3 (IL-3; 10 ng/mL; PeproTech, Rocky Hill, IL, USA), 10% fetal bovine serum (FBS), and gentamicin (8 µg/mL).

Human *KIT* wild-type cDNA was cloned into the pLVX IRES ZsGreen viral vector (Clontech, Mountain View, CA, USA) and *KIT* exon 11 (W557\_K558del), exon 13 (N655K), and exon 14 (T670I) mutant alleles were generated by PCR. Correct mutation introduction was checked by sequencing. To generate *KIT* lentiviral particles, human embryonic kidney HEK 293T cells



(ATCC) were transfected with vectors encoding *KIT* mutants. HEK 293T cells were cultured in DMEM medium supplemented with 10% FBS and gentamicin (8 µg/mL). Ba/F3 cells were infected with HEK 293T-derived lentiviral supernatants in the presence of polybrene (8 µg/mL). Ectopically *KIT* expressing cells were selected by IL-3 withdrawal. Lentiviral infection efficiency was monitored in situ by green fluorescence. Expression of the ectopic *KIT* alleles was checked by Western blot. Briefly, cells were lysed in RIPA buffer (Santa Cruz Biotechnology, Dallas, TX, USA). Protein lysates were separated by SDS-PAGE and transferred onto a nitrocellulose membrane (Protran Whatman, Merck, Darmstadt, Germany). Expression analyses were performed with the following antibodies: anti c-KIT (H300; Santa Cruz Biotechnology) and anti-GAPDH (MAB374, Chemicon International, Temecula, CA, USA), for total protein loading normalization. A ChemiDoc imaging system (Bio-Rad, Hercules, CA, USA) was used for visualization. Ba/F3 cells expressing comparable levels of ectopic *KIT* mutants were used in TKI cell viability assays.

#### 2.4. TKI Cell Viability Assay

Ba/F3 cells engineered to express the test mutation (*KIT* exon 13 N655K), an imatinib-sensitive mutation (*KIT* exon 11 W557\_K558del), or an imatinib-resistant mutation (*KIT* exon 14 T670I) were seeded on a 48-well plate at a density of 7500 cells/mL. The following day, cells were exposed to the indicated doses of TKIs for 72 h, as previously described [7]. TKIs (Selleckchem, Munich, Germany) were dissolved in DMSO (dimethyl sulfoxide) as a vehicle. Drug dosage ranges were selected based on literature data and were as follows: imatinib (0–1000 nM), sunitinib (0–36 nM), regorafenib (0–480 nM), cabozantinib (0–24 nM), avapritinib (0–250 nM), and ripretinib (0–80 nM). Cell viability was evaluated by Trypan Blue staining and expressed as percentage of cells surviving the treatment, normalized to vehicle (DMSO)-treated cells. Four replicates per dose were evaluated. Results were confirmed on at least two independent Ba/F3 cell infections.

#### 2.5. Ethical Approval

All procedures followed were in accordance with the Helsinki Declaration and with institutional and national ethical standards. The study was approved by the CRO Aviano institutional review board (IRB-04-2017). Written informed consent to be included in the study was obtained from patients.

### 3. Results

In March 2019, a 52-year-old woman was referred for genetic counseling after a diagnosis of multifocal GIST. She displayed diffuse freckles on her arms, legs, and trunk, and an atypical junctional nevus was surgically removed in February 2019. She had a history of estrogen-receptor-positive intraductal breast carcinoma diagnosed at the age of 43. She was also under surveillance for a thyroid nodule.

GIST was an incidental finding during bilateral salpingo-oophorectomy for uterine myomas and ovarian cyst (November 2018). Multiple nodules, the largest of 6 cm, were detected at the small bowel. At histopathological examination, these nodules showed spindle cells arranged in fascicles, and interlacing bundles with eosinophilic cytoplasm and elongated nuclei. Immunohistochemistry showed positivity for KIT/CD117 and DOG1, weak/focal reactivity for SMA and CD34, negativity for desmin and S100 (Figure 1A). Mitotic index was low (1 per 50 high-power fields). Diagnosis was of GIST of intermediate risk of progression according to Miettinen [9]. The diagnostic workup included a 18FDG-PET (fluorine-18-fluorodeoxyglucose positron emission tomography) that showed two lesions at the small bowel and one at the gastric fundus. Upper gastrointestinal endoscopy and ultrasound endoscopy showed a 2 cm submucosal nodule at the gastric fundus (Figure 1A). A second surgery was performed in January 2019 for resection of the gastric tumor and multiple small bowel nodules (size range 0.5–2 cm). Pathological examination corroborated the diagnosis of multinodular GIST. Molecular analysis, performed using a comprehensive GIST-specific NGS panel, revealed in both 2018 and 2019 tumor specimens a heterozygous T-to-G transversion at codon 655 of *KIT* exon 13

(c.1965T > G) resulting in an N655K amino acid change (Figure 1B). Besides the N655K *KIT* mutation, no other pathogenic mutation in GIST driver genes (*PDGFRA*, *BRAF*, *SDHA*, *SDHB*, *SDHC*, *SDHD*, *HRAS*, *KRAS*, *NRAS*, *SPRED1*, *NF1*, *NF2*, and *TP53*) was found.

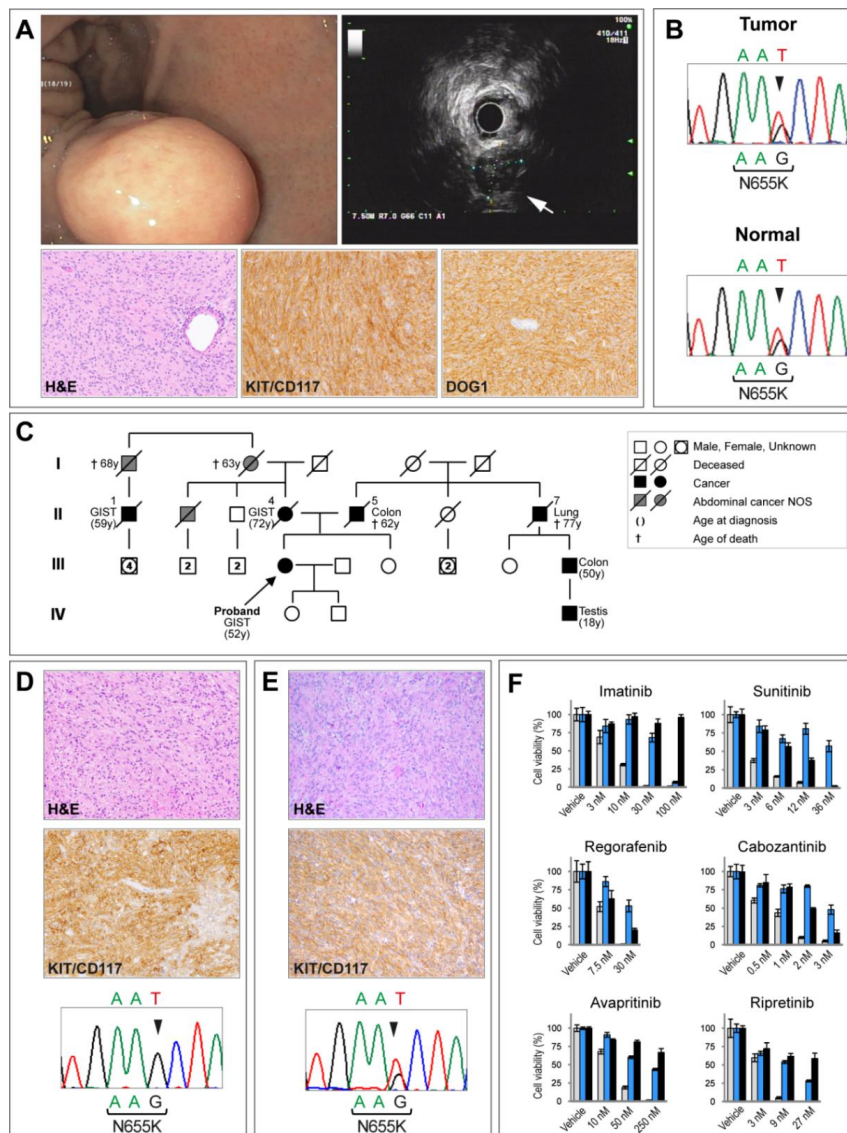


**Figure 1.** (A) Index case: endoscopic and histopathologic characteristics. Endoscopic (upper panel, left) and endoscopic ultrasound (upper panel, right) appearance of the submucosal gastric tumor of the index case (arrow). Lower panels: hematoxylin and eosin (H&E) staining of the lesion revealed bundles of spindle cells arranged in fascicles. Tumor cells displayed positive immunoreactivity for KIT/CD117 and DOG1 (original magnification:  $\times 20$ ). (B) Index case: molecular analysis. Sanger sequencing of tumor DNA revealed a T-to-G transversion at codon 655 of *KIT* exon 13 resulting in an N655K amino acid change (upper panel). The same *KIT* mutation was subsequently detected in the peripheral blood DNA (normal), indicating a germline origin (lower panel). (C) Family pedigree. (D) Index case's mother: pathological and molecular characterization of the gastrointestinal stromal tumor (GIST). H&E staining of the tumor showing a proliferation of spindle cells. Tumor cells were positive for KIT/CD117 expression (original magnification:  $\times 20$ ). Molecular analysis of tumor DNA revealed a *KIT* exon 13 N655K mutation. No significant signal for the wild-type nucleotide (T) was detected, indicating that the mutation in the tumor of the index case's mother was homozygous/hemizygous.

(E) Index case's second-degree cousin. Pathological and molecular characterization of the GIST. H&E staining showing spindle-shaped tumor cells disposed in fascicles. KIT/CD117 immunostaining demonstrating diffuse and strong membranous and cytoplasmic reactivity (original magnification:  $\times 20$ ). Sanger sequencing of tumor DNA revealing a *KIT* exon 13 N655K mutation. (F) In vitro tyrosine kinase inhibitor (TKI) sensitivity assay. Ba/F3 cells, engineered to express *KIT* mutant alleles, were treated with different TKIs at the indicated dosages. Cell viability is expressed as percentage of cells surviving the treatment, normalized to vehicle (DMSO)-treated cells. Color coding for *KIT* mutants: Light grey: imatinib-sensitive *KIT* exon 11 W557\_K558del; Blue: the *KIT* exon 13 N655K mutation detected in the familial GIST syndrome described here; Black: imatinib-resistant *KIT* exon 14 T670I. Error bars represent standard error of the mean.

Regarding family history (Figure 1C), the index case has a healthy sister (47 years old) with freckles on the trunk. Their mother died in 2012 at the age of 74 of metastatic GIST. She presented with multifocal intestinal GIST (positive for KIT/CD117, DOG1, and CD34; negative for S100, SMA, and desmin) and hepatic metastasis at diagnosis. Sequencing of tumor DNA revealed the same *KIT* N655K mutation detected in the proband (Figure 1D).

In 2000, the maternal second-degree cousin of the index case (II-1 at pedigree) was diagnosed at the age of 59 with multiple gastric and small-bowel mesenchymal malignant neoplasms compatible with GIST. The patient received two lines of combination chemotherapy for sarcomas (epidoxorubicine plus ifosfamide first, followed by CYVADIC, a combination of cyclophosphamide, vincristine, doxorubicin, and dacarbazine). Five years later (January 2006), he was referred to our center where PET/CT scan showed multifocal abdominal and hepatic increased uptake. Histological revision of the primary tumor supported the diagnosis of KIT/CD117-positive, DOG1-positive, GIST (immunohistochemistry was negative for CD34, S100, SMA, and desmin). Numerous microscopic GIST-like lesions (microGISTs) were also identified alongside the intestinal wall. Molecular analysis revealed a *KIT* exon 13 N655K mutation (Figure 1E). He started imatinib (400 mg daily). The disease progressed slowly until January 2007 when he underwent surgery for multiple abdominal masses. The patient was shifted to sunitinib for 15 months and, on progression, a rechallenge with imatinib at 800 mg allowed a progression-free interval of 9 months. A last line of treatment with nilotinib did not provide benefit and was stopped after 2 months.

The index case's uncle (mother's brother) and the maternal grandmother died of abdominal malignancy of unknown site and pathology (NOS). Colon cancer appeared as a recurrent event in the proband's paternal branch.

In light of multifocal presentation, family history, and the recurrence of the same rare *KIT* exon 13 mutation in the neoplasms of the family, genetic testing was proposed to the proband. Analysis of peripheral blood DNA highlighted the presence of the same *KIT* N655K mutation detected in the tumors thus supporting its germline origin (Figure 1B).

Due to the intermediate risk of recurrence and the fact that *KIT* exon 13-mutated sporadic GISTs are in general scarcely responsive to imatinib, after curative surgery, the index case was put on close surveillance with alternating CT scan and 18FDG-PET every six months. A papillary thyroid carcinoma, follicular variant, was diagnosed in January 2020.

Genetic counseling was considered for the proband's first-degree relatives. The sister refused genetic testing. Thus, annual abdominal ultrasound and upper-gastrointestinal endoscopy were suggested. The proband's children were under age 18 and were therefore considered not eligible for genetic testing.

In sporadic GISTs, the *KIT* exon 13 N655K detected in this family is very uncommon. Thus, it is poorly characterized [7,8]. To address its sensitivity to TKIs approved or under trial for GIST treatment, we performed in vitro cytotoxicity assays. Specifically, the response to imatinib, sunitinib, regorafenib, avapritinib, cabozantinib, and ripretinib of Ba/F3 cells engineered to express the N655K mutation was compared with that of cells expressing a prototypical imatinib-sensitive (*KIT* exon 11 W557\_K558del) and an imatinib-resistant (*KIT* exon 14 T670I) mutation (Figure 1F). Compared to the canonical *KIT*

exon 11 sensitizing mutation (W557\_K558del), the N655K mutation displayed a lower sensitivity to all TKIs tested. Compared to the reference resistant mutation (*KIT* exon 14 T670I), N655K appeared less responsive to sunitinib, regorafenib, and cabozantinib; it was instead slightly more sensitive to imatinib, especially at higher dosages, in keeping with previous results [7]. In addition, last-generation TKIs such as avapritinib and ripretinib [10] demonstrated a certain degree of activity toward this mutation (Figure 1F).

#### 4. Discussion

Very few cases of *KIT*/*PDGFRA*-associated familial GIST syndromes have been reported so far. A PubMed search retrieved 51 reports, 45 describing hereditary GISTs due to germline *KIT* mutations, most of which involving exon 11, and 6 reports of familial GIST associated with germline *PDGFRA* mutations (Table 1) [11–58].

**Table 1.** Currently reported cases of *KIT*- or *PDGFRA*-associated familial Gastrointestinal Stromal Tumors (GISTs).

Gene	Exon	Mutation	No. of Kindreds	Main Clinical Features [Reference]
<i>KIT</i>	8	D419del	1	systemic mastocytosis, multiple GISTs, dysphagia [11]
	9	K509I	2	systemic mastocytosis, multiple GISTs [12]; achalasia; mastocytosis, multiple GISTs [13]
	11	Y533C	1	multiple GISTs [14]
	11	W557R	4	multiple GISTs, skin hyperpigmentation, dysphagia [15]; multiple gastrointestinal autonomic nerve tumor [16]; multiple GISTs; skin hyperpigmentation [17]; multiple GISTs [18]
	11	W557S	1	multiple GISTs; lentigines [19]
	11	W557L_K558E	1	multiple GISTs, hereditary breast cancer [20]
	11	V559A	7	multiple GISTs; lentigines, cafe-au-lait macules [21]; multiple GIST, cutaneous hyperpigmentation [22]; multiple GISTs, melanosis, lentiginosis, hyperpigmentation, dysphagia [23]; multiple GISTs, hyperpigmentation, urticaria pigmentosa [24]; multiple GISTs, cutaneous hyperpigmentation [25]; multiple GISTs [26]
	11	V559_V560del	1	multiple GISTs, cutaneous hyperpigmentation [27]
	11	V560del	1	multiple GISTs [28]
	11	V560G	1	multiple GISTs, cutaneous hyperpigmentation [29]
	11	V560A	1	multiple GISTs [29]
	11	Q575_P577delinsH	1	rectal GIST [30]
	11	L576P	2	multiple GISTs; skin hyperpigmentation, achalasia-like stenosis [31]; multiple GISTs [32]
	11	L576_P577insQL	1	multiple GISTs, cutaneous hyperpigmentation [33]
	11	D579del	7	multiple GISTs, cutaneous hyperpigmentation, dysphagia [34]; GIST [35]; GIST, cutaneous hyperpigmentation [36]; multiple GISTs [37]; multiple GISTs [38]; multiple GIST, nevi, hyperpigmentation [39]
	13	K642T	1	multiple GISTs, dysphagia [40];
	13	K642E	7	multiple GISTs, breast cancer [41]; multiple GISTs, dysphagia, multiple nevi and lentigines [42]; multiple GISTs [43]; multiple GISTs including rectal GIST [44]; multiple GISTs, dysphagia, pigmentary defects (hyper- and hypopigmentation) [45]; multiple GISTs including rectal GIST, pigmentary defects (hyper- and hypopigmentation) [46]
13	N655K	1	multiple GISTs, lentigines, atypical junctional nevus, breast and thyroid cancer [present report]	
17	D820Y	3	multiple GISTs, dysphagia [47]; multiple GISTs [48]; multiple GISTs including rectal GIST [49]	
17	D820G	1	multiple GISTs [50]	
17	N822Y	1	multiple GISTs [51]	
<i>PDGFRA</i>	12	Y555C	1	multiple GISTs, intestinal neurofibromatosis, glaucoma, coarse facies, broad hands [52]
	12	V561D	1	multiple GISTs, fibrous tumors, lipoma [53,54]
	14	P653L	2	multiple GISTs, fibrous tumors, inflammatory fibroid polyps [55,56]
	18	D846Y	1	multiple GISTs, broad hands [57]
	18	D846V	1	multiple GISTs, coarse facies/skin, broad extremities [58]

Here, we report a new kindred with familial GISTs caused by a *KIT* exon 13 germline mutation (N655K). In sporadic GISTs, *KIT* exon 13 mutations, which affect the ATP-binding pocket of



the kinase, are uncommon and usually arise as secondary/imatinib-resistance events [1,2]. Among *KIT* exon 13 mutations, N655K is extremely rare, accounting for less than 0.1% of all GIST-associated *KIT* variants recorded in the Catalogue of Somatic Mutations in Cancer (COSMIC) database. With the only exception of a single, undetailed entry in the ClinVar database, to the best of our knowledge, there are no literature reports implicating this mutation in hereditary GISTs. Owing to its rarity, the N655K variant is poorly characterized and scanty literature data exist about its sensitivity to TKIs [7,8].

Our *in vitro* assay results indicate that N655K conveys a limited sensitivity to most TKIs approved for the treatment of GISTs. However, compared to a canonical resistance mutation (T670I), N655K was slightly more sensitive to imatinib, especially at higher dosages, a finding that is somehow in line with the response observed in the proband's second-degree cousin. Always with reference to the T670I resistance mutation, N655K appeared more sensitive also to avapritinib and ripretinib. These latter are new-generation TKIs that have been proven to be effective in controlling a wide range of *KIT* and *PDGFRA* mutations, including classical resistant mutations [10].

The limited number of kindreds reported so far prevents genotype–phenotype correlations and the presentation pattern of these tumor forms and the management of patients carrying GIST-predisposing gene mutations still need to be defined [2,5].

As far as the treatment is concerned, there is currently no evidence supporting a differential therapeutic approach for GISTs developing in a background of germline *KIT/PDGFR*A mutations compared to sporadic GISTs, although tumor multiplicity and, hence, surgery-requiring complications (e.g., intestinal hemorrhages and occlusions) are more likely to occur in the former.

Definitively, when a familial GIST syndrome is suspected, based on early age of onset, tumor multifocality, and family history, genotyping is highly recommended and, if positive, counseling and predictive genetic testing should be offered to all first-degree relatives. Moreover, it is worth bearing in mind that individuals affected by hereditary GISTs seem to have an increased risk for other tumor types [2,5]. Indeed, our index case also developed breast and papillary thyroid cancers.

In our opinion, GIST-predisposing-mutation carriers should undergo close surveillance for early detection of cancer. This is even more important when the genetic setting makes the tumor poorly amenable to pharmacological inhibition, as in the family presented here, and the earliest diagnosis of neoplastic growth would increase the chance of curative surgery. Unfortunately, no specific guidelines exist on how to manage these subjects. In particular, consensus recommendations for clinical surveillance are lacking and whether regular esophagogastroduodenoscopy (EGD) or 18FDG-PET examinations are useful options remain open questions.

In this context, single case reports such as the one described here are fundamental to build up a body of information that may lay down the ground for the development of evidence-based guidelines.

## 5. Conclusions

In this paper we report the identification and characterization of a new kindred affected by multiple GISTs due to a rare *KIT* germline N655K mutation. Very few cases of syndromic *KIT/PDGFR*A-associated familial GISTs have been described so far. Case studies such as ours may help in defining the presentation pattern of these tumor forms and contribute to the formulation of clinical practice guidelines. In addition, *in vitro* evaluation of drug sensitivity may provide a basis for treatment personalization.

**Author Contributions:** Conceptualization and drafting of the manuscript, M.F., D.G., L.F., and R.M.; patient treatment and genetic counselling: M.F., L.F., M.C., A.B., F.P., and R.C.; pathological analyses: S.S. and V.C.; molecular analyses: D.G., S.L., E.D.S., and R.M.; study supervision and funding acquisition, R.M. All authors have read and agreed to the published version of the manuscript.

**Funding:** This study was supported by the Italian Ministry of Health and by the Italian Association for Cancer Research (AIRC).

**Conflicts of Interest:** The authors declare no conflict of interest.

## References

1. Corless, C.L. Gastrointestinal stromal tumors: What do we know now? *Mod. Pathol.* **2014**, *27*, S1–S16. [[CrossRef](#)]
2. Mei, L.; Smith, S.C.; Faber, A.C.; Trent, J.; Grossman, S.R.; Stratakis, C.A.; Boikos, S.A. Gastrointestinal Stromal Tumors: The GIST of Precision Medicine. *Trends Cancer* **2018**, *4*, 74–91. [[CrossRef](#)]
3. Brenca, M.; Rossi, S.; Polano, M.; Gasparotto, D.; Zanatta, L.; Racanelli, D.; Valori, L.; Lamon, S.; Dei Tos, A.P.; Maestro, R. Transcriptome sequencing identifies ETV6-NTRK3 as a gene fusion involved in GIST. *J. Pathol.* **2016**, *238*, 543–549. [[CrossRef](#)]
4. Gasparotto, D.; Rossi, S.; Polano, M.; Tamborini, E.; Lorenzetto, E.; Sbaraglia, M.; Mondello, A.; Massani, M.; Lamon, S.; Bracci, R.; et al. Quadruple-Negative GIST Is a Sentinel for Unrecognized Neurofibromatosis Type 1 Syndrome. *Clin. Cancer Res.* **2017**, *23*, 273–282. [[CrossRef](#)]
5. Ricci, R. Syndromic gastrointestinal stromal tumors. *Hered. Cancer Clin. Pract.* **2016**, *14*, 15. [[CrossRef](#)]
6. Agarwal, R.; Robson, M. Inherited predisposition to gastrointestinal stromal tumor. *Hematol. Oncol. Clin. N. Am.* **2009**, *23*, 1–13. [[CrossRef](#)]
7. Garner, A.P.; Gozgit, J.M.; Anjum, R.; Vodala, S.; Schrock, A.; Zhou, T.; Serrano, C.; Eilers, G.; Zhu, M.; Ketzer, J.; et al. Ponatinib inhibits polyclonal drug-resistant KIT oncoproteins and shows therapeutic potential in heavily pretreated gastrointestinal stromal tumor (GIST) patients. *Clin. Cancer Res.* **2014**, *20*, 5745–5755. [[CrossRef](#)]
8. Kinoshita, K.; Hirota, S.; Isozaki, K.; Nishitani, A.; Tsutsui, S.; Watabe, K.; Tamura, S.; Ishikawa, T.; Kanda, T.; Nishida, T.; et al. Characterization of tyrosine kinase I domain c-kit gene mutation Asn655Lys newly found in primary jejunal gastrointestinal stromal tumor. *Am. J. Gastroenterol.* **2007**, *102*, 1134–1136. [[CrossRef](#)]
9. Miettinen, M.; Lasota, J. Gastrointestinal stromal tumors: Pathology and prognosis at different sites. *Semin. Diagn. Pathol.* **2006**, *23*, 70–83. [[CrossRef](#)]
10. Farag, S.; Smith, M.J.; Fotiadis, N.; Constantinidou, A.; Jones, R.L. Revolutions in treatment options in gastrointestinal stromal tumours (GISTs): The latest updates. *Curr. Treat. Options Oncol.* **2020**, *21*, 55. [[CrossRef](#)]
11. Hartmann, K.; Wardelmann, E.; Ma, Y.; Merkelbach-Bruse, S.; Preussner, L.M.; Woolery, C.; Baldus, S.E.; Heinicke, T.; Thiele, J.; Buettner, R.; et al. Novel germline mutation of KIT associated with familial gastrointestinal stromal tumors and mastocytosis. *Gastroenterology* **2005**, *129*, 1042–1046. [[CrossRef](#)]
12. Speight, R.A.; Nicolle, A.; Needham, S.J.; Verrill, M.W.; Bryon, J.; Panter, S. Rare, germline mutation of KIT with imatinib-resistant multiple GI stromal tumors and mastocytosis. *J. Clin. Oncol.* **2013**, *31*, e245–e247. [[CrossRef](#)]
13. Halpern, A.L.; Torphy, R.J.; McCarter, M.D.; Sciotto, C.G.; Glode, L.M.; Robinson, W.A. A familial germline mutation in KIT associated with achalasia, mastocytosis and gastrointestinal stromal tumors shows response to kinase inhibitors. *Cancer Genet.* **2019**, *233–234*, 1–6. [[CrossRef](#)]
14. Nakai, M.; Hashikura, Y.; Ohkouchi, M.; Yamamura, M.; Akiyama, T.; Shiba, K.; Kajimoto, N.; Tsukamoto, Y.; Hao, H.; Isozaki, K.; et al. Characterization of novel germline c-kit gene mutation, KIT-Tyr553Cys, observed in a family with multiple gastrointestinal stromal tumors. *Lab. Investig.* **2012**, *92*, 451–457. [[CrossRef](#)]
15. Robson, M.E.; Glogowski, E.; Sommer, G.; Antonescu, C.R.; Nafa, K.; Maki, R.G.; Ellis, N.; Besmer, P.; Brennan, M.; Offit, K. Pleomorphic characteristics of a germ-line KIT mutation in a large kindred with gastrointestinal stromal tumors, hyperpigmentation, and dysphagia. *Clin. Cancer Res.* **2004**, *10*, 1250–1254. [[CrossRef](#)]
16. Hirota, S.; Okazaki, T.; Kitamura, Y.; O'Brien, P.; Kapusta, L.; Dardick, I. Cause of familial and multiple gastrointestinal autonomic nerve tumors with hyperplasia of interstitial cells of Cajal is germline mutation of the c-kit gene. *Am. J. Surg. Pathol.* **2000**, *24*, 326–327. [[CrossRef](#)]
17. Farag, S.; van der Kolk, L.E.; van Boven, H.H.; van Akkooi, A.C.J.; Beets, G.L.; Wilmink, J.W.; Steeghs, N. Remarkable effects of imatinib in a family with young onset gastrointestinal stromal tumors and cutaneous hyperpigmentation associated with a germline KIT-Trp557Arg mutation: Case report and literature overview. *Fam. Cancer* **2018**, *17*, 247–253. [[CrossRef](#)]
18. Antonescu, C.R.; Viale, A.; Sarran, L.; Tschernyavsky, S.J.; Gonen, M.; Segal, N.H.; Maki, R.G.; Socci, N.D.; DeMatteo, R.P.; Besmer, P. Gene expression in gastrointestinal stromal tumors is distinguished by KIT genotype and anatomic site. *Clin. Cancer Res.* **2004**, *10*, 3282–3290. [[CrossRef](#)]

19. Hasegawa, M.; Shimizu, A.; Ieta, K.; Shibusawa, K.; Ishikawa, O.; Ishida-Yamamoto, A.; Tamura, A. Generalized lentiginos associated with familial gastrointestinal stromal tumors dramatically improved by imatinib treatment. *J. Dermatol.* **2020**, *47*, e241–e242. [[CrossRef](#)]
20. Sekido, Y.; Ohigashi, S.; Takahashi, T.; Hayashi, N.; Suzuki, K.; Hirota, S. Familial Gastrointestinal Stromal Tumor with Germline KIT Mutations Accompanying Hereditary Breast and Ovarian Cancer Syndrome. *Anticancer Res.* **2017**, *37*, 1425–1431. [[CrossRef](#)]
21. Gupta, D.; Chandrashekar, L.; Larizza, L.; Colombo, E.A.; Fontana, L.; Gervasini, C.; Thappa, D.M.; Rajappa, M.; Rajendiran, K.S.; Sreenath, G.S.; et al. Familial gastrointestinal stromal tumors, lentiginos, and café-au-lait macules associated with germline c-kit mutation treated with imatinib. *Int. J. Dermatol.* **2017**, *56*, 195–201. [[CrossRef](#)] [[PubMed](#)]
22. Maeyama, H.; Hidaka, E.; Ota, H.; Minami, S.; Kajiyama, M.; Kuraishi, A.; Mori, H.; Matsuda, Y.; Wada, S.; Sodeyama, H.; et al. Familial gastrointestinal stromal tumor with hyperpigmentation: Association with a germline mutation of the c-kit gene. *Gastroenterology* **2001**, *120*, 210–215. [[CrossRef](#)] [[PubMed](#)]
23. Adela Avila, S.; Peñalosa, J.; González, F.; Abdo, I.; Rainville, I.; Root, E.; Carrero Valenzuela, R.D.; Garber, J. Dysphagia, melanosis, gastrointestinal stromal tumors and a germinal mutation of the KIT gene in an Argentine family. *Acta Gastroenterol. Latinoam.* **2014**, *44*, 9–15. [[PubMed](#)]
24. Beghini, A.; Tibiletti, M.G.; Roversi, G.; Chiaravalli, A.M.; Serio, G.; Capella, C.; Larizza, L. Germline mutation in the juxtamembrane domain of the kit gene in a family with gastrointestinal stromal tumors and urticaria pigmentosa. *Cancer* **2001**, *92*, 657–662. [[CrossRef](#)]
25. Kuroda, N.; Tanida, N.; Hirota, S.; Daum, O.; Hes, O.; Michal, M.; Lee, G.H. Familial gastrointestinal stromal tumor with germ line mutation of the juxtamembrane domain of the KIT gene observed in relatively young women. *Ann. Diagn. Pathol.* **2011**, *15*, 358–361. [[CrossRef](#)]
26. Kim, H.J.; Lim, S.J.; Park, K.; Yuh, Y.J.; Jang, S.J.; Choi, J. Multiple gastrointestinal stromal tumors with a germline c-kit mutation. *Pathol. Int.* **2005**, *55*, 655–659. [[CrossRef](#)] [[PubMed](#)]
27. Nishida, T.; Hirota, S.; Taniguchi, M.; Hashimoto, K.; Isozaki, K.; Nakamura, H.; Kanakura, Y.; Tanaka, T.; Takabayashi, A.; Matsuda, H.; et al. Familial gastrointestinal stromal tumours with germline mutation of the KIT gene. *Nat. Genet.* **1998**, *19*, 323–324. [[CrossRef](#)]
28. Bamba, S.; Hirota, S.; Inatomi, O.; Ban, H.; Nishimura, T.; Shioya, M.; Imaeda, H.; Nishida, A.; Sasaki, M.; Murata, S.; et al. Familial and multiple gastrointestinal stromal tumors with fair response to a half-dose of imatinib. *Intern. Med.* **2015**, *54*, 759–764. [[CrossRef](#)]
29. Kang, D.Y.; Park, C.K.; Choi, J.S.; Jin, S.Y.; Kim, H.J.; Joo, M.; Kang, M.S.; Moon, W.S.; Yun, K.J.; Yu, E.S.; et al. Multiple gastrointestinal stromal tumors: Clinicopathologic and genetic analysis of 12 patients. *Am. J. Surg. Pathol.* **2007**, *31*, 224–232. [[CrossRef](#)]
30. Woźniak, A.; Rutkowski, P.; Sciot, R.; Ruka, W.; Michej, W.; Debiec-Rychter, M. Rectal gastrointestinal stromal tumors associated with a novel germline KIT mutation. *Int. J. Cancer* **2008**, *122*, 2160–2164. [[CrossRef](#)]
31. Neuhaus, T.M.; Mansmann, V.; Merkelbach-Bruse, S.; Klink, B.; Hellinger, A.; Höffkes, H.G.; Wardelmann, E.; Schildhaus, H.U.; Tinschert, S. A novel germline KIT mutation (p.L576P) in a family presenting with juvenile onset of multiple gastrointestinal stromal tumors, skin hyperpigmentations, and esophageal stenosis. *Am. J. Surg. Pathol.* **2013**, *37*, 898–905. [[CrossRef](#)] [[PubMed](#)]
32. Vale Rodrigues, R.; Santos, F.; Pereira da Silva, J.; Francisco, I.; Claro, I.; Albuquerque, C.; Lemos, M.M.; Limbert, M.; Dias Pereira, A. A case of multiple gastrointestinal stromal tumors caused by a germline KIT gene mutation (p.Leu576Pro). *Fam. Cancer* **2017**, *16*, 267–270. [[CrossRef](#)] [[PubMed](#)]
33. Carballo, M.; Roig, I.; Aguilar, F.; Pol, M.A.; Gamundi, M.J.; Hernan, I.; Martinez-Gimeno, M. Novel c-KIT germline mutation in a family with gastrointestinal stromal tumors and cutaneous hyperpigmentation. *Am. J. Med. Genet. A* **2005**, *132*, 361–364. [[CrossRef](#)] [[PubMed](#)]
34. Forde, P.M.; Cochran, R.L.; Boikos, S.A.; Zabransky, D.J.; Beaver, J.A.; Meyer, C.F.; Thornton, K.A.; Montgomery, E.A.; Lidor, A.O.; Donehower, R.C.; et al. Familial GI Stromal Tumor With Loss of Heterozygosity and Amplification of Mutant KIT. *J. Clin. Oncol.* **2016**, *34*, e13–e16. [[CrossRef](#)]
35. Tarn, C.; Merkel, E.; Canutescu, A.A.; Shen, W.; Skorobogatko, Y.; Heslin, M.J.; Eisenberg, B.; Birbe, R.; Patchefsky, A.; Dunbrack, R.; et al. Analysis of KIT mutations in sporadic and familial gastrointestinal stromal tumors: Therapeutic implications through protein modeling. *Clin. Cancer Res.* **2005**, *11*, 3668–3677. [[CrossRef](#)]

36. Wali, G.N.; Halliday, D.; Dua, J.; Ieremia, E.; McPherson, T.; Matin, R.N. Cutaneous hyperpigmentation and familial gastrointestinal stromal tumour associated with KIT mutation. *Clin. Exp. Dermatol.* **2019**, *44*, 418–421. [[CrossRef](#)]
37. Jones, D.H.; Caracciolo, J.T.; Hodul, P.J.; Strosberg, J.R.; Coppola, D.; Bui, M.M. Familial gastrointestinal stromal tumor syndrome: Report of 2 cases with KIT exon 11 mutation. *Cancer Control* **2015**, *22*, 102–108. [[CrossRef](#)]
38. Lasota, J.; Miettinen, M. A new familial GIST identified. *Am. J. Surg. Pathol.* **2006**, *30*, 1342. [[CrossRef](#)]
39. Kleinbaum, E.P.; Lazar, A.J.F.; Tamborini, E.; Mcauliffe, J.C.; Sylvestre, P.B.; Sunnenberg, T.D.; Strong, L.; Chen, L.L.; Choi, H.; Benjamin, R.S.; et al. Clinical, histopathologic, molecular and therapeutic findings in a large kindred with gastrointestinal stromal tumor. *Int. J. Cancer* **2008**, *122*, 711–718. [[CrossRef](#)]
40. Yamanoi, K.; Higuchi, K.; Kishimoto, H.; Nishida, Y.; Nakamura, M.; Sudoh, M.; Hirota, S. Multiple gastrointestinal stromal tumors with novel germline c-kit gene mutation, K642T, at exon 13. *Hum. Pathol.* **2014**, *45*, 884–888. [[CrossRef](#)]
41. Wadt, K.; Andersen, M.K.; Hansen, T.V.O.; Gerdes, A.M. A new genetic diagnosis of familial gastrointestinal stromal tumour. *Ugeskr. Laeg.* **2012**, *174*, 1462–1464. [[PubMed](#)]
42. Bachet, J.B.; Landi, B.; Laurent-Puig, P.; Italiano, A.; Le Cesne, A.; Lévy, P.; Safar, V.; Duffaud, F.; Blay, J.Y.; Emile, J.F. Diagnosis, prognosis and treatment of patients with gastrointestinal stromal tumour (GIST) and germline mutation of KIT exon 13. *Eur. J. Cancer* **2013**, *49*, 2531–2541. [[CrossRef](#)] [[PubMed](#)]
43. Isozaki, K.; Terris, B.; Belghiti, J.; Schiffmann, S.; Hirota, S.; Vanderwinden, J.M. Germline-activating mutation in the kinase domain of KIT gene in familial gastrointestinal stromal tumors. *Am. J. Pathol.* **2000**, *157*, 1581–1585. [[CrossRef](#)]
44. Graham, J.; Debiec-Rychter, M.; Corless, C.L.; Reid, R.; Davidson, R.; White, J.D. Imatinib in the management of multiple gastrointestinal stromal tumors associated with a germline KIT K642E mutation. *Arch. Pathol. Lab. Med.* **2007**, *131*, 1393–1396. [[CrossRef](#)]
45. Vilain, R.E.; Dudding, T.; Braye, S.G.; Groombridge, C.; Meldrum, C.; Spigelman, A.D.; Ackland, S.; Ashman, L.; Scott, R.J. Can a familial gastrointestinal tumour syndrome be allelic with Waardenburg syndrome? *Clin. Genet.* **2011**, *79*, 554–560. [[CrossRef](#)]
46. Engin, G.; Eraslan, S.; Kayserili, H.; Kapran, Y.; Akman, H.; Akyuz, A.; Aykan, N.F. Imatinib response of gastrointestinal stromal tumor patients with germline mutation on KIT exon 13: A family report. *World J. Radiol.* **2017**, *9*, 365–370. [[CrossRef](#)]
47. Hirota, S.; Nishida, T.; Isozaki, K.; Taniguchi, M.; Nishikawa, K.; Ohashi, A.; Takabayashi, A.; Obayashi, T.; Okuno, T.; Kinoshita, K.; et al. Familial gastrointestinal stromal tumors associated with dysphagia and novel type germline mutation of KIT gene. *Gastroenterology* **2002**, *122*, 1493–1499. [[CrossRef](#)]
48. O’Riain, C.; Corless, C.L.; Heinrich, M.C.; Keegan, D.; Vioreanu, M.; Maguire, D.; Sheahan, K. Gastrointestinal stromal tumors: Insights from a new familial GIST kindred with unusual genetic and pathologic features. *Am. J. Surg. Pathol.* **2005**, *29*, 1680–1683. [[CrossRef](#)]
49. Veiga, I.; Silva, M.; Vieira, J.; Pinto, C.; Pinheiro, M.; Torres, L.; Soares, M.; Santos, L.; Duarte, H.; Bastos, A.L.; et al. Hereditary gastrointestinal stromal tumors sharing the KIT Exon 17 germline mutation p.Asp820Tyr develop through different cytogenetic progression pathways. *Genes Chromosomes Cancer* **2010**, *49*, 91–98. [[CrossRef](#)]
50. Arima, J.; Hiramatsu, M.; Taniguchi, K.; Kobayashi, T.; Tsunematsu, I.; Kagota, S.; Sakane, J.; Suzuki, Y.; Hirota, S. Multiple gastrointestinal stromal tumors caused by a novel germline KIT gene mutation (Asp820Gly): A case report and literature review. *Gastric Cancer* **2020**, *23*, 760–764. [[CrossRef](#)]
51. Thalheimer, A.; Schlemmer, M.; Bueter, M.; Merkelbach-Bruse, S.; Schildhaus, H.U.; Buettner, R.; Hartung, E.; Thiede, A.; Meyer, D.; Fein, M.; et al. Familial gastrointestinal stromal tumors caused by the novel KIT exon 17 germline mutation N822Y. *Am. J. Surg. Pathol.* **2008**, *32*, 1560–1565. [[CrossRef](#)] [[PubMed](#)]
52. de Raedt, T.; Cools, J.; Debiec-Rychter, M.; Brems, H.; Mentens, N.; Sciot, R.; Himpens, J.; de Wever, I.; Schöffski, P.; Marynen, P.; et al. Intestinal neurofibromatosis is a subtype of familial GIST and results from a dominant activating mutation in PDGFRA. *Gastroenterology* **2006**, *131*, 1907–1912. [[CrossRef](#)]
53. Pasini, B.; Matyakhina, L.; Bei, T.; Muchow, M.; Boikos, S.; Ferrando, B.; Carney, J.A.; Stratakis, C.A. Multiple gastrointestinal stromal and other tumors caused by platelet-derived growth factor receptor alpha gene mutations: A case associated with a germline V561D defect. *J. Clin. Endocrinol. Metab.* **2007**, *92*, 3728–3732. [[CrossRef](#)] [[PubMed](#)]



54. Carney, J.A.; Stratakis, C.A. Stromal, fibrous, and fatty gastrointestinal tumors in a patient with a PDGFRA gene mutation. *Am. J. Surg. Pathol.* **2008**, *32*, 1412–1420. [[CrossRef](#)] [[PubMed](#)]
55. Ricci, R.; Martini, M.; Cenci, T.; Carbone, A.; Lanza, P.; Biondi, A.; Rindi, G.; Cassano, A.; Larghi, A.; Persiani, R.; et al. PDGFRA-mutant syndrome. *Mod. Pathol.* **2015**, *28*, 954–964. [[CrossRef](#)]
56. Ricci, R.; Martini, M.; Cenci, T.; Riccioni, M.E.; Maria, G.; Cassano, A.; Larocca, L.M. Divergent gastrointestinal stromal tumors in syndromic settings. *Cancer Genet.* **2016**, *209*, 354–358. [[CrossRef](#)]
57. Chompret, A.; Kannengiesser, C.; Barrois, M.; Terrier, P.; Dahan, P.; Tursz, T.; Lenoir, G.M.; Bressac-De Paillerets, B. PDGFRA germline mutation in a family with multiple cases of gastrointestinal stromal tumor. *Gastroenterology* **2004**, *126*, 318–321. [[CrossRef](#)]
58. Manley, P.N.; Abu-Abed, S.; Kirsch, R.; Hawrysh, A.; Perrier, N.; Feilotter, H.; Pollett, A.; Riddell, R.H.; Hookey, L.; Walia, J.S. Familial PDGFRA-mutation syndrome: Somatic and gastrointestinal phenotype. *Hum. Pathol.* **2018**, *76*, 52–57. [[CrossRef](#)]

**Publisher’s Note:** MDPI stays neutral with regard to jurisdictional claims in published maps and institutional affiliations.



© 2020 by the authors. Licensee MDPI, Basel, Switzerland. This article is an open access article distributed under the terms and conditions of the Creative Commons Attribution (CC BY) license (<http://creativecommons.org/licenses/by/4.0/>).